Strategies in umbilical cord-derived mesenchymal stem cells expansion

Von der Naturwissenschaftlichen Fakultät

der Gottfried Wilhelm Leibniz Universität Hannover

zur Erlangung des Grades

Doktorin der Naturwissenschaften

Dr. rer. nat

genehmigte Dissertation

von

M.Sc. Antonina Lavrentieva

Geboren am 21.05.1976 in Dmitrow (Russland)

2012

Referent: Prof. Dr. Thomas Scheper
Institut für Technische Chemie
Leibniz Universität Hannover
Korreferent: Prof. Dr. Cornelia Kasper
Department für Biotechnologie,
Universität für Bodenkultur, Wien

Tag der Promotion: 29. August 2012

Erklärung

Ich versichere, dass ich diese Dissertation selbstständig und nur unter Verwendung der angegebenen Hilfsmittel und Quellen durchgeführt habe. Diese Arbeit wurde nicht als Diplomarbeit oder ähnliche Prüfungsarbeit verwendet.

Hannover, im Mai 2012

Kurzfassung

Die Nutzung von mesenchymalen Stammzellen (MSC) für zelltherapeutische Verfahren und die Gewebezüchtung ist vielversprechend. MSC, aus einer Vielzahl an Geweben isoliert, werden bereits in zahlreichen klinischen Untersuchungen eingesetzt. Die Nabelschnurmatrix stellt eine bedeutende Quelle für MSC dar. Aus Nabelschnur (umbilical cord – UC) isolierte MSC haben kurze Verdopplungszeiten und ihre Gewinnung und ihr Einsatz werden nicht durch ethische Probleme eingeschränkt. Des Weiteren gibt es bislang keine gesetzlichen Beschränkungen in der Anwendung von UC-MSC im Vergleich zu Embryonalen Stammzellen. Da für therapeutische Anwendungen in der Regel mehrere Millionen MSC pro Patient erforderlich sind, müssen optimierte Kultivierungsprotokolle entwickelt werden.

In dieser Arbeit wurden zwei verschieden Strategien zur Optimierung der Expansionsausbeute sowie der Qualität der MSC untersucht: 1.) der Einfluss der Sauerstoff-Konzentration auf die statische Kultivierung von UC-MSC, 2.) der Einfluss der dynamischen Kultivierung von UC-MSC in einem Bioreaktor, dem Einweg Z®RP 2000 H.

Die Ergebnisse der vorliegenden Arbeit zeigten, dass sich UC-MSC unter Hypoxie an die natürliche in vivo Mikroumgebung dieser Zellen anpassten. Im Hinblick auf die Fähigkeit in einem nahrungsbeschränkten Milieu nach der Transplantation zu überleben, bietet die hypoxische Kultivierung Vorteile. Kultivierungen von UC-MSC unter hypoxischen Bedingungen wurden sowohl über kurze Zeiträume von 3 Tagen, als auch über längere Perioden von 3 Monaten mit Sauerstoffkonzentrationen zwischen 1,5 % und 5% O_2 durchgeführt. Dabei wurden Einflüsse auf die Zellproliferation, die metabolische Aktivität, die Differenzierungskapazität und mögliche in vitro Transformationen der Zellen untersucht. Kultivierungen unter hypoxischen Bedingungen (2,5% und 5% O_2) resultierten in einer Zunahme der Proliferationsaktivität. Die UC-MSC passten ihren Sauerstoffverbrauch und ihren Metabolismus der jeweiligen hypoxischen Umgebung an. Bei Kultivierung unter hypoxischen Bedingungen bei 2,5% O_2 wurden im Vergleich zur Kultivierung bei 21% O_2-Gehalt 300 Gene unterschiedlich exprimiert.

Die Kultivierung der UC-MSC im Einweg Z®RP 2000 H Bioreaktor resultierte in einer 8-fachen Zunahme der Zellzahl nach 5-tägiger Kultivierung.

Abstract

The use of mesenchymal stem cells (MSC) in the field of tissue engineering and cell therapy is a promising development, since these cells can be expanded *ex vivo* to clinically relevant numbers. Moreover, these cells retain their ability to differentiate into different cell lineages after expansion. MSC, isolated from various tissues, are already used in hundreds of running clinical trials as cell suspensions or as part of tissue engineered constructs. The umbilical cord (UC) matrix represents a very promising MSC source, since cells from the UC can be easily obtained and have short doubling-times. Furthermore, their harvest is not ethically restricted and there are no medico-legal limitations in their application.

Millions of MSC are required for each treatment. In this regard, the use of optimized culturing protocols may result in better defined cell populations and reduced patient response variability. In order to optimize the yield and quality of *in vitro* expanded MSC, two different strategies were investigated in this work. First of all, the influence of oxygen concentration on the static cultivation of UC-MSC was explored. And second, a dynamic cultivation in a disposable Z®RP 2000 H bioreactor was performed.

Cultivation of UC-MSC in hypoxic conditions may help to: (I) further adapt cells to their natural *in vivo* microenvironment and (II) test the capability of MSC to survive in a nutrition-limited milieu after transplantation, as well as to function according to the local tissue requirements. Short-term (3 days) and long-term (3 month) cultivation of UC-MSC in hypoxic conditions (between 1.5% to 5% oxygen (O_2)) was performed and cell proliferation, metabolic activity, differentiational capacity and possible spontaneous malignant *in vitro* transformation of the cells were studied. Hypoxic conditions (2.5% and 5% O_2) caused an increase in the proliferational activity of the UC-MSC. MSC adapted their oxygen consumption and metabolism according to the appropriate hypoxic environment. Almost 300 genes were regulated differently under hypoxia (2.5% O_2) as compared to normoxia (21% O_2).

Dynamic cultivation in bioreactors provides active nutrient transport, better on-line control, documentation and also allows expansion of the cells without subcultivation. Cultivation of the UC-MSC in a disposable Z®RP 2000 H bioreactor resulted in an 8-fold increase of cell numbers after 5 days of cultivation.

1 Contents

List of abbreviations

αMEM	Minimal essential medium alpha
ALP	Alkaline phosphatise
ATP	adenosine triphosphate
AD	Adipose-derived
ATM	Ataxia telangiectasia mutated
b-FGF	Basic fibroblast growth factor
BM	Bone marrow
bp	Base pair
cDNA	Complementary deoxyribonucleic acid
CD	Cluster of differentiation
C-MYC	V-myc myelocytomatosis viral oncogene homolog
DKK-1	Dickkopf-1 protein
EGF	Endothelial growth factor
ESC	Embryonic stem cell
FCS	Foetal calf serum
FITC	Fluorescein isothiocyanate
GAG	Glycosaminoglycan
GMP	Good manufacturing practice
GvHD	Graft-versus-host disease
GLUT-1	Glucose transporter-1
G6PD	Glucose-6-phosphate dehydrogenase
h	Human
H-RAS	v-Ha-ras Harvey rat sarcoma viral oncogene homolog
HBEGF	Heparin-binding EGF-like growth factor
HIF	Hypoxia-inducible factors
HLA	Human leukozyte antigen
HPLC	High performance liquid chromatography
HPRT1	Hypoxanthine phosphoribosyltransferase-1
IGFBP	Insulin-like growth factor binding protein
ISCT	International Society for Cellular Therapy
LDHA	Lactate dehydrogenase A
MAPK	Mitogen-activated protein kinases

MMPs	Matrix metalloproteases
MRI	Magnetic resonance imaging
MSC	Mesenchymal stromal cell
NAD	Nicotinamide adenine dinucleotide
PBMC	Peripheral blood mononuclear cells
PGF	Plancetal growth factor
PPP	Pentose-phosphate pathway
iPSC	Induced pluripotent stem cells
PBL	Peripheral blood lymphocytes
PBS	Phosphate buffer saline
PD	Pyruvate dehydrogenase
PE	Phycoerythrin
PG	Proteoglycan
PLGA	Poly (L-lactide-co-glycolide)
PFF	Pulsating fluid flow
PTEN	Phosphatase and tensin homolog
p39	Jun proto-oncogene
p53	Tumor protein p53
r	Rabbit
ROS	Reactive oxygen species
RNS	Reactive nitrogen species
Rpm	Rotations per minute
RT-PCR	Reverse-transcriptase polymerase chain reaction
qRT-PCR	Quantitative reverse-transcriptase polymerase chain reaction
RUNX2	Runt-related transcription factor 2
SCF-R	Stem cell factor receptor
SDF	Stromal cell-derived factor
TCA	Tricarboxylic acid cycle
TE	Tissue Engineering
hTERT	Human telomerase reverse transcriptase
TGF-β	Transforming growth factor-beta
UC	Umbilical cord
UCB	Umbilical cord blood
VEGFA	Vascular endothelial growth factor A

VHL	von Hippel–Lindau tumor suppressor protein
WJ	Wharton’s jelly
3D	Three-dimensional

Keywords: Mesenchymal stem cells, mesenchymal stromal cells, umbilical cord, hypoxia, oxygen tension, long-term cultivation, bioreactor cultivation

Schlüsselwörter: Mesenchymale Stammzellen, Mesenchymale Stromazellen, Nabelschnur, Hypoxie, Bioreaktorkultivierung

2 Introduction

The field of regenerative medicine has grown dramatically over the past decades. Starting with simple surgical implants, nowadays it includes bone-marrow and organ transplants, tissue engineering and cell therapies. But independent of the technologies applied, the central focus of regenerative medicine remains human cells. The cell source can be embryonic stem cells (ESC), adult stem cells (e.g. mesenchymal stem cells (MSC)), reprogrammed differentiated cells (induced pluripotent stem cells (iPSC)) or adult tissue-specific differentiated cells. Despite of the great differential potential of ESC, ethical limitations and accompanying risks present a great challenge in the utilisation of these cells. Adult tissue-specific cells, unfortunately, cannot be easily isolated and expanded *in vitro*, a fact which is making it difficult to use these cells routinely in tissue engineering and cell therapies. Taking these considerations into account, MSC represent a valuable compromise as a cell source. On one hand, there are very little or no ethical constraints using these cells. On the other hand, despite being isolated from adult tissues, they still retain self-renewal and proliferational capacity, and they can be differentiated into various cell types in a controlled fashion. Moreover, MSC demonstrate various immunomodulatory capacities.

MSC, isolated from various tissues were intensively studied and characterized by many working groups. Umbilical cord (UC) tissue represents a very promising source of MSC, since cells from this source can be easily obtained and expanded. UC-derived MSC have a short doubling time, their harvest is not ethically restricted and there are no medico-legal limitations in their application.

The first animal and *in vitro* studies performed with MSC have given encouraging results. To obtain clinically relevant cell numbers or functionally active differentiated tissues, MSC must be intensively expanded *in vitro*. Hundreds of clinical trials recruiting MSC for the treatment of spinal cord injuries, burns, liver cirrhosis or failure, graft versus host disease,

diabetes mellitus, progressive multiple sclerosis and cardiac ischemia are carried out at the moment. For each treatment, millions of cells are required and optimal expansion methods can help in obtaining MSC of good quality within a short period of time, enhancing chances for treatment optimization and patient survival.

Methods of cell expansion include conventional static cultivation in cell culture flasks and, more recently, dynamic cultivation in bioreactors under controlled conditions. Applied techniques include special cell culture media, addition of signaling molecules, variation of physical and chemical factors, as well as application of different mechanical stimulations. Knowledge of the different aspects that affect MSC proliferation differentiation *in vivo* and *in vitro* will help researches to achieve directed cell fate without addition of supraphysiological concentrations of growth factors. Oxygen concentration appears to be a significant factor which influences MSC proliferation, stemness and differentiation capacity. *In vivo*, tissue oxygen concentrations are maintained within a narrow range (perceived as "physiological normoxia") minimizing the risk of oxidative damage from excess oxygen. Depending on the vascularization and functional state of the tissue, MSC develop in different hypoxic microenvironments, but are never exposed to the atmospheric oxygen concentrations in which traditional *in vitro* cell cultivations are performed. On the other hand, directly after transplantation in the site of injured or necrotic tissue, MSC are exposed to severe pathophysiological hypoxia, so that the ability of these cells to survive in such conditions can be a key factor in the treatment success.

Another important factor of MSC-mediated treatments are safety aspects. MSC treatment of disorders should not lead to uncontrolled cell growth and subsequent tumorigenesis *in vivo*. Thus, possible malignant transformation during *in vitro* expansion of MSC must be studied in order to exclude any possible risks for the patient.

The possibility to expand MSC under controlled conditions in bioreactors is another step towards processing these cells for clinical applications. MSC are anchorage-dependant cells which cannot be expanded as cell suspension. Several techniques were developed over the past few years including cultivation on microcarriers, on a three-dimensional matrix and on polycarbonate cell carrier slides. These techniques may allow researchers to obtain the necessary cell numbers without MSC subcultivation (reattachment and seeding), since proteases used to detach the cells not only digest the extracellular matrix, but also damage important cell surface markers and receptors. Moreover, the cultivation in bioreactors without subcultivation reduces the risk of bacterial and fungal contamination, as well as cross-

contamination with other cell lines. Continuous on-line monitoring and control of important cultivation parameters like pH, temperature, oxygen, CO_2 and metabolite concentrations will help to provide the optimal growth-conditions for the cells and assure reproducible cell expansion.

Aims of the work

The present study was designed to investigate a number of variables in order to optimize the processing of UC-MSC, in particular studying the role of hypoxia and the possibility of dynamic cell expansion. The three major aims which were defined were:

First of all, to study the effect of different oxygen concentrations on the *short-term* cultivation of UC-MSC in terms of proliferation capacities and metabolic activities, oxygen consumption rates, gene expression profile, cytokine expression on RNA and protein level, as well as MSC migratory capacity.

Secondly, to study the effect of *long-term* cultivation of UC-MSC in hypoxic conditions in terms of proliferation capacity, possible spontaneous *in vitro* transformation, surface immunophenotype marker expression and differential potential.

Thirdly, to test the possibility of expanding UC-MSC in a disposable Z®RP 2000 H bioreactor (Zellwerk, Germany) and to examine the yield and properties of UC-MSC after dynamic expansion.

3 Theoretical background

3.1 Mesenchymal stem cells: sources and capacities

Mesenchymal stem cells (MSC), often also called multipotent stromal cells are a population of cells with self-renewal and differentiation capacity [1]. Since their first isolation in 1970 from guinea pig bone marrow aspirates [2], MSC were found in almost all postnatal tissues (Table 3.1). The term "mesenchymal" reflects only the origin of these cells, but not their differentiation potential. *In vivo* these cells can participate in tissue regeneration via differentiation or paracrine rescue function. MSC isolated from different sources must fulfill the minimal criteria, established by the International Society for Cellular Therapy (ISCT). These include: (i) adherence on plastic under standard culture conditions, (ii) *in vitro* differentiation capacity towards osteogenic, chondrogenic and adipogenic lineage, and (iii) specific surface antigen expression positivity (CD73, CD90, CD105) and negativity (CD45, CD34, HLA-DR) [3].

Table 3.1: Sources and differentiational potential of mesenchymal stem cells.

Tissue	Differential potential	Reference
Bone marrow	Adipogenic, Chondrogenic, Osteogenic, Myogenic, Neuronal	[4]
Adipose tissue	Adipogenic, Chondrogenic, Osteogenic, Myogenic	[4, 5]
Cartilage	Adipogenic, Chondrogenic, Osteogenic	[6]
Dermis	Adipogenic, Chondrogenic, Osteogenic, Myogenic	[4]
Dental pulp	Adipogenic, Chondrogenic, Osteogenic, Myogenic, Neuronal	[7]
Breast milk	Adipogenic, Chondrogenic, Osteogenic	[8]
Blood	Adipogenic, Osteogenic, Osteoclastic, Fibroblastic	[4, 9]
Umbillical cord blood	Adipogenic, Chondrogenic, Osteogenic, Neuronal, Epithelial, Hepatogenic, Myogenic	[10-13]
Urine	Urothelial, Myogenic	[14]
Wharton's jelly	Adipogenic, Chondrogenic, Osteogenic, Myogenic, Neuronal, Endothelial, Hepatogenic, Pancreagenic	[15-17]
Placenta/Chorion	Chondrogenic, Osteogenic, Myogenic, Neuronal	[15]
Placenta/Amnion	Adipogenic, Chondrogenic, Osteogenic, Myogenic, Endothelial	[15]

Human MSC are of great interest for cell-based therapies, tissue engineering and tissue replacement, since these cell populations are characterized by high proliferative activity, self-renewal capacity, low immunogenicity and their potential to differentiate *in vitro* and *in vivo* toward desired lineages [18-20]. Apart from their differentiation capacity, MSC demonstrate various *in vitro* immunosuppressive effects. MSC suppress T-lymphocyte and natural killer proliferation and function [21, 22], inhibit differentiation and function of monocyte-derived dendritic cells [23] and modulate B-cell function [24].

Another very important property of MSC which has been discovered recently, is their rescue function. Either via delivery of growth factors or through cell contact-mediated events, these cells demonstrate astonishing abilities to support other cells and help them to survive and recover after damage. MSC isolated from umbilical cord, for example, can rescue photoreceptors and visual functions in a rodent model of retinal disease [25]. In a mouse model of cerebellar ataxia bone marrow-derived MSC (BM-MSC) were able to rescue Purkinje cells and improve motor function [26]. In another mouse model, BM-MSC contributed to the recovery of the kidney during acute renal failure [27]. MSC have been also shown to improve motor function and prolong survival through trophic support in Huntington's disease mouse models [28]. *In vitro* MSC can rescue neuronal cells after ischemia via trophic support [29]. MSC-conditioned medium accelerates skin wound healing [30], can protect myocardium from ischemia/reperfusion injury [31], increases axon growth [32] and promotes neuronal survival [33].

However, to fulfil such local trophic rescue functions, MSC must be capable to recognize and reach appropriate injured tissues [34]. Indeed, these cells demonstrate the unique capacity to arrive into injured brain sites independent of the way they are injected into the body – intravenously [35], intraarterial [36] or directly into the brain [37]. Damage of cells is usually accompanied by the release of specific signals. Tissue damage has been associated with local increase in mediators, like e.g. stromal cell-derived factor-1 (SDF-1), which mediates MSC-homing to injured myocardium [38]. Injury or trauma initiates the mobilization of MSC into peripheral blood [39, 40] and then these circulating MSC are suggested to arrive at the damaged tissues in a way similar to leukocyte recruitment to sites of inflammation.

In comparison to other postnatal MSC sources, umbilical cord (UC) tissue (Wharton’s jelly) represents a very promising source MSC, since cells can be easily obtained from this birth-associated tissue by initial culturing of the tissue pieces. UC-derived MSC represent a heterogeneous population of cells with varying cell size, which have shorter doubling times if

compared to BM-MSC [16, 17, 41]. Their harvest is not ethically restricted and there are no medico-legal limitations in their application [41-43]. Accumulated studies have shown that UC-MSC transplantation can promote neuroprotection and locomotion recovery in experimental models of brain disease [44, 45]. Moreover, UC-MSC can survive after transplantation, migrate in the host spinal cord after transplantation and promote functional recovery after spinal cord injury [46].

3.2 MSC applications in clinical trials

At the time of writing (February 2012) there were more than 200 global clinical trials using MSC registered at *clinicaltrials.gov* – the official website of the National Institute of Health, USA. Spinal cord injuries, burns, liver cirrhosis or failure, immune reconstitution in HIV-infected patients, diabetes mellitus, progressive multiple sclerosis, cardiac ischemia – are just a small selection of disorders where MSC are used for treatment.

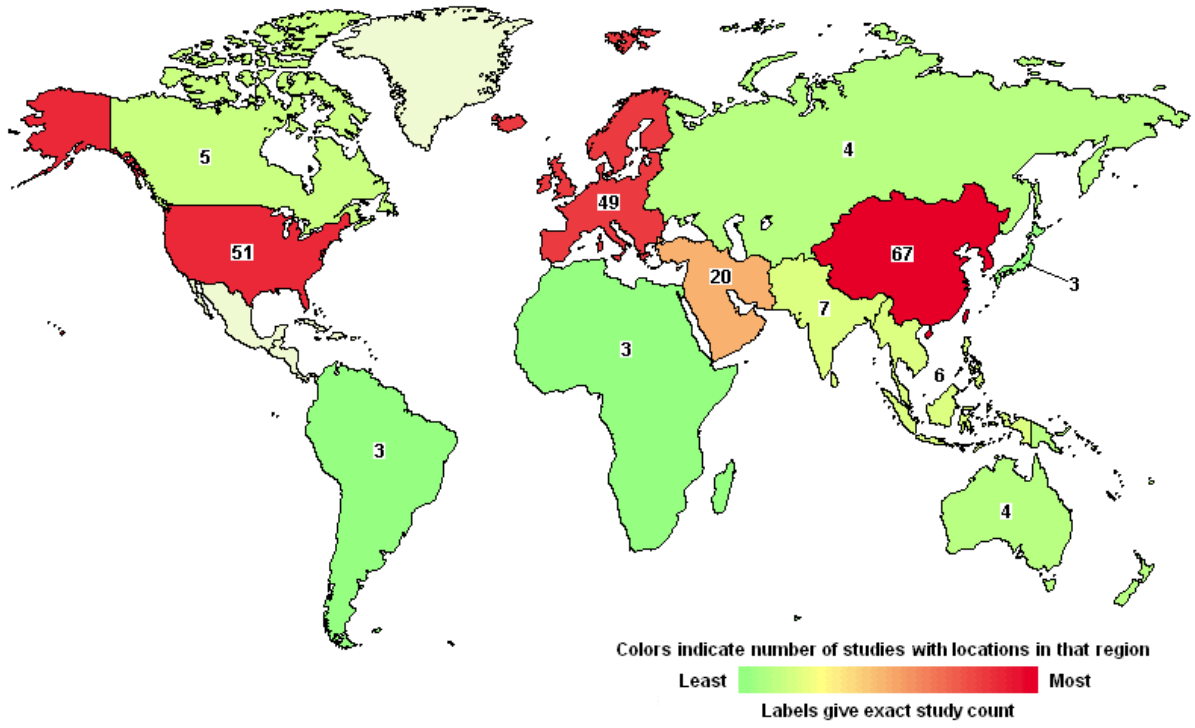

Figure 1: Map of geographical distribution of clinical trials performed with MSC. Source: *www.clinicaltrials.gov*

As it can be seen in the map (fig.1), most of the clinical trials run in the USA, Europe and China. In Europe, the highest number of clinical trials are conducted in Spain.

The biggest groups of disorders treated with MSC are multiple sclerosis (10 trials), graft versus host disease (GVHD) (18 trials), diabetes mellitus (40 trials), rheumatic diseases (18 trials), degenerative arthritis (20 trials) and ischemia (32 trials). Table 3.2 reflects the distribution of clinical trials depending on the conditions. The sum number of trials in the table greatly exceeds the number of trials reflected on the map. This happens because every single registered clinical trial can involve multiple disorders, for example in the case of diabetes, when not only diabetes itself (as a hormone related disorder), but also secondary, accompanying complications like retinal degeneration, neuropathic syndromes, autoimmune disorders and diabetic foot are treated by MSC therapy.

Table 3.2: Numbers of clinical trials using MSC for different conditions (Source: www.clinicaltrials.gov)

Condition	Example	Number of trials
Bacterial and fungal diseases	Chronic obstructive pulmonary disease	4
Behaviors and mental disorders	Autism	21
Nervous system diseases	Parkinson's disease	212
Blood and lymph conditions	Aplastic anemia	119
Cancers and other neoplasms	Leukaemia	178
Heart and blood diseases	Acute myocardial infarction	250
Digestive system diseases	Crohn's disease	131
Diseases and abnormalities at or before birth	Severe bronchopulmonary dysplasia	56
Gland and hormone related diseases	Diabetes mellitus	48
Eye diseases	Retinitis pigmentosa	38
Immune system diseases	GVHD	128
Respiratory tract (lung and bronchial) diseases	Idiopathic pulmonary fibrosis	25
Muscle, bone, and cartilage diseases	Degenerative arthritis	141

GVHD is a major cause of mortality after allogenic hematopoietic stem cell (HSC) transplantations and was historically one of the first conditions studied. Despite of the traditional treatment with corticosteroids, acute GVHD patients have a poor prognosis with less that 30% exhibiting 5-year survival [47]. Because of their immunomodulating capacities, MSC were first used for the treatment of GVHD in 2001 [48]. Several larger studies were performed later, as reviewed in 2011 by Lin and Hogan [49]. In the majority of studies it was shown that most GVHD patients responded to BM-MSC injection. However, larger

randomized trials must be performed to clarify the risks of disease relapse and infection. Moreover, standardization and optimization of the MSC manufacturing process may play an important role in the outcome and also in the better understanding of the efficiency of treatments.

Application of MSC for acute myocardial infarction is another promising development in cell-based therapy. Several clinical studies demonstrated the beneficial role and safety of MSC injection in treatment of postinfarcted tissues [50, 51]. Infusion of MSC after acute myocardial infarction was associated with a significantly lower mortality during further follow-up [52]. Intracardiac transplantation of MSC led to coronary revascularization, improvement of ventricular geometry and function, as well as reduced myocardial scar proportion and heart failure symptoms [53].

3.3 MSC cell numbers and introduction methods used in clinical trials

As mentioned above, the large scale production of MSC and the mode of injection play an important role in treatment outcome. Different cell numbers are needed to treat diverse disorders, but all cells injected must be expanded *in vitro*. Several examples of cell numbers, required for selected clinical trials are shown in table 3.3. As it can be seen, millions of cells (range $0.6x10^6$ - $2x10^6$ per kilogram of body weight) must be available for one injection. Moreover, some treatments consist of several injections, which increases even further the number of MSC required.

Table 3.3: MSC cell number and injection methods in selected clinical trials (source: *www.clinicaltrials.gov*)

Disorder	**Required number of MSC**	**Method of injection**
Diabetic foot	$5x10^7$ per limb	Intramuscular
Ulcerative colitis	$2x10^7$, later $1x10^7$	Intravenous, later to mesenteric artery
Liver cirrhosis	$1x10^6$/kg	Intravenous
Multiple sclerosis	$1x10^6$/kg	Intravenous
GVHD	$1x10^6$/kg	Intravenous
Spinal cord injury	$1x10^6$/kg	Intravenous
Parkinson's disease	$0.6x10^6$/kg	Intravenous
Myocardial ischemia	$60x10^6$	Trans-endocardial intramyocardial injections

The dose and frequency of MSC injections for reaching maximal clinical efficacy are still intensively studied, since it is not clear what happens to most of the cells after injection. In the case of autologous transplantation, extensive *in vitro* cell expansion is required if more than one injection should be performed. In the case of allogenic MSC transplantation, it is still unclear if MSC from the same donor should be used for repeated injections, since they may induce an immune response even if none such occurred during the first injection. In this regard, it should be noted that expanded MSC from one donor can be frozen, banked and used later when required. It has been also discussed which factor has a higher impact on the treatment efficiency – the quality of injected MSC or the recipient state (biological/physiological parameters). In any case, the use of optimized culturing protocols may result in better defined cell populations and reduced patient response variability.

3.4 Safety aspects during treatment with MSC

Despite of the encouraging results of *in vitro* experiments, animal models and clinical trials, the question of safety of MSC for clinical use is still a point of discussion. It is essential to understand the advantages and disadvantages of the use of MSC in patients with regard to tumorigenesis. Dramatic titles of scientific review-articles like “Mesenchymal stem cells: angels or demons?” [54], “Concise review: mesenchymal tumors: when stem cells go mad” [55], “Concise review: adult multipotent stromal cells and cancer: risk or benefit?”[56] reflect strongly the controversial opinions and findings regarding MSC treatment safety. There are three major ways which can lead to MSC-associated tumorigenesis: (1) *in vitro* spontaneous transformation of MSC due to their chromosomal instability during long-term expansion cultures; (2) *in vivo* tumor enhancing property of MSC via their ability to suppress the immune system and (3) direct tumor growth support *in vivo* by positive chemotaxis and release of growth factors (e.g. for tumor vascularization).

3.4.1 Spontaneous transformation of MSC

In 2009 a working group from Israel published a case report about a 13-year-old boy with ataxia telangiectasia (a neurogenerative disease), who developed a brain tumor after stem cell treatment [57]. The boy received three fetal stem cell transplants in Russia between 2001 and 2004 and had a MRI in 2005 because of recurrent headaches. Tumors were found in the brain and spinal cord. After tumor resection from the spinal cord (identified as a glioneuronal tumor), DNA analysis of the tumor cells revealed their origin as coming from the donor cells. These cells expressed XX and XY phenotype, two normal copies of the ATM gene and HLA typing showing that the tumor contained cells from at least two donors. Although the exact type of injected cells was not clear (ESC or MSC), this report raised intensive discussion if MSC can be safely used in patients.

Again in the year 2009, a scientific group from Norway published alarming results of frequent spontaneous malignant transformation of human BM-MSC *in vitro* [58], although another working group did not reveal any transformation of these cells two years earlier [59]. Rubio and colleagues also reported spontaneous transformation of AD-MSC *in vitro*, indicating the importance of biosafety studies of MSC biology to efficiently exploit their full clinical therapeutic potential [60]. In the year 2010, however, after publication of the editorial letter “Identity crises” in Nature [61], where the misidentification of a tremendous amount of cell lines used in laboratories around the word was discussed, numerous working groups decided to carefully identify the origin of the cells they are working with. The results of DNA fingerprint analysis revealed that the above reported malignant transformation of BM-MSC was reflecting cross-contamination with the human HT1080 fibrosarcoma, U251 and U373 glioma and U-2 OS osteosarcoma cell lines [62] in two independent laboratories. The working group that reported spontaneous transformation of AD-MSC also identified cross-contamination of MSC with a HT1080 cell line [63]. Although these findings provide support for future MSC applications in patients, they also demonstrate the importance of safety regulations during *in vitro* expansion of these cells, in particular with regard to cross-contaminations.

There are several factors that can lead to *in vitro* transformation. Although life-span limiting antitumor pathways protect MSC from malignant transformation, massive expansion of MSC can lead to mutations, with some of them targeted to cancer-relevant genes [64]. It was demonstrated that spontaneous transformation of neuronal stem cells to cancer cells is

driven by genomic instability [65]. With the help of karyotype analysis, accumulated chromosomal abnormalities were revealed in transformed BM-MSC [66]. The major reasons for MSC malignant transformation include the introduction of oncogenes, as well as change in their activity, due to mutations or transduction with telomerase reverse transcriptase activity (hTERT). All these factors can lead to loss of contact inhibition, anchorage independence and tumor formation *in vivo* [56, 67]. H-RAS was shown to be an important tumor suppressor, since the lost of its activity leads to transformation of MSC [68]. This means that besides cross-contamination controls, expanded cells should be studied for the presence or absence of certain oncogene expression profiles.

3.4.2 Interactions between MSC and tumors

MSC express numerous growth factors and exhibit tropism for sites of tissue damage. Tumor microenvironment was shown to contain the same proinflammatory mediators as injured tissue, attracting MSC [69]. In this way, tumors can be described as "wounds that never heal", which continuously produce a variety of chemokines and cytokines, recruiting corresponding cells, including MSC [70]. Numerous *in vitro* and *in vivo* studies demonstrated tumor-directed migration and incorporation of MSC, including homing into a wide range of cancer cell lines, like e.g. lung cancer, breast cancer, malignant glioma, pancreatic cancer and colon carcinoma [71-76]. Although the tropism of MSC for the tumor microenvironment is obvious, the exact mechanisms of action, fate and function inside the tumors, as well as the influence on tumor progression is still unclear and often the data is even paradoxical.

On one hand, the growth of solid tumors requires supply of oxygen and nutrients to the tumor cells, and MSC can provide necessary growth factors (e.g. VEGF) which will support tumor vascularization and growth [77]. On the other hand, MSC can trigger apoptosis of tumor cells or inhibit tumor growth. It was demonstrated that MSC can contribute to tumor protection, drug resistance, growth and metastasis. MSC were shown to protect breast cancer cells and increase breast cancer tumor growth by immune protection of tumor cells [74]. The working group of Li demonstrated dual effects of MSC on tumor cells *in vitro* and *in vivo*. They showed that MSC suppress proliferation and cause apoptosis of lung cancer cells *in vitro*, while when injected *in vivo*, MSC enhanced tumor formation and growth [78]. Another working group demonstrated that MSC can prevent apoptosis of acute myeloid leukemia cells by up-regulation of antiapoptotic proteins [79]. Another effect of MSC on tumors is their

participation in the drug resistance of cancer cells [54, 80, 81]. Furthermore, being possibly advantageous for patients with immune disorders, immunomodulating properties of MSC can be deleterious in those patients who harbor a malignant tumor, since anti-cancer mechanisms can be altered by MSC injection, causing tumor growth. This "double-edged sword" must lead to more careful patient selection and in the case of cancer patients, the benefits of treatment should outweigh the risks that these cells could bring to the patient [54].

While some working groups report enhancing effects of MSC on tumor growth, others show a negative influence of MSC on tumorigenesis. Zhu and colleagues demonstrated inhibitory effect of MSC on proliferation of myelogenous leukemia cells via production of DKK-1 (dickkopf-1) protein [82]. MSC were also shown to completely inhibit outgrowth of colon carcinoma cells in vivo [83]. BM-MSC decrease Kaposi sarcoma tumor size via increased inflammatory infiltration [84], they decrease metastasis and tumor growth in Lewis lung carcinoma and melanoma cells [85], they decrease tumor burden and increase survival in non-Hodgkin lymphoma [86, 87]. AD-MSC decrease tumor size *in vivo* and provoke cell death *in vitro* in pancreatic cancer via G1 cell cycle arrest [88]. UCB-MSC decrease tumor size in gliomas via cell-cell contact and up-regulation of PTEN [89-91]. Moreover, recently published studies demonstrated that UC-MSC completely abolished breast carcinomas with no evidence of metastasis or recurrence in rats [92].

Although no simple paradigm can account for the conflicting findings in the studies of MSC, no evidence of tumor formation has been reported in over 1000 patients treated with MSC for a variety of indications under controlled conditions [87]. Moreover, MSC engineered to express tumor suicide genes can be a very useful tool for anti-cancer therapies because of their tumor-tropism and migratory potentials. Gene modified MSC can synthesize anti-tumoral molecules, usually derived from immune effectors like e.g. natural killer cells, making MSC "mesenkillers" [93].

Taken together, these data show the importance of strict control and safety measures in MSC production. To minimize the risk of malignant transformation, MSC must be handled according to standardized protocols and expanded cells must be checked for possible cross-contamination and expression/mutations of oncogenes. Moreover, careful selection of patients can help avoid the possible risk of tumor progression.

3.5 Strategies in MSC expansion

The effective and economic expansion of MSC plays an important role for their application in tissue engineering and cell-based therapies. There are many approaches to expand MSC to obtain clinically relevant cell numbers.

3.5.1 Conventional static cultivation

Conventional static cultivation involves flat, two-dimensional cell cultures in plastic flasks. Because of the limited available surface area (maximum up to 225 cm^2 per flask), only moderate amounts of cells can be produced. Therefore, if production is to be scaled-up, the number of units (T flasks) has to be increased, making the cultivation of cells time-consuming and prone to the danger of contamination. Furthermore, human errors may occur, especially when high cell numbers are needed and cells from one donor must be cultivated in dozens of flasks.

On the next level, cell factories, represent a special type of cell culture flask where 5, 10 or more chambers are arranged in multi-layer stacks. This technique decreases the risk of contamination, is easier to handle and provides a large growth surface in limited-space areas. MSC expansion in cell culture flasks, however, still represents a static method and it does not provide any online monitoring on cell growth. It also makes it difficult to observe the cells under the microscope, because of the cell factory height. During conventional MSC expansion, cells are usually subcultivated over several passages by detachment with the help of various proteases. Such a treatment, however, damages cells, since proteases not only digest extracellular matrix proteins, but also destroy important cell surface receptors and markers, changing the biological properties of MSC in the process.

3.5.2 Cultivation on microcarriers (static and dynamic)

Another method is the cultivation of MSC on microcarriers. The “microcarrier” culture system represents the cultivation of cells (anchorage-dependent or anchorage-proffered) on small solid particles (microspheres) suspended in a growth medium. The term

"microcarrier" was introduced in 1967 by van Wezel [94]. First introduced for virus production [95] in primary adherent cells, this expansion method rapidly showed good results in terms of cell density. Later, along with the development of recombinant DNA-technology and cell transfection methods for protein production, cultivation on microcarriers got a new impulse.

Diverse types of microcarriers were developed over the next years [96]. In general, microcarriers can be divided in two main groups: smooth and macroporous microcarriers. In the first case, cells grow on the surface of the particles without penetration into the core. In the case of macroporous particles, cells are trapped and grow inside of the microcarrier. Macroporous particles can be used for the cultivation of both, suspension and anchorage-dependent cells. Moreover, they support high cell numbers and avoid shear-stress. There are several types of commercially available macroporous microcarriers made of glass (Schott, USA), collagen/gelatin (Percell Biolytica), cellulose (GE Healthcare) and polyethylene (Amersham Biosciences). Smooth microcarriers have the advantage of a better microscopic control of cell growth, easier cell sampling and can be used in stirred-tank bioreactors, developed for suspension cell culture and providing good mass-transfer characteristics, ease of monitoring (better control of pH, pO_2, pCO_2) and scale-up possibilities. Smooth microcarriers are available in different materials: e.g. dextran (GE Healthcare), gelatin (MP Biomedicals,) or polystyrene (Nunc). Besides commercially available microcarriers, a multitude of other microcarriers were developed in laboratories all over the world [96].

In the past several years different research groups have used microcarrier-based expansion of MSC in glass spinner-flasks [97-99]. Frauenschuh and his group, as well as Schop with colleagues tested cytodex 1 (dextran) and cytodex3 (gelatin coated dextran, GE) for BM-MSC expansion [97, 99]. It was shown that cell type, as well as microcarrier type and the selected medium/serum concentration all play an important role in cell adhesion time and expansion efficiency. Sart with colleagues examined the influence of the MSC source, taking murine MSC from the bone marrow and ear conch for cultivation under the same cultivation conditions [98]. Despite promising results, an important issue to be considered with the cultivation on microcarriers, is that MSC cultivated on microcarriers or free-floating 3D scaffolds can be exposed to lower gravity (simulated microgravity environment), which may affect their differentiation capacity [100, 101].

3.5.3 Dynamic cultivation in bioreactors

The expansion of MSC in bioreactors is a promising development for the future application of MSC in cell-based therapies and tissue engineering. The cultivation in bioreactors with integrated sensors provides important information about cell growth and nutrient consumption. It is possible to control and document numerous cultivation parameters like nutrient, gas and metabolite concentrations, pH, temperature, pressure, shear forces and cell mass growth. Moreover, automated controlling systems help maintain constant nutrition and gas supply, and withdraw toxic metabolites during all periods of cultivation. Furthermore, most of the newly developed bioreactors are disposable, which reduces the risk of cross-contamination and provides a "one patient-one bioreactor" approach. There are numerous types of bioreactors used to expand adherent anchorage-dependent cells (for full review see [102]). Wave-bioreactors can be used to expand MSC on the above mentioned microcarriers in one-way cell culture bags. For example, GE Healthcare (Little Chalfont, UK) produces a wide spectrum of WAVE-bioreactors (fig. 2A), starting from the low-scale systems (System 2/10 with 0.1 - 5 liter capacity) up to large-scale reactors (System500/1000 with 100 - 500 liter capacity). Recently, GE Healthcare together with Biosciences AB (Uppsala, Sweden), registered a patent (US 2011/0070648 A1) for expansion of MSC to therapeutic amounts on Cytodex microcarriers in plastic bag bioreactors.

The PluriX™ 3D bioreactor, developed by Pluristem (Haifa, Israel) represents a bioreactor, where adherent cells grow on the 3D fibracel polyester matrix (fig. 2B). On September 14, 2010 Pluristem reported that data from its "first-in-man" clinical trials, which began in 2009, indicate that its placenta-derived cell therapy appears to be safe and improves objective and subjective measurements in patients with critical limb ischemia, the end-stage of peripheral artery disease. Several clinical trials are running or have already been performed with placenta-derived pluripotent stromal cells expanded in the PluriX™ 3D bioreactor. Pluristem used a 1-liter bioreactor for phase 1 trials and a 5-liter bioreactor for phase 2 or 3 trials. According to the manufacturer, newly developed 75 liter bioreactors can produce 1000 doses of cells with 300 million cells per dose.

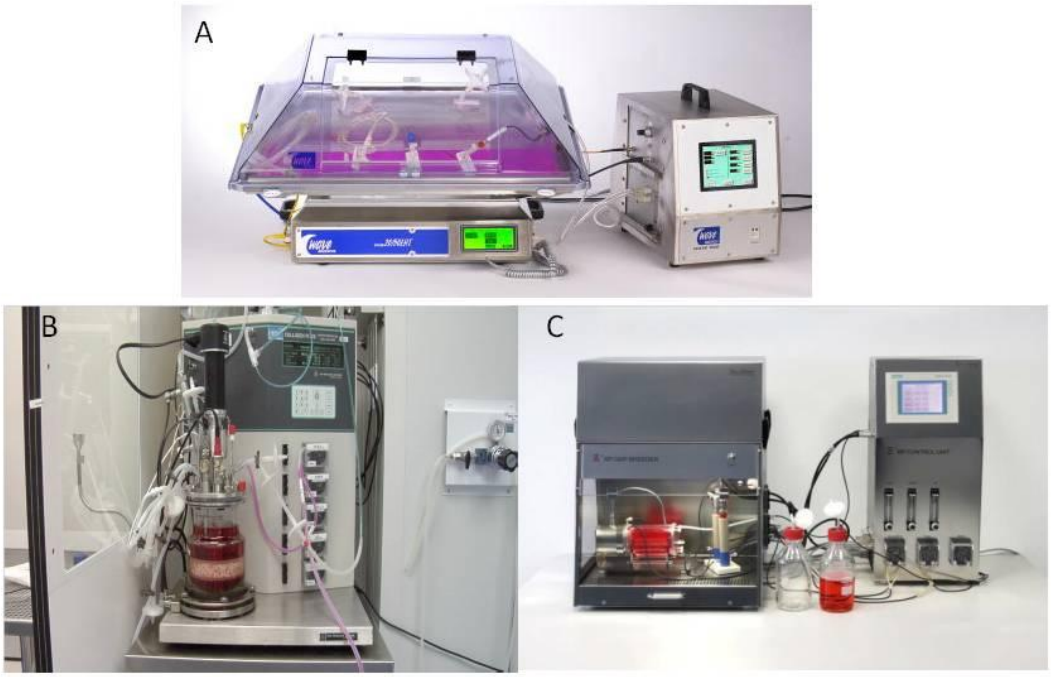

Figure 2: Selected bioreactors used for MSC expansion; A: the WAVE Bioreactor with a disposable cell culture bag and control unit (GE Healthcare), B: PluriX™ 3D Bioreactor (Pluristem), C: Z®RP 2000 H bioreactor and GMP-breeder (Zellwerk)

A new approach in the expansion of adherent MSC is offered by Zellwerk GmbH (Berlin, Germany), where cells are cultivated on rotating stalked polycarbonate cell carrier slides (fig. 2C). The Z®RP 2000 H bioreactor is connected to the pH and pO_2 sensors, which are integrated into the tubing system. Besides of cell culture medium mixing via rotation, medium is also constantly circulating via tubing system, where feed- and waste-flasks are connected, making it possible to cultivate cells in fed-batch or perfusion modus. Disposable Z®RP 2000 H bioreactor provides a surface of 2000 cm^2 for cell growth, while Z®RP 8000 H offers 8000 cm^2. Cultivation of cells is performed in a GMP-breeder under full automated control with documentation. According to the manufacturer's data, MSC in a Z®RP 8000 H system can be expanded in 9 days to 400 million cells without subcultivation.

3.6 Influence of oxygen concentration on the cultivation of MSC

Many different *in vitro* cell culture parameters influence the proliferation and differentiation capacities of MSC. Cell culture media composition, type of serum, addition of different cytokines and supplements – all these factors have an effect on MSC cell fate and play a critical role in successful cell expansion. Another crucial cell cultivation parameter is the oxygen tension. The amount of available oxygen led to the development of different forms of life on our planet and its concentration in the air is a result of the balance between its consumption by one organism and its production by another. In aerobic organisms oxygen is an essential, but also toxic molecule, which leads to the formation of reactive oxygen species (ROS). Even aerobic organisms could not survive without defense mechanisms against oxidative stress and damage. Multicellular organisms developed complex mechanisms of oxygen sensing, delivery and homeostasis.

3.6.1 Hypoxia-inducible factors

The cellular response to variations in oxygen concentration is mediated by changes in gene expression. Alterations of gene expression are particularly important with regard to hypoxia-inducible factors (HIF), a family of transcription factors which bind to specific DNA sequences (hypoxia regulated elements, 5'-TACGTGCT-3') in promoter or enhancer regions of the target gene [103]. The HIF family consists of HIF-1α, HIF-1β, HIF-2α, HIF-2β, HIF-3α and HIF-3β proteins. HIF-1 protein, the main regulator of oxygen homeostasis, is found to be expressed in all animal tissues. HIF-1 is a heterodimeric transcription factor that is composed of a constitutively expressed HIF-1β subunit and an oxygen-regulated HIF-1α subunit [104]. HIF-1α is constantly translated, but rapidly degraded in cells with normal (depending on physiological requirements) oxygen concentration. This degradation is triggered by the hydroxylation of two proline residues in the highly conserved oxygen-dependent degradation domain. The hydroxylation is catalyzed by proline hydroxylase and leads to the binding of the von Hippel–Lindau tumor suppressor protein (VHL), the recognition component of E3 ubiquitine ligase [103, 104]. After ubiquitiniation, HIF-1α is targeted into the 26S proteosomes for consequent degradation. If the oxygen level decreases

below a certain threshold, proline hydroxylation stops and HIF-1α becomes stabilized. Afterwards, it enters the cell nucleus, binds to a constitutively expressed HIF-1β, and then attaches to hypoxia regulated elements in the target gene's enhancer. Hundreds of genes were found to be regulated by HIF-1[104, 105]. HIF-1, in turn is also regulated by various factors including oxygen concentration, pH, growth factors and hormones (fig. 3).

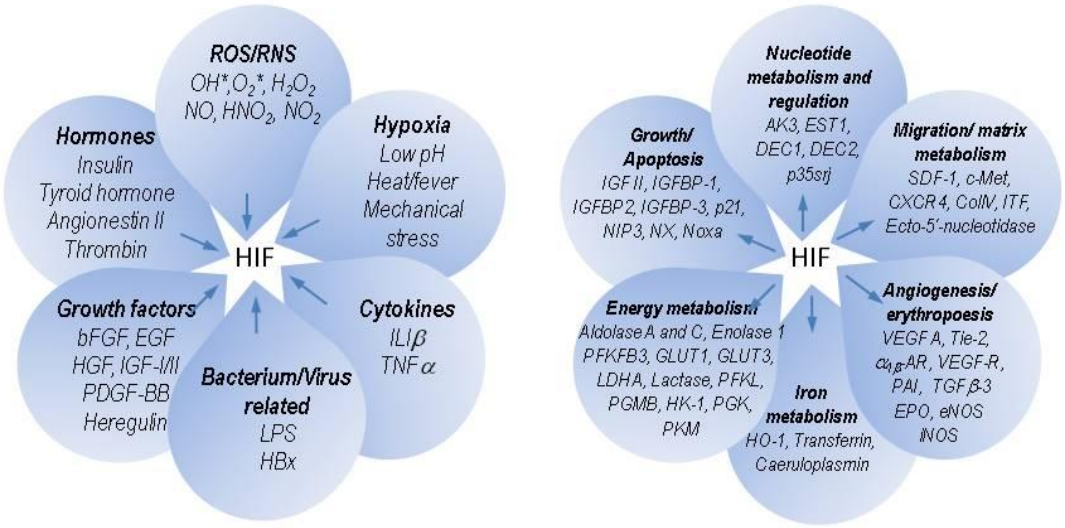

Figure 3: Factors inducing HIF- activity (A) and selected HIF target genes (B); adopted from [105]

It was shown that HIF-1α is required for mesenchymal cell survival during embryonic development and *HIF-1α* knockout leads to death of mice embryos around midgestation, resulting in cardiovascular malformations and open neural tube defects [106, 107]. In naturally hypoxic tissues (e.g. cartilage), HIF-1 is essential for normal development, homeostasis and functioning. In life-threatening states such as stroke, cardiovascular diseases and injuries HIF-1 plays a crucial role in tissue survival and regeneration [108].

3.6.2 Role of oxygen in cell metabolism

In animal cells there are two major glucose metabolic pathways which lead to energy production in form of adenosine triphosphate (ATP): anaerobic glycolysis and oxidative phosphorylation. The largest part of oxygen consumption by the cells is the use of oxygen as a terminal electron acceptor in oxidative phosphorylation. Oxidative phosphorylation takes

place in cell mitochondria and results in 36 molecules of ATP per one molecule of glucose, while glycolysis in the cytoplasm produces only 2 ATP per one glucose molecule. Figure 4 shows schematically the mechanism of metabolic shift from oxidative phosphorylation (A) to glycolysis (B). After transport into the cell, glucose is converted into glucose-6-phosphate, then via several steps into two molecules of pyruvate. Pyruvate, in turn, is the substrate for two enzymes – lactate dehydrogenase (LDH) which turns it into lactate and pyruvate dehydrogenase (PD), converting it into acetyl-CoA, which enters the Krebs cycle (tricarboxylic acid cycle (TCA)) in the mitochondria. Conversion of glucose into pyruvate and further into lactate is called glycolysis and does not require oxygen. If oxygen is present, conversion of acetyl-CoA in the Krebs cycle leads to its oxidation to CO_2 with simultaneous reduction of NAD to NADH, which is used by the electron transport chain in the production of ATPs via oxidative phosphorylation. If oxygen concentration in the cell drops, PD is immediately phosphorylated by pyruvate dehydrogenase kinase (PDK) (fig. 4B), which inhibits the utilization of pyruvate as a fuel for the Krebs cycle and regulates mitochondrial oxygen consumption, keeping intracellular oxygen concentration constant [109]. In this case, all pyruvate is converted into lactate.

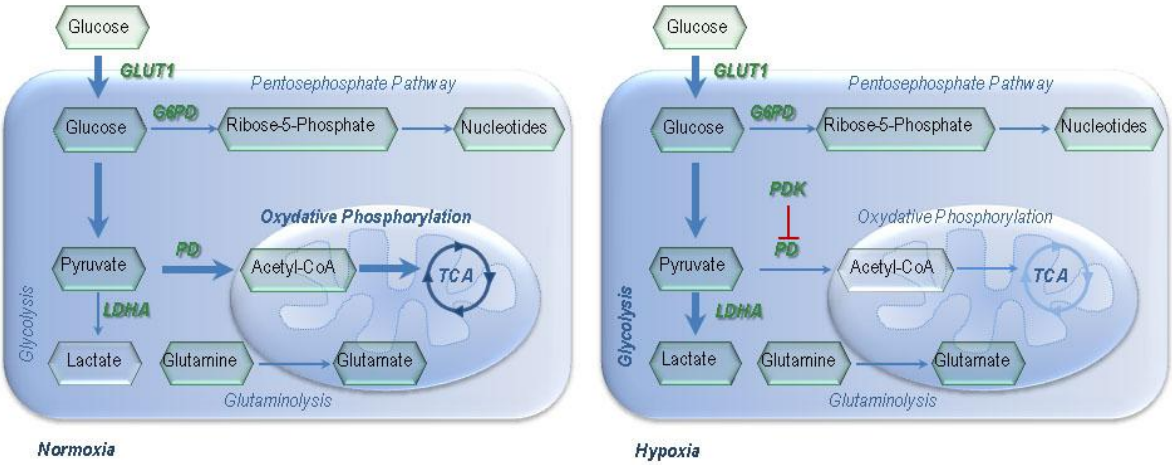

Figure 4: Schematic representation of glucose metabolic shift in differentiated cells. In the case of normoxia (A) pyruvate is converted into acetyl-CoA and enters TCA cycle in mitochondria, where oxidative phosphorylation takes place. In the absence/deficit of oxygen (B) all pyruvate is converted into lactate by lactate dehydrogenase A

Cancer cells tend to ferment glucose into lactate even in the presence of sufficient oxygen to support mitochondrial oxidative phosphorylation. This phenomenon was first

discovered by Otto Warburg, who noticed already in the year 1924 that glucose metabolism of cancer cells is distinct from that of normal mammalian cells [110]. The researcher postulated that these changes in cell metabolism may cause cancer and the metabolic shift itself was named the "Warburg effect". Nowadays, although the Warburg effect was confirmed by many research groups, it is still not clear if these metabolic changes are the cause of malignant transformation or a consequence of it, as a reaction of the cells on the hypoxic tumor microenvironment [111]. Moreover, the Warburg effect was also described in highly-proliferative adult and embryonic stem cells [112, 113]. There are several explanations why proliferating cells use energetically disadvantaged pathways. First, proliferating mammalian cells are exposed to a continuous supply of glucose and other nutrients in circulating blood and the ATP level is easily maintained by a high rate of glucose conversion. Second, the utilization of O_2 as a substrate for energy production is not without risks. A fraction of electrons escape the respiratory chain and generate reactive oxygen species, which can oxidize lipids, proteins and DNA, and may result in cellular dysfunction or death [114]. Avoiding the involvement of mitochondria decreases the risk of ROS production and possible damage to lipids, proteins and DNA. And last but not least, proliferating cells have important metabolic requirements that extend beyond ATP [111].

Besides ATP production, glucose is involved in NADPH and nucleotide synthesis via the pentose-phosphate pathway (PPP). PPP takes place in the cytosol and along with glycolysis is a main glucose metabolic pathway. In general, there are three major outcomes of PPP: production of ribose-5-phosphate for nucleotide synthesis, generation of NADPH for further reductive reactions like e.g. fatty acid synthesis and production of erythrose-4-phosphate for subsequent aromatic amino acid synthesis. NADPH is used by the cells to prevent the oxidative stress by reduction of glutathione, a major antioxidant, which prevents damage to important cellular components caused by ROS such as free radicals. PPP activity was shown to be a sufficient indicator to indirectly determine changes of intacellular levels of ROS in response to increasing oxygen concentrations [115]. At low oxygen concentrations the activity of PPP was lower when compared to hyperoxia [115]. Although most of the enzymes involved in glucose metabolism are controlled by HIF-1, the data about changes in PPP under hypoxia are controversial. Some authors suggest that under hypoxia glucose flux through PPP is inhibited by hypoxia-induced depletion of glucose-6-phosphate, the substrate for the rate-limiting enzyme of the PPP, which then promotes accumulation of NADP+ and depletion of NADPH [116]. Another study showed that in e.g. cancer cells, glucose flux through PPP

under hypoxia is increased in order to enhance nucleotide synthesis for fast-dividing cells [117].

An alternative major energy source and metabolic precursor is glutamine, which is either deamidated to enter the TCA cycle or directly used for protein synthesis. The influence of oxygen concentration on glutaminolysis (which results in ammonia and glutamate) is also debated. It was reported that glutamine consumption by BM-MSC is increased under hypoxia [112]. On the other hand, cultivation of embryonic stem cells (ESC) under hypoxia does not have an impact on glutamine consumption [118]. Interestingly, it was demonstrated that in hyperoxia, glutamine protects cellular structures, especially mitochondria, from damage due to oxygen toxicity [119].

3.6.3 Oxygen concentrations *in vivo*

There are only few cell types in the human organism which are exposed to atmospheric oxygen concentration: e.g. keratinocytes and melanocytes in the epidermis, pneumocytes and macrophages in lung alveoli, and cells of the corneal epithelium. The remainder of the cells divide, grow and function under much lower oxygen tensions (fig. 5). The partial pressure of oxygen in various organs and tissues is measured in mmHg. For better comparison, these values are presented in this work as volumetric oxygen concentrations (figure 5 and see also chapter 8.2). Depending on the consumption rate and tissue vascularization, oxygen tensions as low as 6% - 7% (48 mmHg - 54.9 mmHg) were measured in bone marrow and between 10% and 15% in adipose tissue (AT) [120-122]. Measured oxygen tension in avascularized articular cartilage ranges from 7% (53 mmHg) on the surface to less than 1% (7.6 mmHg) in the deep zone [123, 124]. In lung parenchyma and circulation, the oxygen level exceeds only16% and in the retina – its maximum is 5% [125, 126].

The brain is one of the largest oxygen consumers in the body, accounting for 20% of total oxygen consumption. Despite a highly developed cerebral circulation system, the oxygen tension in different parts of the brain varies between 2% and 5% (23.8 mmHg at 27 mm below the dura to 33 mmHg at 12 mm below the dura) [127, 128].

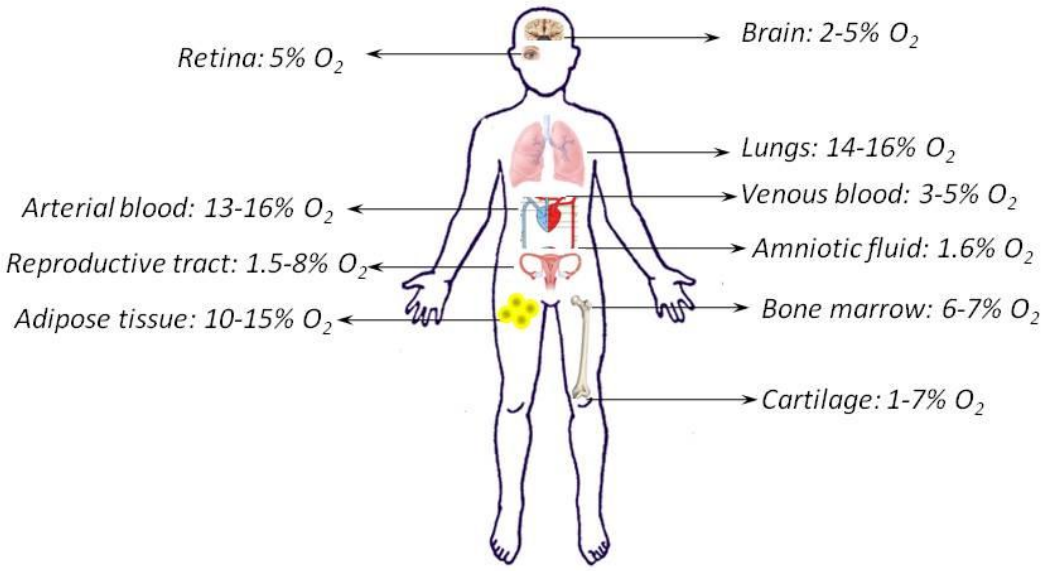

Figure 5: *In vivo* oxygen concentrations in different organs

Oxygen tension within the mammalian female reproductive tract was shown to be low, about 1.5 % to 8 % (11 mmHg – 55 mmHg) which lasts throughout the fetal development [129, 130]. During late gestation, even after placental gas exchange is established, oxygen concentrations in the umbilical artery, vein, and the amniotic fluid are still constrained below maternal venous levels (fetal vein – 4% (29.2 mmHg), fetal artery – 2.3% (18 mmHg), amniotic fluid – 1.6% (12.1 mmHg)) [131-133]. The umbilical cord with its blood vessels – two arteries and one vein - is lacking capillaries or lymphatic channels, thus stimulating UC-MSC cells to develop in a hypoxic atmosphere.

Together, these data indicate that low oxygen tensions (1% - 15%) present a so-called "physiological hypoxia", which is the steady state of physiological oxygenation or "*in situ* normoxia". This means that MSC, independent of their origin, develop in oxygen concentrations much lower than those used in standard cell culture techniques [134]. Moreover, efficient respiratory chain function occurs only within a narrow range of O_2 concentrations, which is dissimilar for cells of different origins [114].

3.6.4 Influence of oxygen concentration on MSC

There is increasing interest in studies of the influence of oxygen concentration on survival, proliferation and differentiation of MSC. *In vitro*, hypoxic conditions are usually modeled in cell incubators, where required oxygen concentrations are established by substitution of ambient air with nitrogen (in volumetric %). Although published results are sometimes contradictory, most of the studies demonstrate increased proliferation of MSC under hypoxia (table 3.6). The effect of hypoxia on MSC is certainly dependent on several parameters, including the degree of experimental hypoxia, the type of MSC and the presence or absence of cell culture media supplements. For example, Zhu and coauthors demonstrated that hypoxia (3% O_2) along with serum deprivation induced rat BM-MSC apoptosis [135]. On the other hand, cultivation of human BM-MSC in 2% O_2 without serum deprivation resulted in increased proliferation and higher expression of stem cell genes when compared to normoxic conditions [136, 137]. This was supported by another study, where human BM-MSC were also shown to proliferate faster in 2% oxygen [112]. Long-term cultivation of UC-MSC under 2% oxygen concentration increased proliferation, while maintaining the immunophenotypic characteristics of these cells [138, 139]. AD-MSC cultivated in 2% oxygen demonstrated increased proliferation along with decreased chondrogenesis [140]. In addition, another study has shown that low oxygen tension can be preferential for the cultivation of MSC, where rat BM-MSC were cultivated in 5% oxygen resulting in increased proliferation and osteogenic differentiation [141].

Table 3.6 : Influence of oxygen concentration on proliferation and differentiation capacity of MSC

Oxygen concentration	Type of cells	Observed effect	Reference
≤ 1%	rBM-MSC	Increased proliferation, induced ALP activity and production of Col I/III	[142]
≤ 1%	hBM-MSC	Down-regulation of several osteoblastic markers	[143]
≤ 1%	hBM-MSC	Decreased osteogenesis via suppression of RUNX2	[144]
1%	hBM-MSC	Decreased proliferation and differentiation	[145]

2%	hBM-MSC	Prolonged stemness, increased proliferation	[146]
2%	hBM-MSC	Increased proliferation and metabolism	[112]
2%	hWJ-MSC	Increased proliferation and increased expression of mesodermal and endothelial markers	[147]
2%	hAD-MSC	Increased proliferation, decreased chondrogenesis and osteogenesis	[140]
2%	hUC-MSC	Increased proliferation, stable karyotype	[139]
3%	hBM-MSC	Decreased osteogenesis	[148]
3%	ratBM-MSC	In combination with serum deprivation -apoptosis	[135]
5%	ratBM-MSC	Increased proliferation, ALP activity and osteogenesis *in vivo* and *in vitro*	[141]
5%	hAD-MSC	Increased proliferation, collagen II synthesis and chondrogenesis	[149]
5%	hAD-MSC	Increased chondrogenesis, decreased osteogenesis	[150]

Hirao and colleagues showed that a hypoxic microenvironment promotes a chondrogenic rather than an osteogenic phenotype [151]. Other researchers showed similar results, concluding that hypoxic conditions promote the chondrogenesis of MSC [152-155]. Direct comparison of dynamic compression and low oxygen tension revealed that hypoxia is a more potent pro-chondrogenic stimulus than mechanical stimulation [156]. Moreover, expansion of BM-MSC under low oxygen tension (5%) enhanced their subsequent osteogenesis [155]. Cultivation under low oxygen concentrations had the same effect on AD-MSC, namely stronger chondrogenesis and weaker osteogenesis [150]. Merceron and colleagues concluded that tissue engineered constructs for bone repair should contain a capillary network or angiogenic factors along with sufficient porosity of scaffolds. Annabi and coauthors demonstrated that hypoxia (1% O_2) increased the migratory potential and a capillary-like structure formation by BM-MSC [157].

Besides increased proliferation, cultivation under hypoxia plays an important role in subsequent MSC survival after transplantation. Accordingly, Rosova and colleagues showed that preconditioning of MSC under hypoxia prior to transplantation resulted in increased motility and improved tissue regenerative potential [158]. In the hind limb ischemia injury model, they demonstrated that mice which received hypoxic preconditioned MSC recovered faster than those in a control group, who received normoxic MSC. Another working group

demonstrated that hypoxic preconditioning of MSC could overcome the hypoxia-related inhibition of osteogenic differentiation [159]. Along these lines, Peterson and colleagues found better survival and enhanced function of rat BM-MSC after hypoxic preconditioning [160].

Taken together, these data demonstrate that cultivation of MSC in hypoxic, yet physiological oxygen concentrations may be beneficial for the cells and also helps to obtain higher cell yields within a shorter time frame for expansion. Cultivation under hypoxia is also important in subsequent cell survival after transplantation in avascularized injured tissues.

4 Experimental part

4.1 Static cultivation

4.1.1 Online measurements of oxygen concentration during short-term culture in hypoxic and normoxic conditions

Cultivation of MSC in hypoxic conditions which mimic the natural microenvironment of these cells represents an important prerequisite to study cell proliferation, differentiation, senescence, metabolic balance and other physiological processes [158]. Thus, a variety of studies for *in vitro* cell cultivation and subsequent clinical applications suggested MSC culture in hypoxic (1 % to 10 % O_2) rather than normoxic (21 % O_2) conditions [161, 162]. Moreover, implanted MSC in clinical applications without well-developed blood vessels would suffer from limited nutrient and oxygen supply which requires more knowledge about the ability of these cells to survive and adapt to the altered microenvironment. Part of the following work is already published in [163].

For online oxygen concentration measurements, 24 hours after seeding, the cell culture medium was changed and cells were placed on the SFR-Shake Flask Reader in an incubator with reduced oxygen concentration (see chapters 8.2 and 8.6). For three days, dissolved oxygen concentrations (in µmol/l) in the medium and pH values were measured and recorded online every 10 to 20 minutes (fig. 6). The measurements showed - even at 1.5% O_2 - only a minor reduction of the available oxygen level as compared to the cell-free medium, indicating a faster gas diffusion into the medium than the rate of cellular oxygen consumption (fig. 6). The measurements showed - even at 1.5% O_2 - only a minor reduction of the available oxygen level as compared to the cell-free medium indicating faster gas diffusion into the medium than the rate of cellular oxygen consumption (fig. 6). Thus, at the end of the cultivations (80% confluency) with 1.5 % O_2, the concentration of oxygen in the cell culture supernatant was 15.03 µmol/l as compared to 15.7 µmol/l in the control medium (fig. 6A). Likewise, 2.5 % O_2 incubation revealed 23.88 µmol/l of oxygen in the culture supernatant versus 25.10 µmol/l in the control medium (fig. 6B), 5 % O_2 resulted in 48.85 µmol/l versus 50.05 µmol/l in the control medium (fig. 6C), and in normoxic conditions at 21 % O_2 values were 196 µmol/l in the cell culture as compared to 198µmol/l in the cell-free control medium (Fig. 6D).

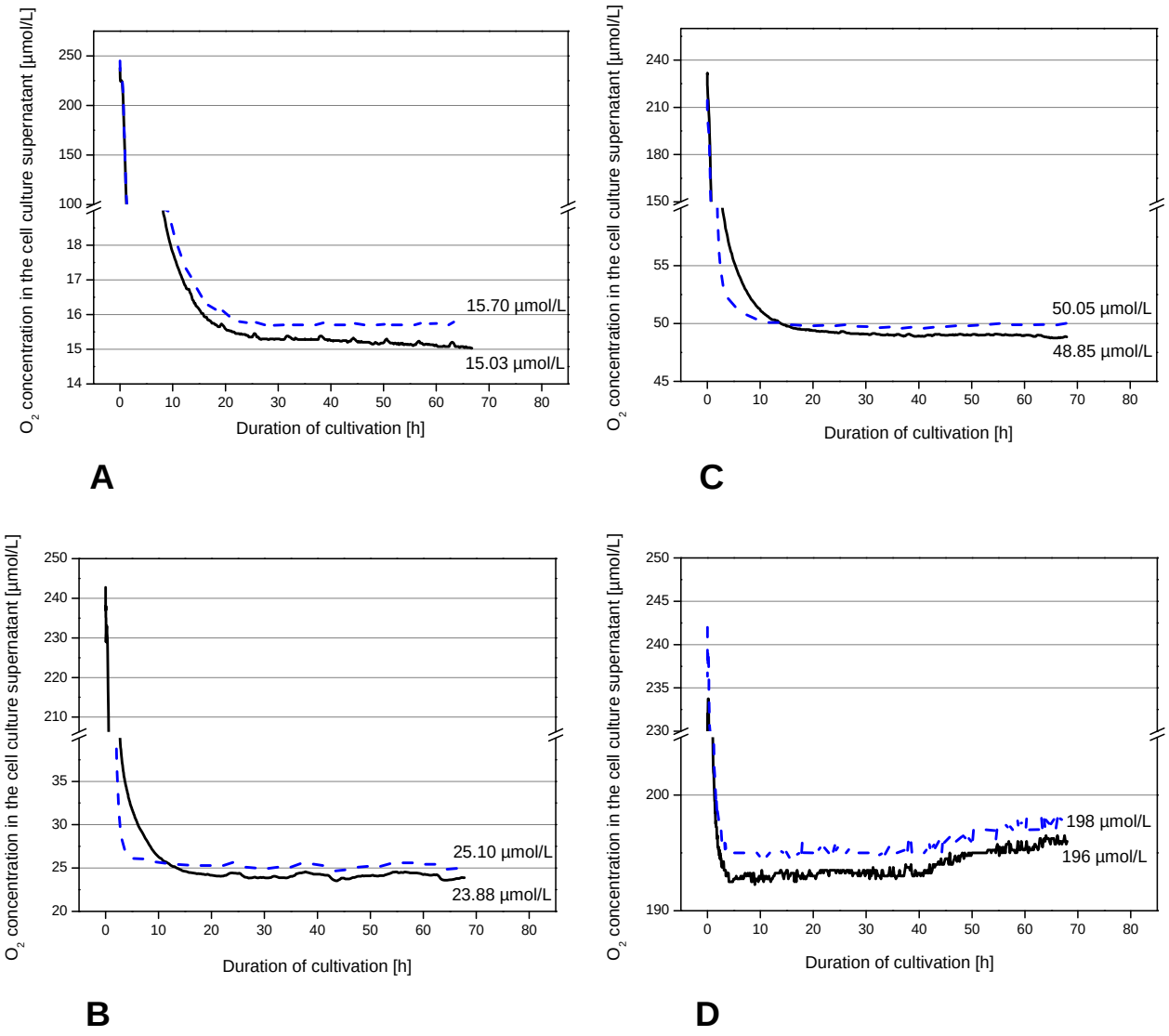

Figure 6: Results of online-measurements of dissolved oxygen concentrations in the cell culture supernatant at 1.5 % (A), 2.5 % (B), 5 % (C) and 21 % (D). The oxygen concentration was subsequently determined for 70h in the 4 different cell cultures.The dissolved oxygen concentrations are demonstrated for the cell culture (black solid line) and for a parallel medium control without cells (blue dashed line)

The calculated oxygen consumption at the end of cultivation (80% confluency) was 0.024 ± 0.002 pmol/h/cell in 1.5 % O_2, 0.035 ± 0.006 pmol/h/cell in 2.5 % O_2, 0.036 ± 0.006 pmol/h/cell in 5 % O_2, and 0.095 ± 0.005 pmol/h/cell in 21 % O_2 (fig. 7).

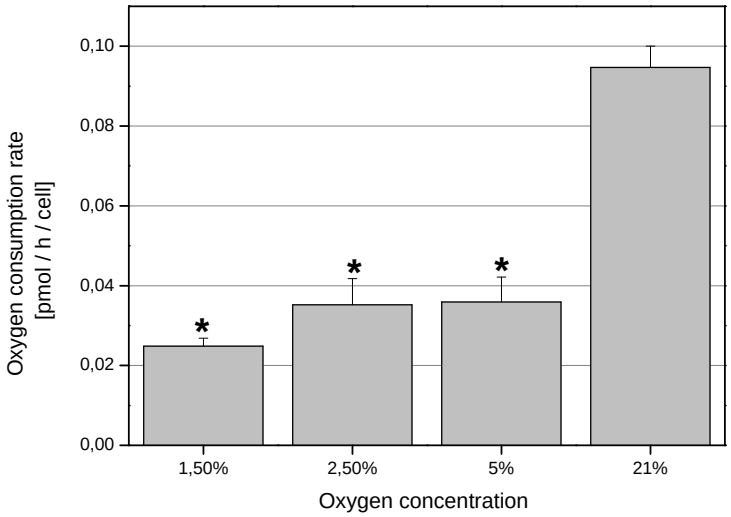

Figure 7: Rates of oxygen consumption by UC-derived MSC from all donors (n=4) at 1.5 %, 2.5 %, 5 % and 21 % O_2. Asterisks indicate statistically significant differences in comparison to the normoxic (21 % O_2) control (* p < 0.001)

The results from the present study reveal that UC-derived stem cells adapt their oxygen consumption and the accompanying energy metabolism according to the available oxygen concentrations. Thus, oxygen consumption rates of MSC in hypoxic conditions were about 3 times lower compared to a normoxic atmosphere. Similar data has been reported in hypoxic primary human fibroblasts [109, 164].

It has been found, that decreased cell respiration in hypoxic conditions is not due to lack of oxygen being able to act as a substrate for oxidative phosphorylation (the major oxygen utilization in the cell) [109]. Under such circumstances oxygen consumption by mitochondria is actively downregulated by hypoxia-inducible factor-1 (HIF-1). HIF-1 was found to induce pyruvate dehydrogenase kinase 1 (PDK 1) which in turn suppresses the utilization of pyruvate as a fuel for the Krebs cycle [109]. This mechanism is used by the cell to maintain intracellular oxygen concentration, i.e. to keep homeostasis. Non-mitochondrial oxygen consumption in hypoxic conditions is unaffected. Cell plasma membranes are not a barrier to oxygen transport into the cell. It was measured that the difference of oxygen concentration across the cell membrane during oxygen consumption stays in the nanomolar range [165]. In our experiments it can be assumed that at the concentration of 15.03 µmol/l (at 1.5 % O_2), oxygen still easily diffuses into the cells and its intracellular concentrations correlate with the concentrations measured in the culture medium.

On-line measurements also showed that a longer time period is needed to reach desired low dissolved oxygen concentrations in freshly changed, not previously deoxygenated medium. This is equivalent to a time interval of 20-30 hours for 1.5 % O_2, 15 h for 2.5 %, and 10 h for 5 % respectively (fig. 1). It also means that in static long-time cultivation experiments, where medium is changed every 2-3 days, cells are still exposed to a higher oxygen concentration for a considerably long period of time after medium change. The use of hypoxic working stations would be a solution if the exposure of the cells to higher oxygen tension is undesirable.

4.1.2 Online measurements of pH during short-term culture under different oxygen tensions

Cultivation under lower oxygen tension suggests alterations in the metabolic activities of the cells. Since all cell culture media were developed for cultivation under atmospheric oxygen concentration, it is important to know if the buffer capacity of the medium is sufficient to keep pH values in a physiological range (pH 7.0-7.5).

Parallel to the measurements of dissolved oxygen concentrations, changes of pH in the cell culture medium were observed online. The pH values in the cell culture supernatant progressively decreased during cultivation time (70h) in parallel to an increasing cell number and reached a difference of about 0.15 pH values compared to control medium at the end of the cultivation (80 % confluency) (fig. 8). Online measurements of pH values in cell culture supernatants in 1.5%, 2.5%, 5% and 21% oxygen, however, revealed no significant differences between different oxygen concentrations. This demonstrates that buffer capacity of the medium is sufficient to provide physiological pH values under hypoxia over short periods of cultivation without medium change.

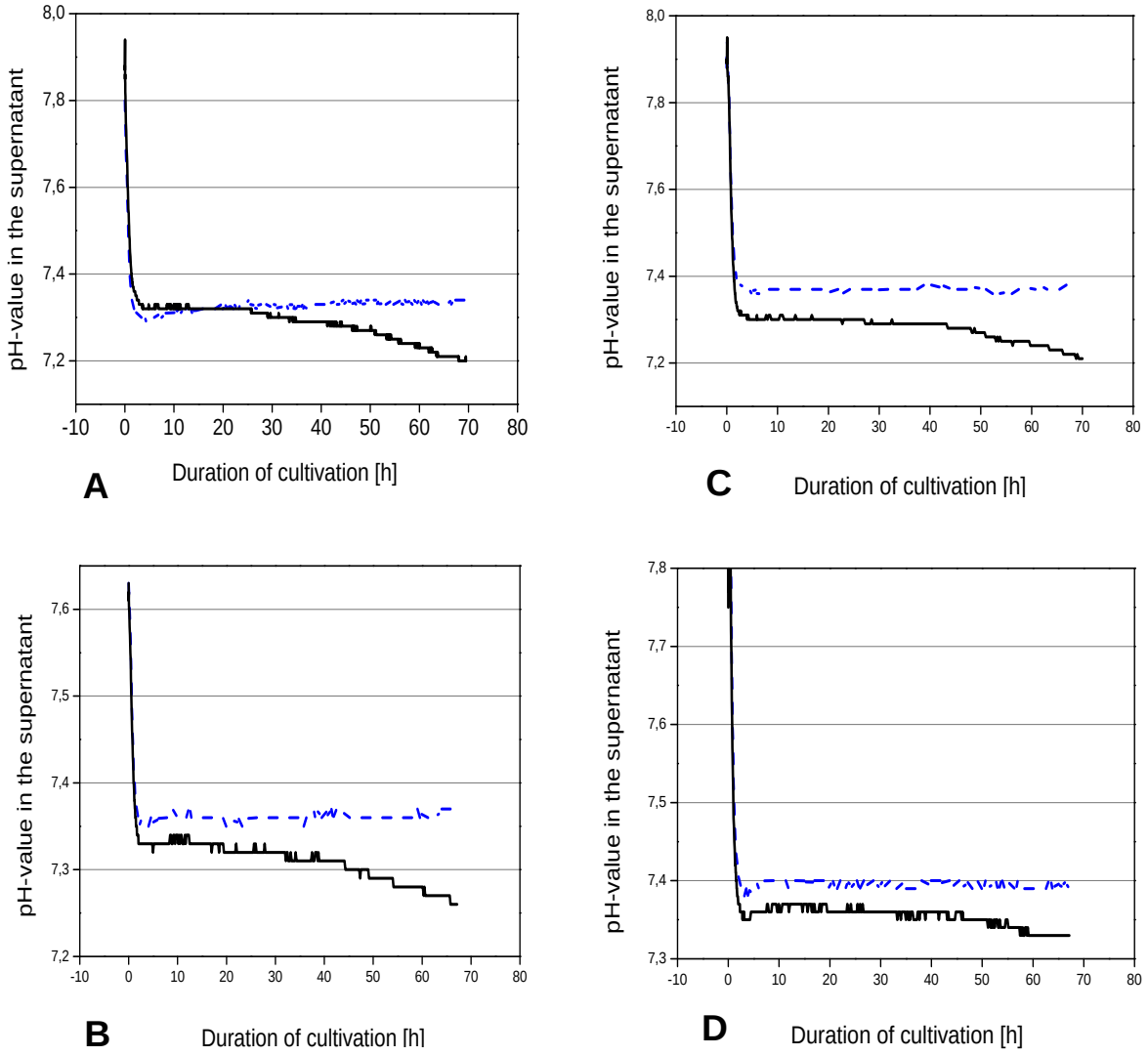

Figure 8: Results of online-measurements of the cell culture supernatant at 1.5 % (A), 2.5 % (B), 5 % (C) and 21 % (D). The pH was subsequently determined for 70h in the 4 different cell cultures

4.1.3 Cell proliferation under different oxygen tensions

The survival of MSC in hypoxic conditions is a key issue if the cells are to be transplanted into necrotic tissues or constitute a part of an avascular TE construct. On the other hand, cultivation of MSC under "physiological hypoxia" can prevent the cells from damage via overproduction of ROS by mitochondria. To check the influence of hypoxia on cell proliferation, MSC were cultivated under 1.5%, 2.5%, 5% or 21% of oxygen tensions.

After a 72 h exposure of UC-derived MSCs to various concentrations of oxygen, the proliferation, apoptosis and cell damage/necrosis in all 4 different cell populations were investigated. Cell growth analysis revealed a statistically significant increase in cell proliferation at 2.5 % O_2 as compared to normoxic 21 % O_2 (fig. 9). There was a statistically insignificant decrease in cell proliferation at 1.5% oxygen concentration when compared to normoxic control.

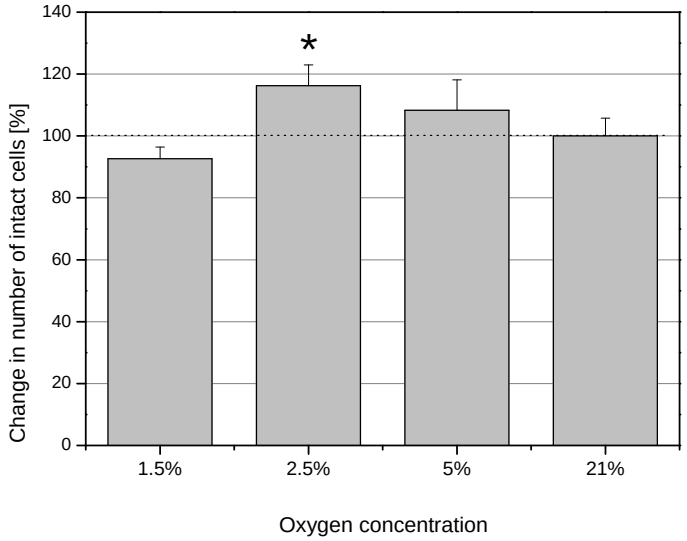

Figure 9: The effect of hypoxia on the cell growth of the UC-derived stem cells from all donors (n=4). Data represent the mean ± SD (*p<0.05)

A more detailed analysis of the hypoxic (1.5 % O_2) MSC cultures revealed little if any increase in apoptosis in cell preparations from all four donors (fig. 10A). In contrast, markedly decreased cell damage or necrosis in all MSC populations became detectable in hypoxic conditions as evaluated by a significantly reduced LDH release in two of the four MSC donors (fig. 10B).

Similar data were obtained earlier in bone marrow-derived MSC [137, 158]. The lower level of cell damage and/or necrosis under hypoxia as compared to the normoxic control suggests an adaptation to the energy requirements during hypoxia as well as reduced production of damaging ROS compounds in hypoxic cells [166].

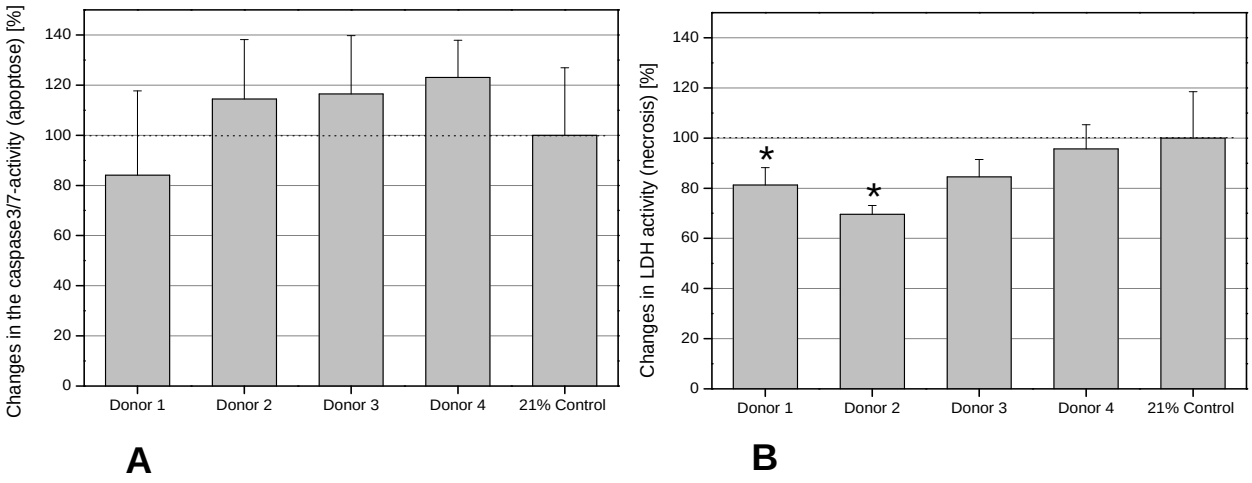

Figure 10: The effect of hypoxia (1.5 % O_2) on apoptosis was tested by the measurement of caspase 3/7 activity (A) and cell damage or necrosis was tested by the measurement of LDH activity in the cell culture supernatant (B) of the 4 different donors of UC-derived stem cells. All measurements were normalized to 10,000 cells whereby the values of all measurements were calculated compared to the normoxic control conditions (21% O_2) at 100 %. Data represent the mean ± SD for three independent measurements of each donor

4.1.4 Metabolic activity of MSC under hypoxia

Energy metabolism is mainly represented by glucose and glutamine, two important molecular carbon and nutrient sources. The analysis of metabolic activities of UC-derived MSC in our experiments was in agreement with previously described increases in glucose consumption and lactate production at low oxygen tension, as a consequence of switching cell metabolism from oxidative phosphorylation to anaerobic glycolysis, as well as an up-regulation of the glucose transport into the cells [137, 167].

UC-MSC cultured at 1.5% O_2 consumed significantly more glucose (22.35 ± 1.56 pmol/day/cell) (fig. 11A) and produced significantly more lactate (30.58 ± 3.58 pmol/day/cell) when compared to normoxic controls (12.00 ± 1.93 and 16. 36 ± 1.07 respectively) (fig. 11B). At 2.5 % glucose consumption and lactate production rates were lower than at 1.5% O_2 (15.10 ± 1.39 and 19.97 ± 3.08 pmol/day/cell respectively), but still higher than in normoxic controls (fig. 11A, B). At 5 % O_2, there were no differences in glucose uptake and lactate production when compared to 21 % O_2.

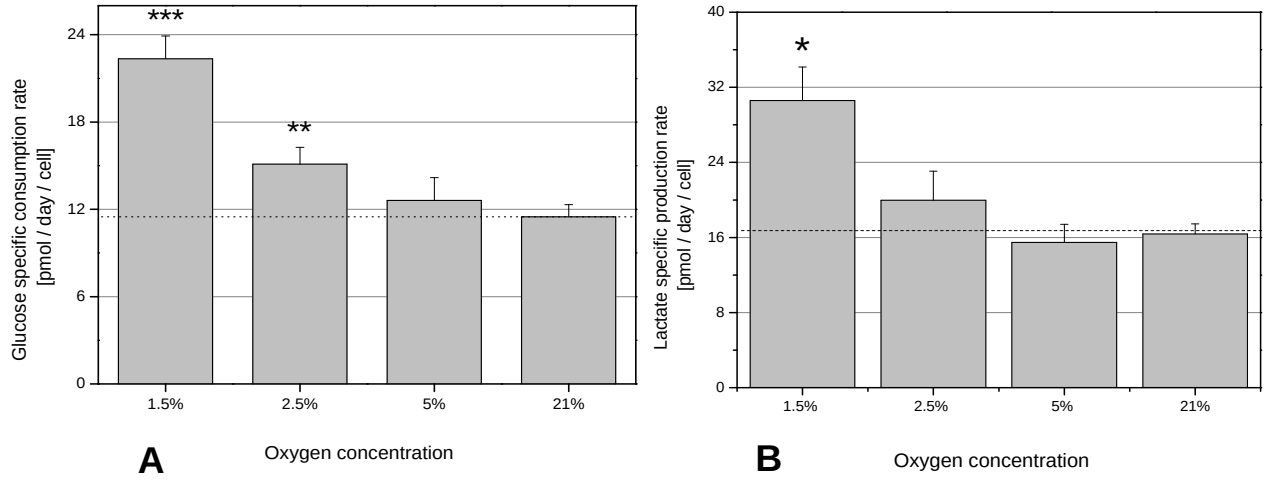

Figure 11: The effect of hypoxia on the glucose consumption (A) and lactate production (B) of the UC-derived stem cells in all donors. Data are the means ± SD for triplicate measurements for each donor, four donors per each oxygen concentration. (p < 0.005,*** p < 0.001, *p<0.05)**

Consumption of glutamine was lower at 1.5% O_2 (1.94 ± 0.53 pmol/day/cell) and at 2.5 % O_2 (2.65 ± 0.95 pmol/day/cell) with no detectable difference at 5% O_2 (2.79 ± 0.72 pmol/day/cell) when compared to 21 % O_2 controls (2.82 ± 1.37 pmol/day/cell) (fig. 12A). Glutamate production was lower at 1.5%, 2.5% and 5% O_2 when compared to 21% O_2 (fig. 12B).

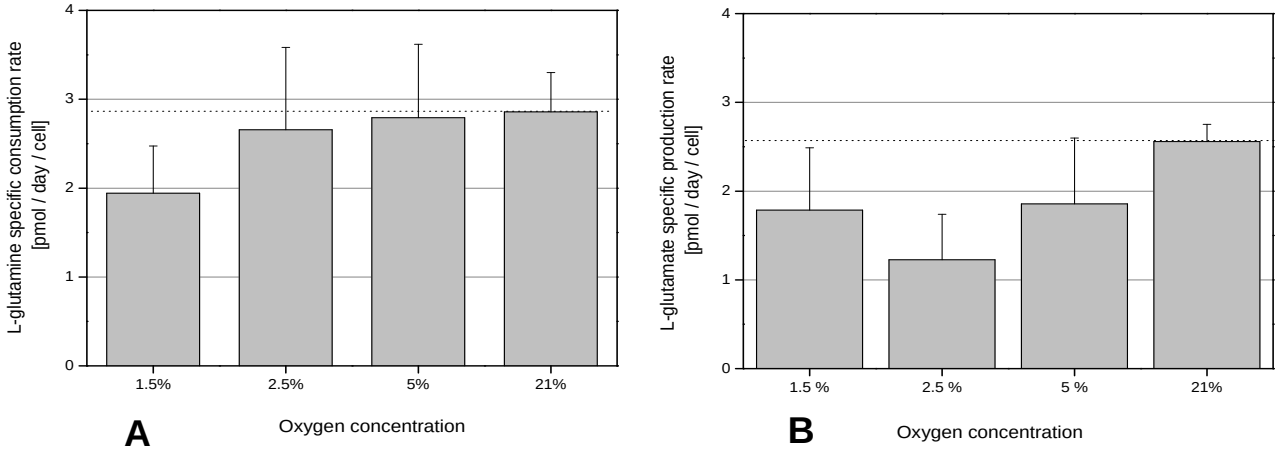

Figure 12: The effect of hypoxia on the glutamine consumption (A) and glutamate production (B) of the UC-derived stem cells. Data are the means ± SD for triplicate measurements for each donor, four donors per each oxygen concentration

These results show that under normoxic conditions, UC-derived stem cells consume less glutamine (about 3 pmol/day/cell) than BM-derived cells, as reported previously (4 pmol/day/cell [168] and 30 pmol/day/cell [167]). Glutamine consumption was lower at 1.5% and 2.5% O_2 as compared to the normoxic (21%) state, also unlike data reported for BM-derived MSC [167]. To check the possible contribution of glutamine to the production of lactate, cultivation at 1.5 % O_2 and 21% O_2 without glutamine was also performed (data are not shown). Without glutamine, both glucose consumption and lactate production were decreased. It is well known that glutamine is essential for the proliferation of many cell types in culture. However, at 1.5% O_2, UC-derived cells did not stop to proliferate without glutamine, which indirectly indicates that in hypoxic conditions glutamine is not used as the main energy or carbon source.

4.1.5 Expression of glucose-metabolism associated genes under hypoxia

In the next step, the regulation of some energy metabolism pathway-associated factors including glucose transporter-1 (*GLUT-1)* (glucose transport into the cell), lactate dehydrogenase A *(LDHA)* (glycolysis), glucose-6-phosphate dehydrogenase *(G6PD)* (pentose phosphate pathway), pyruvate dehydrogenase kinase-1 *(PDK-1)* (glycolysis) was analyzed. Hypoxanthine phosphoribosyltransferase-1 (*HPRT-1*) expression served as an internal control. These genes represent some targets of the transcription factor HIF-1α. Quantitative RT-PCT (qRT-PCR) analysis revealed a significant up-regulation of *GLUT-1*, *LDHA* and *PDK-1* in 1.5% O_2, 2.5% O_2 and 5% O_2 as compared to normoxic (21% O_2) control cells (fig. 13). In contrast, no up-regulation of *G6PD* in hypoxic conditions was detectable (fig. 13).

Quantitative RT-PCR confirmed the up-regulation of the metabolic activity of UC-MSC under hypoxia. In response to lower oxygen concentrations, a metabolic shift to glycolysis helps the cells to produce enough energy to maintain all necessary functions. The PDK 1 level was up-regulated by all oxygen concentrations, when compared to 21% O_2, supporting previous findings that induction of this enzyme suppresses the utilization of pyruvate as a fuel for the Krebs cycle and regulates mitochondrial oxygen consumption, keeping the intracellular oxygen concentration constant [109].

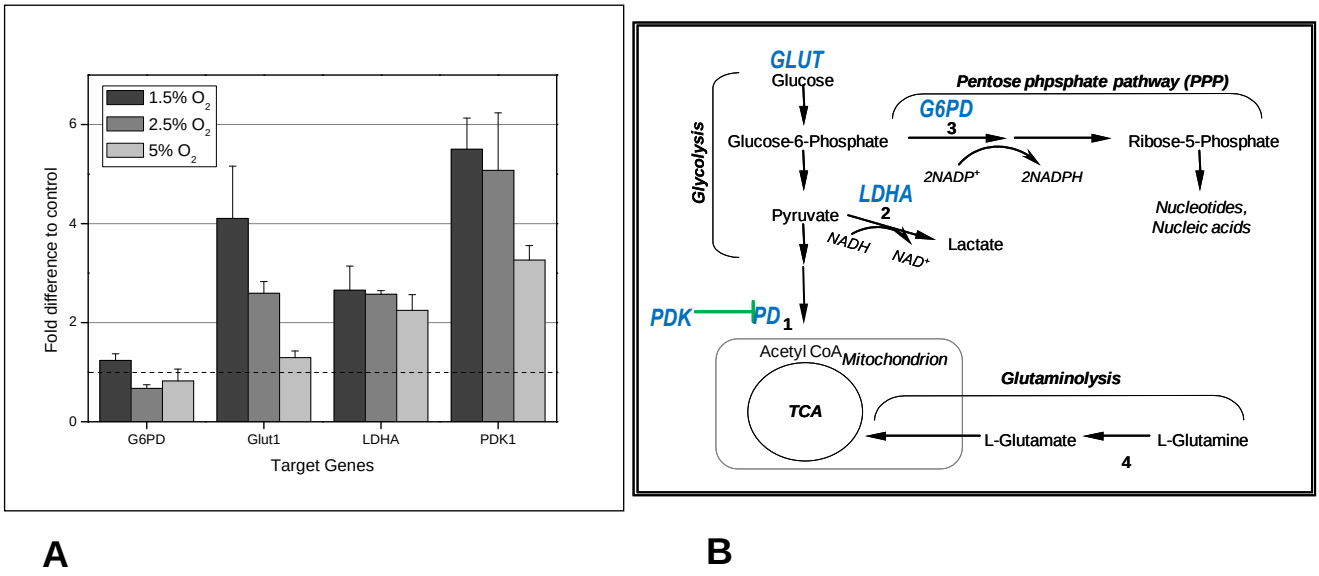

Figure 13: The effect of hypoxia on glucose metabolism-associated gene expression which may also represent HIF-1α target genes. (A) The data represent the expression levels in the UC- MSC at 1.5 % O_2 (black bars), 2.5 % O_2 (dark grey bars) and 5 % O_2 (light grey bars) and compared to the steady state expression levels of normoxic control cultures at 21 % O_2 (dashed line). Data represent the mean ± SD of three independent experiments. (B) Schematic representation of glucose and glutamine metabolic pathways and involved enzymes, gene expression of which was analyzed by qRT-PCR

Gene expression of the glucose transporter GLUT-1 was up-regulated depending on the oxygen concentration – the lower the O_2 tension, the higher the GLUT-1 level. This correlates with an increased glucose consumption rate, as revealed in previous experiments (see chapter 3.1.1). Increased lactate production was also confirmed by the up-regulated expression of lactate dehydrogenase. It seems that PPP is not influenced by the oxygen concentration, since the key rate-limiting enzyme of this pathway (G6PD) was expressed at the same level (fig. 13 A, B).

4.1.6 Cytokine expression profile under hypoxia and normoxia

Short-term (3 days) cultivation under 2.5% oxygen concentration significantly increased UC-MSC proliferation activity (see chapter 3.1.3). To explore further events that lead to increased cell proliferation, cDNA microarray of whole genome, quantitative RT-PCR and protein microarray analysis of cytokines were performed. Increased cell proliferation can be the result of lower cell apoptosis and necrosis, since the cells were cultivated in a more physiological microenvironment and less ROS were produced [129, 130, 169]. Another explanation could be that the UC-MSC produce more cytokines under hypoxia and stimulate their own cell growth via increased cytokine or receptor production. In further experiments, the cytokine expression profiles of UC-MSC in 2.5% O_2 in comparison to 21% O_2 were studied on mRNA and protein levels.

4.1.6.1 Gene expression profile of UC-MSC under hypoxia and normoxia – whole genome cDNA microarray

Whole genome cDNA microarray provides important information about general gene expression for more than 29,000 genes. Gene expression monitoring revealed that in hypoxic conditions (2.5% O_2) about 300 genes were down- or up-regulated as compared to normoxic (21% O_2) conditions (fig.14, detailed overview: supplementary material, tables 8.1 and 8.2). The PANTHER (**P**rotein **AN**alysis **TH**rough **E**volutionary **R**elationships) is a system that classifies genes by their functions, using published scientific experimental evidence and evolutionary relationships to predict function even in the absence of direct experimental evidence. PANTHER biological function analysis tool classifies genes into 17 categories according to the function of proteins, which are encoded by these genes [170, 171]. According to the PANTHER functional analysis, the largest part of regulated genes belongs to metabolic processes (25%), followed by genes responsible for cellular processes (16%), cell communication (11%), transport (8%), immune system processes (7%), developmental and system processes and response to stimulus (6%). Regulated genes were responsible also for cell adhesion, cell cycle regulation, cellular component organization and apoptosis.

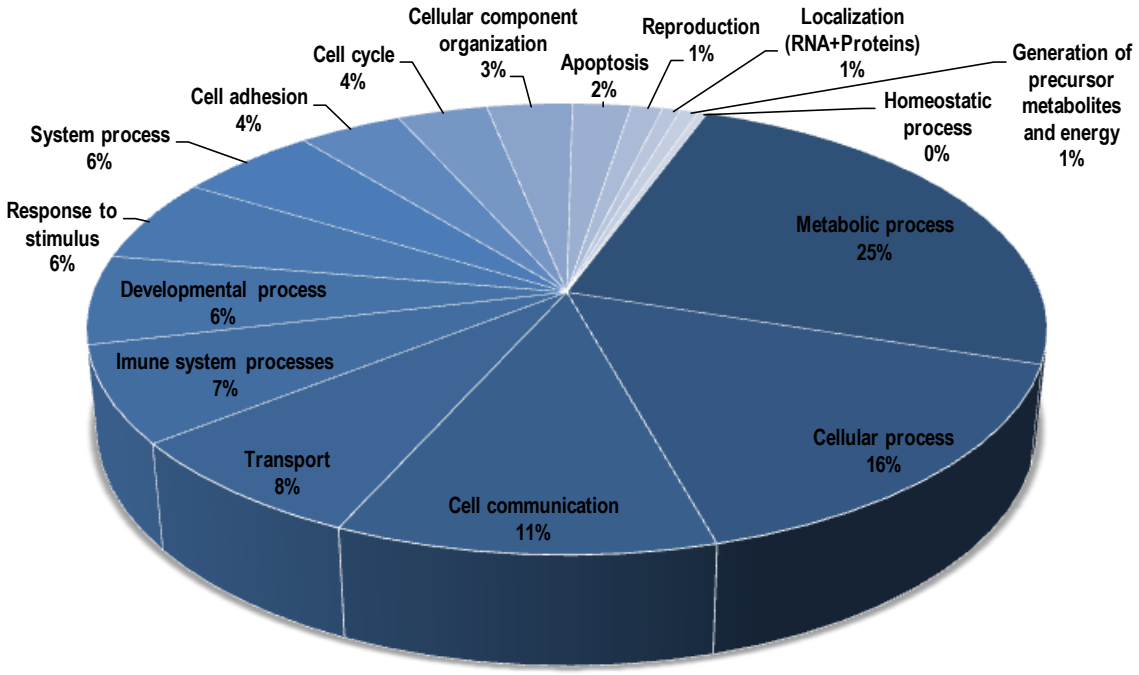

Figure 14: Distribution of biological functions of genes, which were up- or down-regulated in 2.5% oxygen concentration as compared to 21%. Data are presented as percent

If we consider the whole human genome, according to the PANTHER analysis, genes involved in metabolic functions represent the largest population (21.4 % of all genes). Indeed, it is pivotal for cell survival to have a complex and flexible system that helps to keep energetic balance and can adjust to changes in nutrition supply. This is why it is also to be expected, that changes in oxygen concentration result in dynamic response of the metabolic pathways. Data analysis with the PANTHER classification tool did not reveal any genes that were involved in hypoxia-induced regulation (like, e.g. *HIF1α, HIF3α* and *VHL*). Indeed, it was shown that hypoxia does not increase the level of *HIFα* mRNA [172]. The HIF1α protein is constantly expressed independently from oxygen concentration, but it is continuously degraded in the 26S proteosomes. Only above a certain oxygen level HIF1 α is stabilized and functionally active [173]. The VHL protein is a E3 ubiquitin ligase that ubiquitinates HIF1α in the presence of oxygen. Its functional activity is also regulated at the post-translational level. It is still unclear, what concentrations of the HIF1α protein are present in different tissues *in vivo,* since this protein has an extremely short half-life at normal (21%) oxygen

conditions – less than 5 minutes [174, 175]. In UC-MSC cultivated *in vitro* in 2.5% O_2, HIF1α is stabilized at the protein level [163], but it is still unknown how low oxygen tension must be in order to turn the physiological role HIF1α plays in cells into pathophysiological regulation.

Genes involved in cellular processes like cell communication, motion, cytokine production and signaling are significantly regulated in 2.5% oxygen concentration, indicating that UC-MSC actively respond to physiological or pathological hypoxia. It is discussed that MSC in general can play an important role in tissue homeostasis, supporting other differentiated cells with protective cytokines (local paracrine rescue function) or via direction of blood vessel growth into hypoxic tissue in the case of too low oxygen concentration (e.g. VEGF production). In this way, fast regulation of cell communication genes (like receptor expression and production of signaling molecules) via HIF-dependent or HIF-independent pathways is a key condition to fulfill these functions.

Although a whole genome microarray cannot provide an absolute quantitative analysis of gene expression, it gives a very important overview on the genes that respond to different cultivation conditions and offers starting points for further research. In the case of UC-MSC, it is clearly seen that cells cultivated *in vitro* in diverse oxygen concentrations have dissimilar gene expression and additional studies must be performed to evaluate the influence of culture conditions on the functional activity, treatment efficiency and post-implantation survival of these cells.

4.1.6.2 Cytokine gene expression

After 72 hours of cultivation of UC-MSC from 3 donors under 2.5% and 21% O_2, RNA was isolated, transcribed into cDNA and qRT-PCR of selected genes was carried out. Vascular endothelial growth factor A (*VEGFA*), vascular endothelial growth factor receptor (*VEGF-R*), placental growth factor (*PGF*), basic fibroblast growth factor (*bFGF),* stem cell factor receptor (*SCF-R*), insulin-like growth factor binding protein 6 (*IGFBP6*), heparin-binding EGF-like growth factor (*HBEGF*), transforming growth factor beta 3 (TGFβ3) and insulin-like growth factor binding protein 3 (*IGFBP3*) gene expression was analyzed with hypoxanthine phosphoribosyltransferase-1 (*HPRT1*) used as internal control (housekeeping gene) and ΔΔCt-method (fig. 15).

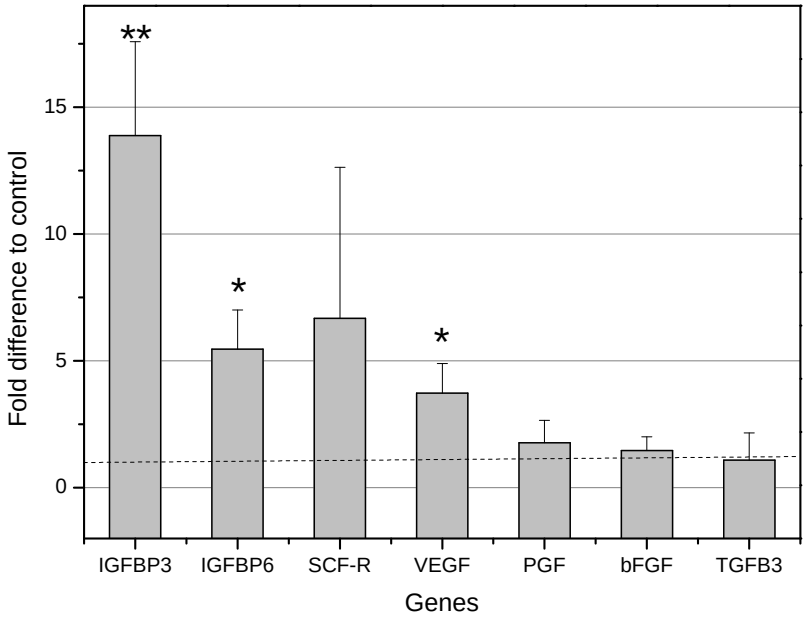

Figure 15: The effect of hypoxia (2.5% O_2) on cytokine gene expression (up-regulated genes). Gene expression was detected by qRT-PCR with hypoxanthine phosphoribosyltransferase-1(HPRT1) expression as an internal control. Data represent the mean ± SD of three independent experiments (p<0.01, *p<0.05)**

Gene expression analysis revealed 3 genes that were significantly up-regulated in 2.5% O_2: IGFBP3 (13.8-fold), IGFBP6 (5.6 fold) and VEGFA (3.7-fold) (fig. 15). Although SCF-R was 6.6-fold up-regulated, there was a big variety in the gene expression levels between donors (from 13-fold to 3.3-fold).

IGFBPs are a family of six homologous multifunctional high-affinity proteins. As can be derived from the name, these proteins bind intra- and extracellular IGFs in biological fluids, acting as carriers and prolonging the half-life of IGFs [176]. IGFs, in turn, regulate growth and embryonic development. Numerous data support the importance of IGFBPs for cell growth by both IGF-dependent and IGF-independent mechanisms. Depending on the cellular context and the IGFBP present, the actions of IGFs can be either enhanced or inhibited [177]. IGFBP6 is found to be an important tumor suppressor in nasopharyngeal carcinoma [178]. IGFBP3 was also found in cell nuclei of lung cancer cells, where it induced their apoptosis and acted as a nuclear tumor suppressor [179]. In prostate cancer cells IGFBP3 was also found in mitochondria. The authors discussed its essential role in prostate cancer apoptosis [180]. On the other hand, it was also suggested that IGFBP3 can act as a shuttle to the nucleus for IGFs [181]. Another important function of IGFBP3 is an immunomodulatory property of MSC – here it was shown that IGFBPs significantly increase inhibition of PBMCs proliferation by MSC [182]. As expected, hypoxia enhanced the expression of VEGFA, the

major primer of vascularisation and cell migration [183]. Moreover, VEGF induces expression of anti-apoptotic proteins and demonstrates mitogenic capacity. Several working groups showed increased levels of VEGF in MSC in response to hypoxia [184, 185]. Notably, mRNA level of bFGF, PGF and TGFβ3 remained unchanged (fig.15).

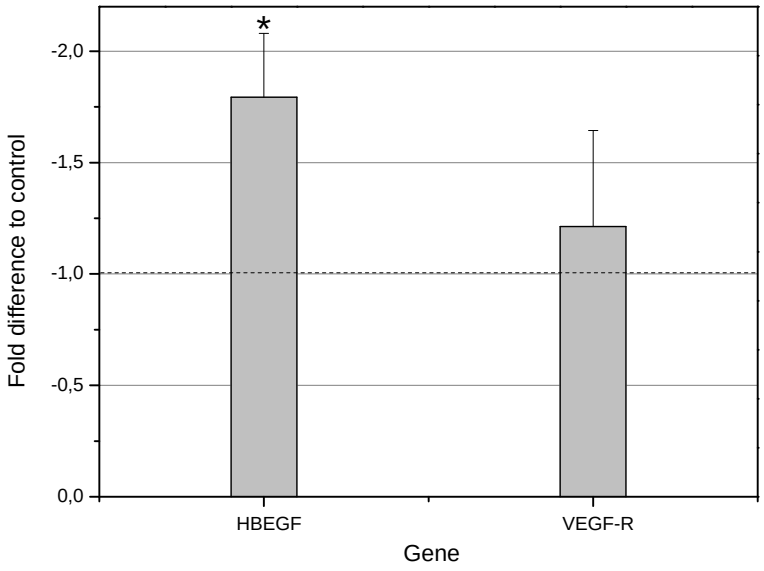

Figure 16: The effect of hypoxia (2.5% O_2) on cytokine gene expression (down-regulated genes). Gene expression was detected by Real-Time RT-PCR with hypoxanthine phosphoribosyltransferase-1(HPRT1) expression as an internal control. Data represent means ± SD of three independent experiments (*p<0.05)

Two of the analysed genes were down-regulated under 2.5% O_2 (HBEGF statistically significant and VEGF-R insignificant) (Fig.16). It can be concluded, that during hypoxia only ligands are increasingly produced, while expression of VEGF receptors remains constant. HBEGF belongs to the family of epidermal growth factors (EGF), which are important cytokines that induce mitosis of cultured epidermal cells, promote DNA synthesis, stimulate translation, and increase protein phosphorylation [186]. EGF was also shown to trigger neuronal differentiation in BM-MSC [187]. It was demonstrated that HBEGF protect epithelial cells from ROS *in vitro* [188]. Authors revealed higher production of HBEGF during oxidative stress. In the case of hypoxia, when cell metabolism is shifted to glycolysis, mitochondria produce less ROS and the protective function of HBEGF is not required.

4.1.6.3 Cytokine expression on the protein level

Quantitative RT-PCR revealed increased gene expression of some cytokines on the mRNA level. Although mRNA levels in the cell often correlate with protein expression, several post-transcriptional and post-translational factors can influence the final receptor expression, cytokine release and their biological activity. One example of post-transcriptional regulation is microRNA, which consists of short chains of nucleotides that can complimentary bind to target mRNA and suppress translation [189]. Human MSC are strictly regulated by microRNA expression during development and differentiation [189]. An example of post-translational regulation is protein degradation via ubiquitination. The HIF-1α protein is constantly degraded in the cell in normoxia and stabilizes only if certain oxygen concentration threshold is reached. To examine cytokine expression on the protein level, Quantibody Human Growth Factor Array I kit (see chapter 8.10) was used. After cultivation in 2.5% and 21% O_2, UC-MSC from 3 donors were disrupted and the intracellular level of 40 cytokines was measured.

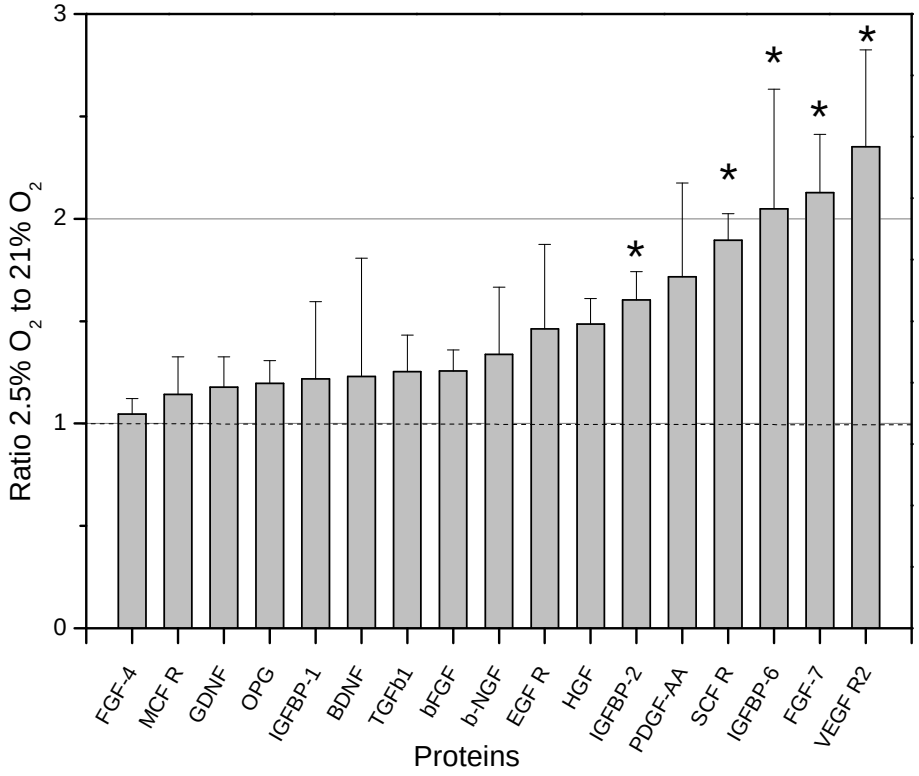

Figure 17: The effect of hypoxia (2.5% O_2) on intracellular cytokine protein expression. Protein expression was detected with the Quantibody Human Growth Factor Array I kit and ratios of protein expression in 2.5% oxygen to protein expression in 21% oxygen were calculated. Data represent means ± SD of three independent experiments (*p<0.05)

It was not possible to detect extracellular cytokine release from UC-MSC since they were cultivated in cell culture medium supplemented with human serum, which is rich in growth factors and soluble receptors. To avoid unspecific detection, culture medium was removed and cell monolayer was washed with PBS before disruption.

With the help of the microarray, 35 proteins were detected in the cell lysates. However, only 17 proteins could be quantified. Five proteins (BMP-4, EGF, IGF-1, TGFα and VEGF R3) were not detected. BMP-4, EGF and TGFα are thee homologous proteins which participate in cell differentiation. Absence of these proteins in the UC-MSC can indirectly indicate an undifferentiated state of the cells. There is no evidence that MSC synthesize IGF-1, but it is known that they can be regulated by IGF as a paracrine (not autocrine) factor. Furthermore, 18 cytokines could be detected in the cell lysates, but their concentrations were below quantification limit. Almost all proteins which were analyzed were up-regulated, but the up-regulation was statistically significant for five proteins only (fig.17).

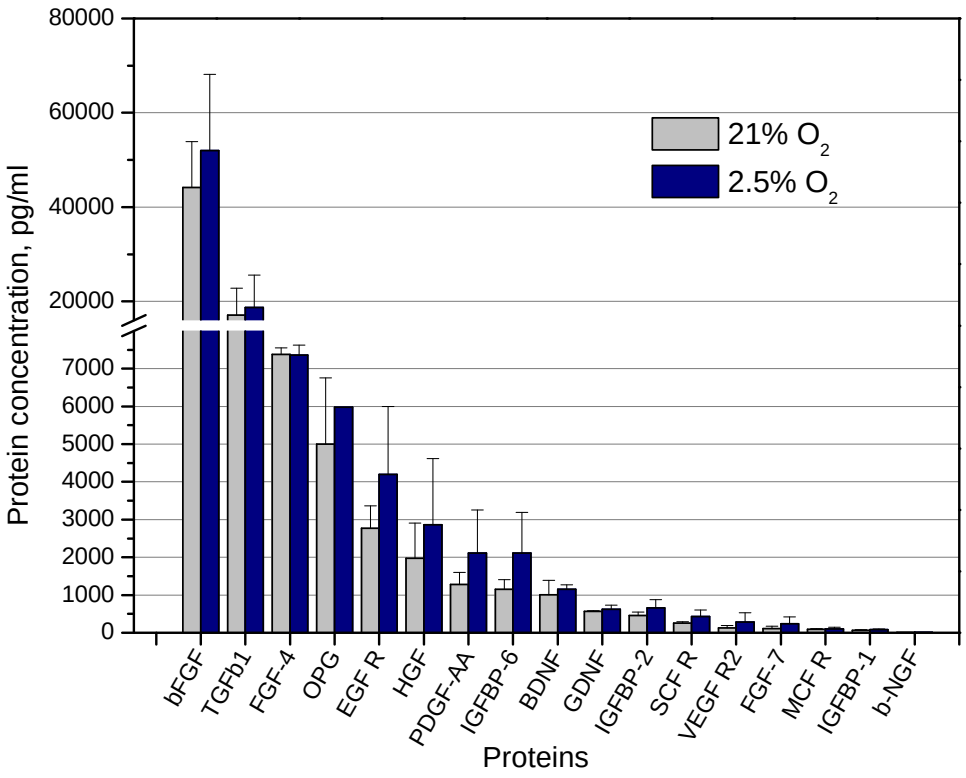

Figure 18: Intracellular concentration of proteins in the cells, cultivated in 21% O_2 (grey columns) and 2.5 % O_2 (blue columns). Protein expression was detected with the Quantibody Human Growth Factor Array I kit. Data represent the means ± SD of three independent experiments

Confirming qRT-PCR results, the level of IGFBP6 was 2.04-fold increased under hypoxia when compared to cells cultivated in ambient oxygen concentrations. IGFBP2 was

also up-regulated, indicating that numerous proteins of this family are regulated depending on the oxygen tension. In contrast to qRT-PCR data, VEGV receptor 2 was significantly over-expressed under hypoxia when compared to normoxic controls.

FGF-7 (also known as *keratinocyte growth factor*) is one of the factors relevant for the ability of MSC to home to sites of injury. It was shown that FGF-7 plays an essential role in liver regeneration [190] and cell migration [191]. The up-regulated SCF receptor (known also as CD117) also participates in cell proliferation and survival, transducting (when binded with SCF) signals via phosphorylation of intracellular signalling molecules. Figure 18 shows actual intracellular concentrations of measured proteins in the cells under hypoxia and normoxia. Concentrations of different proteins vary from7 pg/ml to 47 µg/ml with the highest concentration for bFGF and the lowest for bNGF. It is important to note once more that the proteins were measured only intracellularly, although most of them are released extracellularly. Development of new, chemically-defined cell culture media will make it possible to study also the extracellular release of cytokines by UC-MSC.

4.1.7 Cell migration assay (wound healing assay)

The wound-healing assay is the simplest, most inexpensive and earliest developed assay to study cell migration *in vitro* [192]. In this method, the "wound" is created by scraping the cell monolayer with the pipette tip, followed by observation of cell migration into the scratch.

For the wound-healing assay, UC-MSC from the same donor were cultivated for 8 hours under 21%, 5% and 2.5% O_2. As shown in figure 19, the migration rate of the cells was higher under hypoxia, both at 2.5% and 5% of oxygen tension. It is important to note that infiltration of the MSC into the "wound"-area was a result of migration, but not cell division, since calculated doubling times for UC-MSC (24-30 h) are much longer then the duration of the experiment (8h) (fig.19).

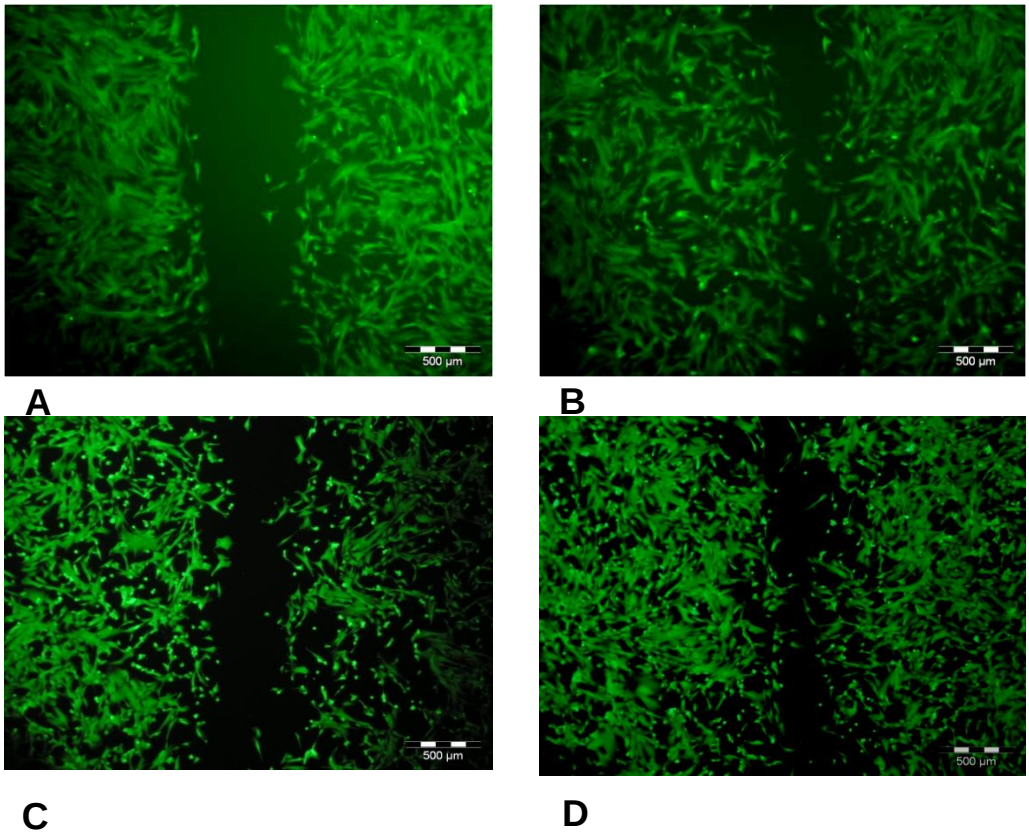

Figure 19: The effect of hypoxia (2.5% and 5% O_2) on UC-MSC migration activity. Cells from the same donors were cultivated for 8 hours under 21% O_2 (A) versus 5% O_2 (B), and under 21% O_2 (C) versus 2.5% O_2 (D)

Hypoxia seems to be a strong stimulator of MSC migration. It was shown previously that both, autocrine and paracrine effects of growth factors involved in enhanced hypoxia-driven migratory potential of MSC [157]. MSC pre-treated by hypoxia before transplantation have better survival chances and can migrate into necrotic tissues [193, 194]. Hypoxic preconditioning also decreases post-transplantation apoptosis of MSC via stabilizing mitochondrial membrane potential and increasing VEGF production [195]. The observation of increased migratory activity of UC-MSC under hypoxia supports the findings with gene and protein expression, showing up-regulation of cell motility under lower oxygen tensions.

4.1.8 Long-term UC-MSC cultivation under different oxygen concentrations

To obtain high cell numbers for clinical use, it is unavoidable to expand the cells over several passages. Millions of cells of good quality with regard to cell viability, paracrine activity and non-tumorigenesis must be obtained in the shortest possible period of time. In the following experiments, UC-MSC were subcultivated over 25 passages under 21%, 5% and 2.5% O_2 (3 donors per each oxygen concentration). Cell numbers, cell senescence, possible spontaneous transformation and the differentiation potential after long-term expansion were analysed.

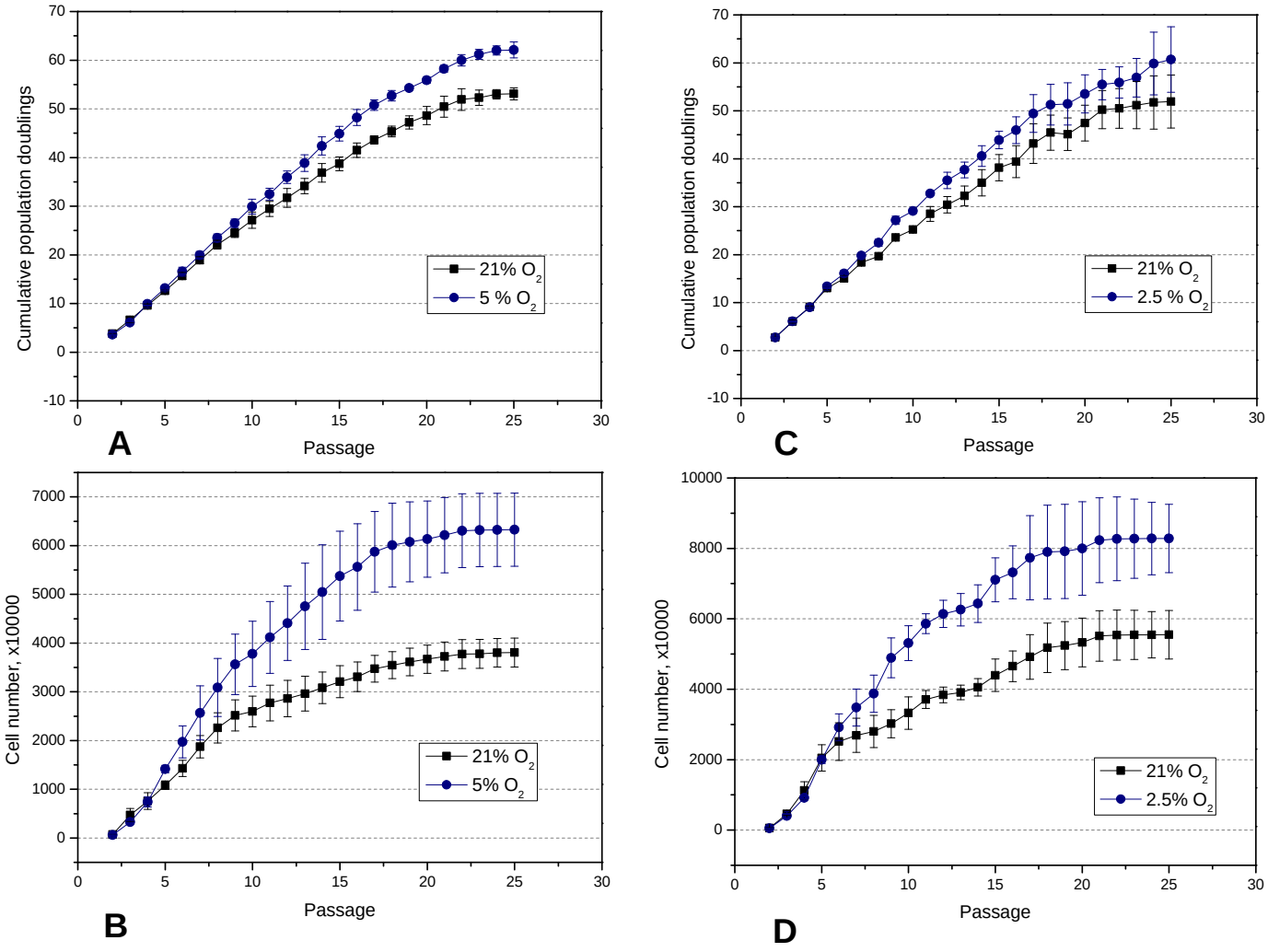

Figure 20: The effect of hypoxia (2.5% and 5% O_2) on UC-MSC long-term culture. Cells from three donors were cultivated over 25 passages under 21% versus 5% O_2 (A, B) and 21% versus 2.5% O_2 (C, D); A, C – cumulative population doublings; B, D – total cell numbers. Data represent means ± SD from 3 donors

Figure 20 shows the results of long-term cultivation of UC-MSC. As can be seen, hypoxic cultures resulted in increased cumulative population doublings and significantly higher total cell numbers in both 2.5% and 5% oxygen when compared to 21% O_2. Starting with the same cell number at passage 1 ($7.5x10^4$ cells), the yield at passage 10 was $5.3x10^7 \pm 0.5\ x10^7$ cells with 2.5% O_2, while it was only $3.3x10^7 \pm 0.4\ x10^7$ at 21% O_2. Similarly, in the experiment where cells were cultivated in 5% O_2 versus 21% O_2, at passage 10 hypoxic culture resulted in $3.97x10^7 \pm 0.7\ x10^7$ cells while at normoxia only $2.61x10^7 \pm 0.3\ x10^7$ cells were counted. Similar results were obtained by Nekanti and colleagues, who demonstrated a higher proliferative activity of UC-MSC in long-term cultivation under 2% oxygen tension [138].

Another working group which studied the long-term cultivation of BM-MSC revealed a better support of the undifferentiated state of the cells and higher colony-forming unit numbers under hypoxia (5% O_2) when compared to 21% O_2 [196]. It should be mentioned, however, that the authors considered "long-term cultivation" only as cultivations of over 2 passages. On the other hand, it is known that BM-MSC have shorter *in vitro* proliferative capacities than UC-MSC.

The results of our study show that UC-MSC can be subcultivated *in vitro* for a very long period of time without losing their proliferative activity. On one hand this is advantageous since larger cell numbers can be obtained. On the other hand, safety considerations play an important role with regard to the clinical perspective of using such cells for stem cell therapy or tissue engineered constructs. Cells should not proliferate endlessly, turning into immortal tumorogenic cell lines. Cultivation over 25 passages showed that UC-MSC slow down their growth after 20 passages, both in normoxic and hypoxic conditions. Cultivation under lower oxygen concentrations, however, helps to achieve higher cell numbers in a shorter period of time.

4.1.9 Cell senescence after long-term cultivation

As it was mentioned above, UC-MSC expanded *in vitro* must not spontaneously transform into malignant immortal cells. To check if cells go into senescence, β-galactosidase staining of UC-MSC after 25 passages under hypoxia and normoxia was performed. Cellular

replicative senescence *in vitro* was first described by Hayflick and Moorhead in 1961 as a phenomenon of growth arrest after a period of normal cell proliferation (Hayflick limit) [197]. Senescent cells stay metabolically active, but demonstrate altered cell morphology – namely hypertrophic cell size, flattened shape and big nuclei (sometimes several of them). One of the reasons of *in vitro* senescence is telomere shortening. In the absence of telomerase reverse transcriptase, telomeres become gradually shorter with each cell division. The rate of telomere shortening in BM-MSC was shown to be about 100 bp at every two passages [198].

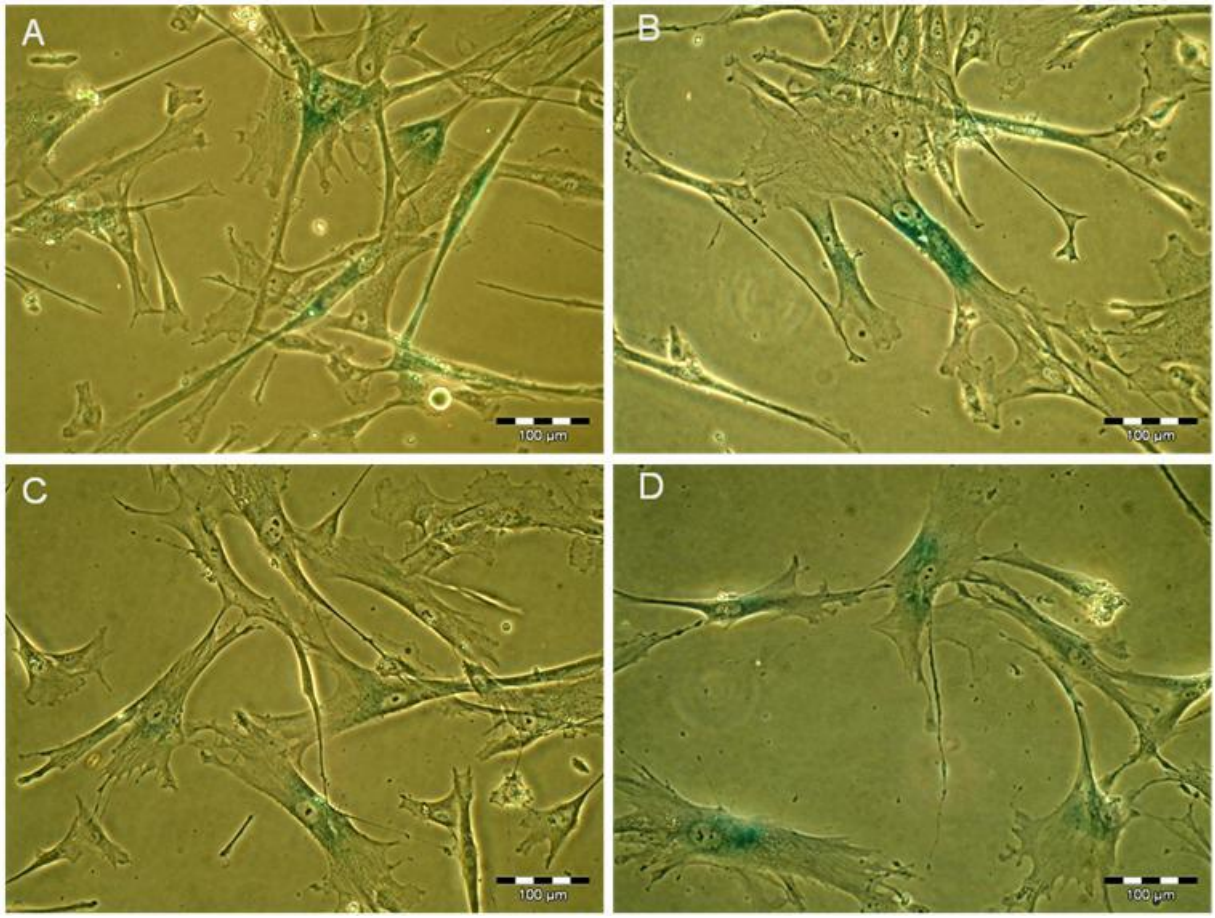

Figure 21: Senescence-associated β-galactosidase staining of UC-MSC cultivated for 25 passages; 21% O_2 (A) versus 5% O_2 (B) and 21% O_2 (C) versus 2.5% O_2 (D)

β-galactosidase staining of the UC-MSC after 25 passages showed that most of the cells become senescent, with blue staining around the cell nuclei and typical morphology (fig. 21). Replicative senescence is an important anti-cancer mechanisms *in vitro* [199] and *in vivo* [200], which opposes neoplastic transformation triggered by activation of oncogenic pathways. The fact, that UC-MSC retain this mechanism when cultivated under normoxic and

hypoxic conditions makes it possible to apply these cells in the clinical contest after *ex vivo* expansion, thus reducing the risk of neoplastic transformation.

4.1.10 Expression of oncogenes, hTERT and tumor suppressors during long-term cultivation of UC-MSC under normoxic and hypoxic conditions

Despite of encouraging results from *in vitro* experiments, animal models and first clinical trials, MSC are still not widely-used in practice. The major factor that will influence the future of clinical applications of UC-MSC is not only the degree of treatment efficiency, but also concern of safety aspects. The treatment cannot be applied to a patient, if it is hazardous by exhibitng side-effects or undesired developments. The direct or indirect involvement of MSC in cancer progress is still under debate. There are three mechanisms by which MSC can be involved in possible cancer development. The first mechanism is direct, via malignant transformation of the implanted MSC, the second mechanism involves the tumor modulatory effects of MSC and the third mechanism is via the MSC influence on the immune system.

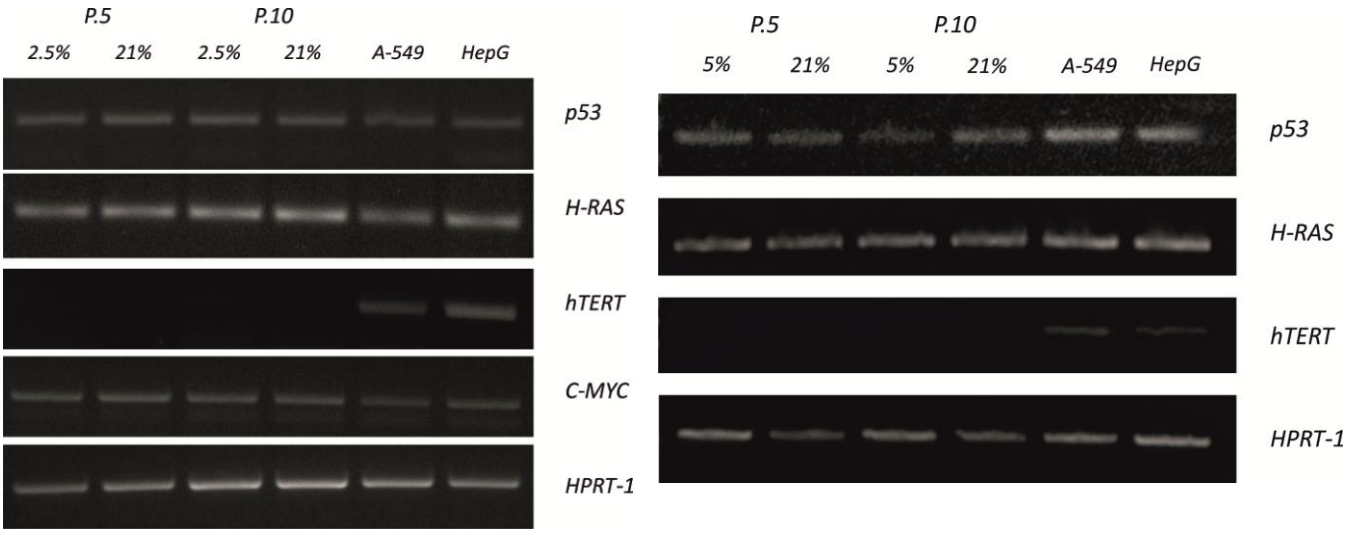

Figure 22: Representative electrophoresis results of RT-PCR products for the genes p53 (tumor supressor protein 53), H-RAS (transforming protein p21), hTERT (human telomerase reverse transcriptase) and C-MYC (human myelocytomatosis viral oncogene homologue;. HPRT-1 (hypoxanthine phosphoribosyltransferase-1) served as housekeeping gene control. (A) UC-MSC cultivated in 2.5% versus 21% O_2. (B) UC-MSC cultivated in 5% versus 21% O_2

In order to examine the safety of long-term culturing of UC-MSC with regard to spontaneous *in vitro* transformation, cells cultivated in 2.5%, 5% and 21% O_2 were studied after passage 5 and after passage 10 for the presence and expression profile of various tumor suppressors and oncogenes (fig. 22).

The tumor suppressor protein 53 (p53) is considered the "guardian of the genome" and a key regulator of the intracellular anti-cancer network [201]. The number 53 in the protein's name reflects its mass on the SDS-PAGE, although its real molecular mass is smaller. p53 is involved in anti-cancer control via several mechanisms, including initiation of apoptosis, activation of DNA-repair proteins and cell growth/cell cycle arrest via cell cycle checkpoints [202, 203]. p53 plays a central role in the biology of MSC, since the absence of p53 implicates spontaneous transformation of MSC in long-term culture [204]. [204]. Recently, p53 was also shown to play an important role in glucose metabolism, increasing the level of oxidative phosphorylation [205]. Hypoxia has divergent effects on the p53 level, depending on its duration and oxygen concentration [206]. In the absence of DNA damage, p53 is ubiquitinated with subsequent proteasomal degradation, but it is immediately stabilized and activated in response to different types of stress. Therefore, it is important to know if the long-term cultivation of MSC can lead to p53 mutations and silencing.

RT-PCR analysis revealed a stable expression profile of p53 in long-term cultivated UC-MSC, both at 2.5%, 5% and 21% O_2 concentrations at passage 5 and at passage 10 (fig. 22A, B). H-RAS, also known as transforming protein 21 (analogous to p53 it is named by its molecular mass), is a proto-oncogene, which (if normally expressed) regulates cell growth, but in the case of mutation or overproduction can lead to malignant transformation. p21 is regulated by p53 and the p21/p53 pathway is one of the major cell-cycle arrest activators in the case of DNA damage. Previous studies demonstrated that over-expression of H-RAS protects from programmed cell death [207]. Although p21-deficiency itself is not sufficient to allow MSC immortalization, when coupled with p53 deficiency, MSC bypass senescence *in vitro* and generate tumors that resemble typical mesenchymal sarcomas *in vivo* [68]. As shown in figure 22, no differences in H-RAS gene expression could be detected after long-term expansion of UC-MSC at all oxygen concentrations during all passages.

Human telomerase reverse transcriptase (hTERT) is the catalytic subunit of telomerase, a RNA-dependent DNA polymerase which stabilizes telomeres and allows cells to avoid the senescence checkpoint [208-210]. Telomerase activity is involved in the immortalization of cancer cells and subsequent tumor growth. It was shown that telomerase is

stringently repressed in normal human somatic tissues, but it reactivates in immortal cancer cells [211]. RT-PCR revealed no spontaneous expression of hTERT in long-term cultivated UC-MSC, both in hypoxic and normoxic cell cultures (fig. 22). The positive control - lung and liver cancer cell lines, in turn, exhibited hTERT-expression, showing that absence of amplicons in UC-MSC cultures was not a result of falsely designed primers.

The level of expression of C-MYC in 2.5% oxygen concentration remained also unchanged over 10 passages (fig. 22A). C-MYC is a transcription factor and also a proto-oncogene, its protein over-expression is linked to senescence bypass and contributes to oncogenesis [212].

Although a more detailed analysis should be performed to assure the safety of MSC applications after *in vitro* expansion in hypoxic conditions, our results demonstrate quite stable expression profiles of selected oncogenes and no spontaneous expression of hTERT.

4.1.11 Surface immunophenotype characterization of UC-MSC during long-term cultivation

No uniform surface marker protein has yet been found to characterize MSC. ISCT recommended a combination of surface antigens which must be positively (≥95%) or negatively (≤2%) expressed by MSC [3]. To identify MSC, ISCT proposed that cells should express CD105 (known as endoglin), CD73 (known as ecto 5' nucleotidase) and CD90 (also known as Thy-1) and must not express CD34 and CD31 which mark primitive hematopoietic progenitors and endothelial cells.

UC-MSC were studied for surface antigen expression during long-term cultivation under normoxic and hypoxic conditions by flow cytometry after staining with FITC- or PE-conjugated antibodies against CD31, CD34, CD44, CD73, CD90, CD105 and corresponding isotype control immunoglobulins. Flow cytometric analysis showed that cells cultivated in 5% and 21% oxygen concentration retained the specific immunophenotypic MSC markers (CD44, CD73, CD90 and CD105) (fig. 23, fig. 24 and table 4.1.11.1) but were negative for hematopoietic (CD34) and endothelial (CD31) markers. According to these data, UC-MSC maintained their surface immunophenotype and did not undergo spontaneous differentiation neither under normoxia nor under hypoxia. Identical results were obtained for UC-MSC cultivated at 2.5% versus 21% O_2 (fig. 25, fig.26 and table 4.1.11.2).

It was shown previously that hypoxia (1% O_2) can induce differentiation of BM-MSC towards endothelial cells [157]. The absence of the specific endothelial marker CD31 during all periods of long-term cultivation of UC-MSC in 2.5% and 5% oxygen indicated that no spontaneous endothelial differentiation took place under hypoxia.

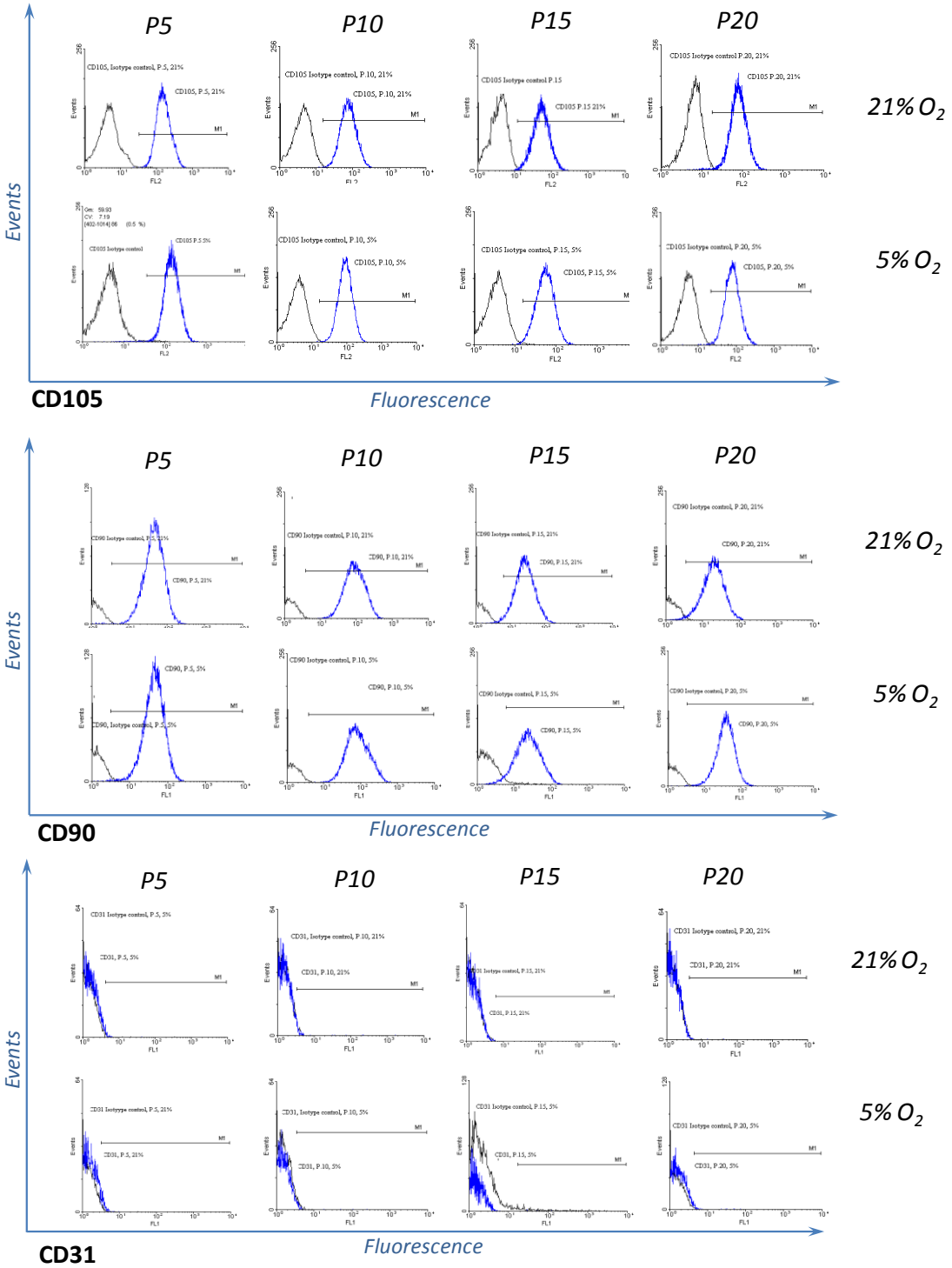

Figure 23: Flow-cytometric analysis of surface antigen expression (CD105, CD90 and CD31) of UC-MSC during long-term cultivation in 5% and 21% oxygen concentration. Grey lines represent isotype control, blue lines – specific antibodies

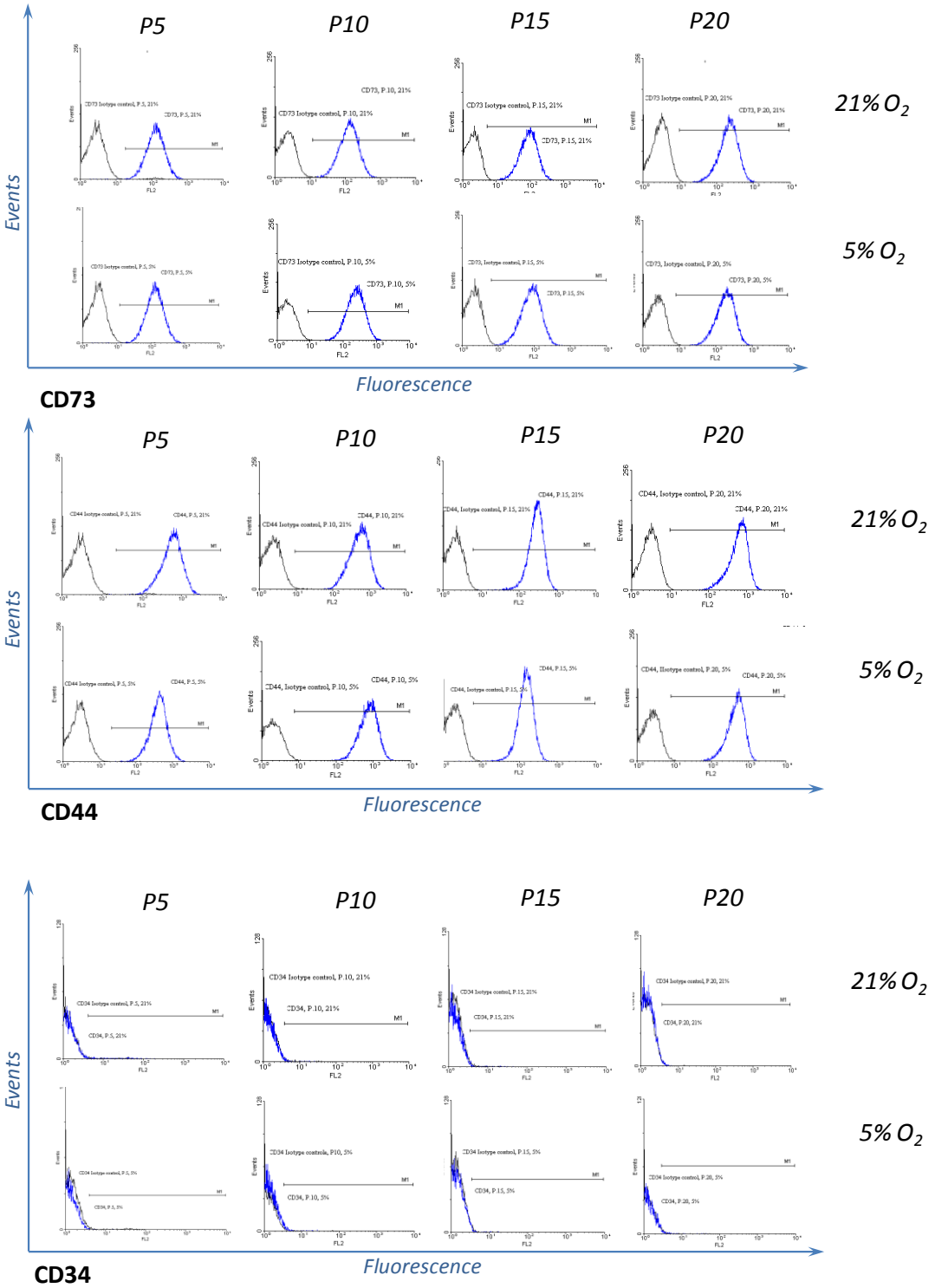

Figure 24: Flow-cytometric analysis of surface antigen expression (CD73, CD44 and CD34) of UC-MSC during long-term cultivation in 5% and 21% oxygen concentration. Grey lines represent isotype control, blue lines – specific antibodies

Table 4.1.11.1: Summarized surface antigen expression during long-term cultivation in 5% and 21% oxygen concentration

Marker	Antigen expression							
	P.5		P.10		P.15		P.20	
	21%	5%	21%	5%	21%	5%	21%	5%
CD31	0.4 %	0.1 %	0.5 %	0.4 %	0.6 %	0.2 %	0.0 %	0.4 %
CD34	0.5 %	0.0 %	0.5 %	0.4 %	0.4 %	0.4 %	0.5 %	0.3 %
CD44	99.9 %	99.9 %	100 %	100 %	100 %	99.9 %	99.9 %	98.3 %
CD73	99.4 %	99.6 %	99.6 %	99.2 %	99.9 %	99.9 %	99.9 %	100 %
CD90	98.9 %	99.5 %	99.7 %	99.9 %	98.0 %	95.2 %	98.2 %	99.6 %
CD105	99.5 %	99.0 %	99.8 %	99.7 %	99.3 %	99.1 %	99.2 %	99.2 %

Table 4.1.11.2: Summarized surface antigen expression during long-term cultivation in 2.5% and 21% oxygen concentration

Marker	Antigen expression							
	P.5		P.10		P.15		P.20	
	21%	2.5%	21%	2.5%	21%	2.5%	21%	2.5%
CD31	0.3 %	0.6 %	0.2 %	0.2 %	0.3 %	0.1 %	0.2 %	1.3 %
CD34	0.8 %	0.8 %	0.1 %	0.3 %	0.4 %	0.6 %	0.6 %	0.4 %
CD44	99.3 %	99.9 %	100 %	100 %	100 %	100 %	99.9 %	99.8 %
CD73	95.6 %	97.32 %	99.3 %	99.8 %	100 %	100 %	99.9 %	100 %
CD90	99.9 %	99.8 %	99.9 %	99.7 %	99.9 %	99.6 %	97.6 %	99.8 %
CD105	99.8 %	97.5 %	97.4 %	99.6 %	99.9 %	98.8 %	97.3 %	97.2 %

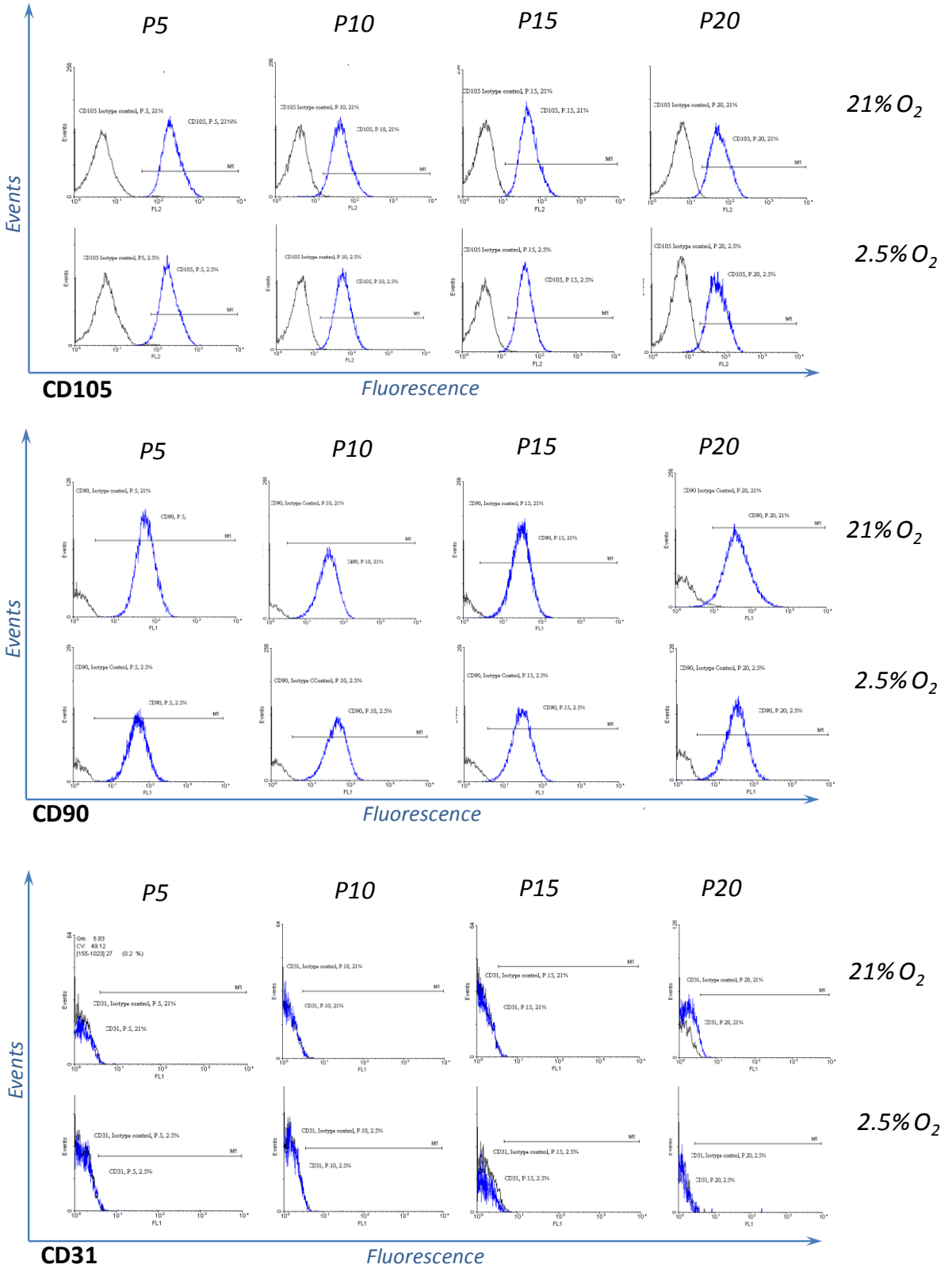

Figure 25: Flow-cytometric analysis of surface antigen expression (CD105, CD90 and CD31) of UC-MSC during long-term cultivation in 2. 5% and 21% oxygen concentration. Grey lines represent isotype control, blue lines – specific antibodies

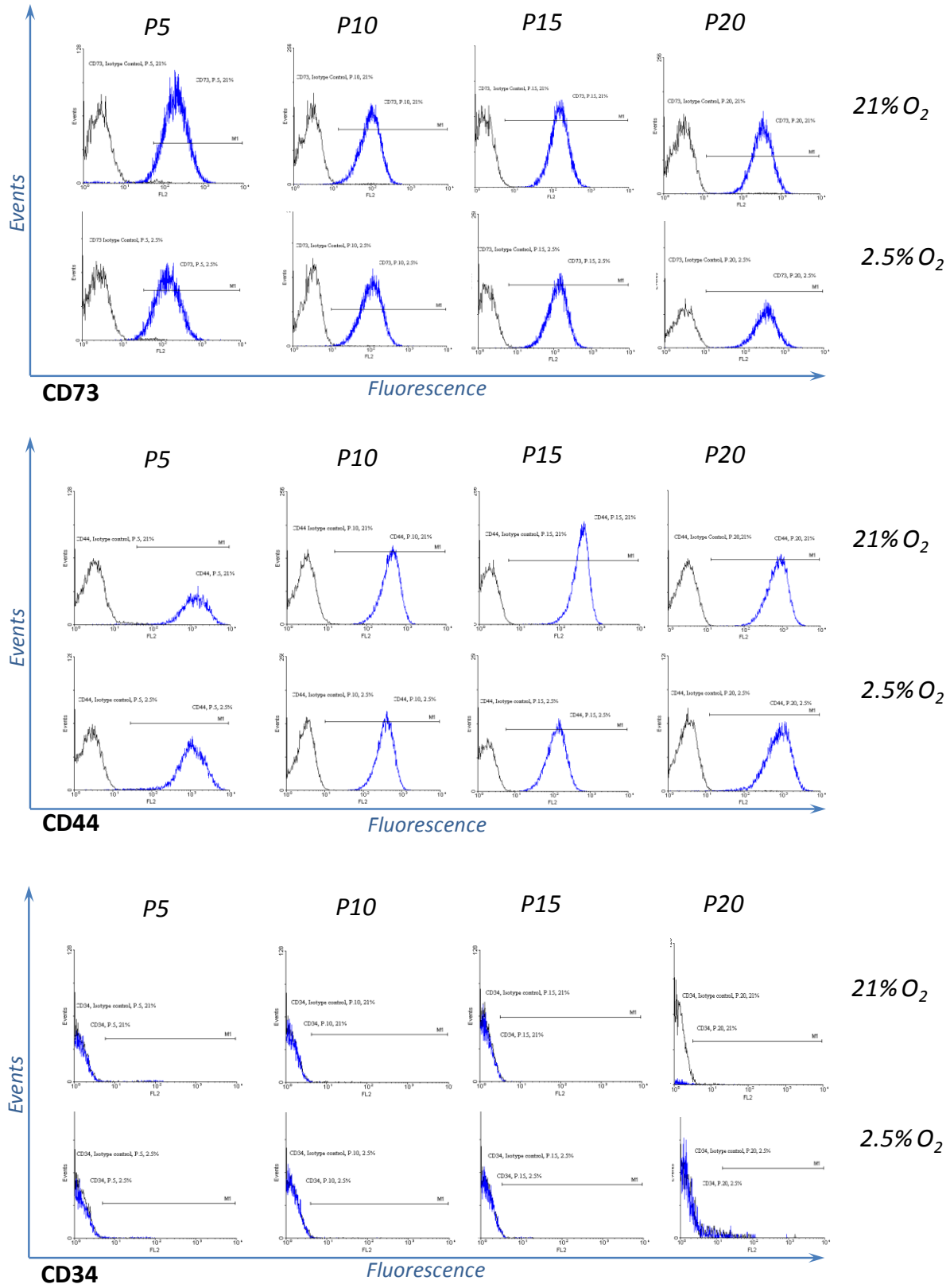

Figure 26: Flow-cytometric analysis of surface antigen expression (CD73, CD44 and CD34) of UC-MSC during long-term cultivation in 2.5% and 21% oxygen concentration. Grey lines represent isotype control, blue lines – specific antibodies

4.1.12 Mitochondrial biogenesis in hypoxic conditions

Mitochondrial biogenesis is a complex process, which is regulated by numerous microenvironmental parameters and which is responsible for sufficient energy supply in eukaryotic cells. Mitochondria are a key component of energy generation and cell survival, since they regulate physiological and stress-related apoptosis via release of caspase activators, loss of mitochondrial transmembrane potential and an altered redox state of the cells [213]. Leakage of electrons during the mitochondrial oxidative phosphorylation and creation of ROS which can damage DNA, proteins and lipids leads to cell dysfunction and death.

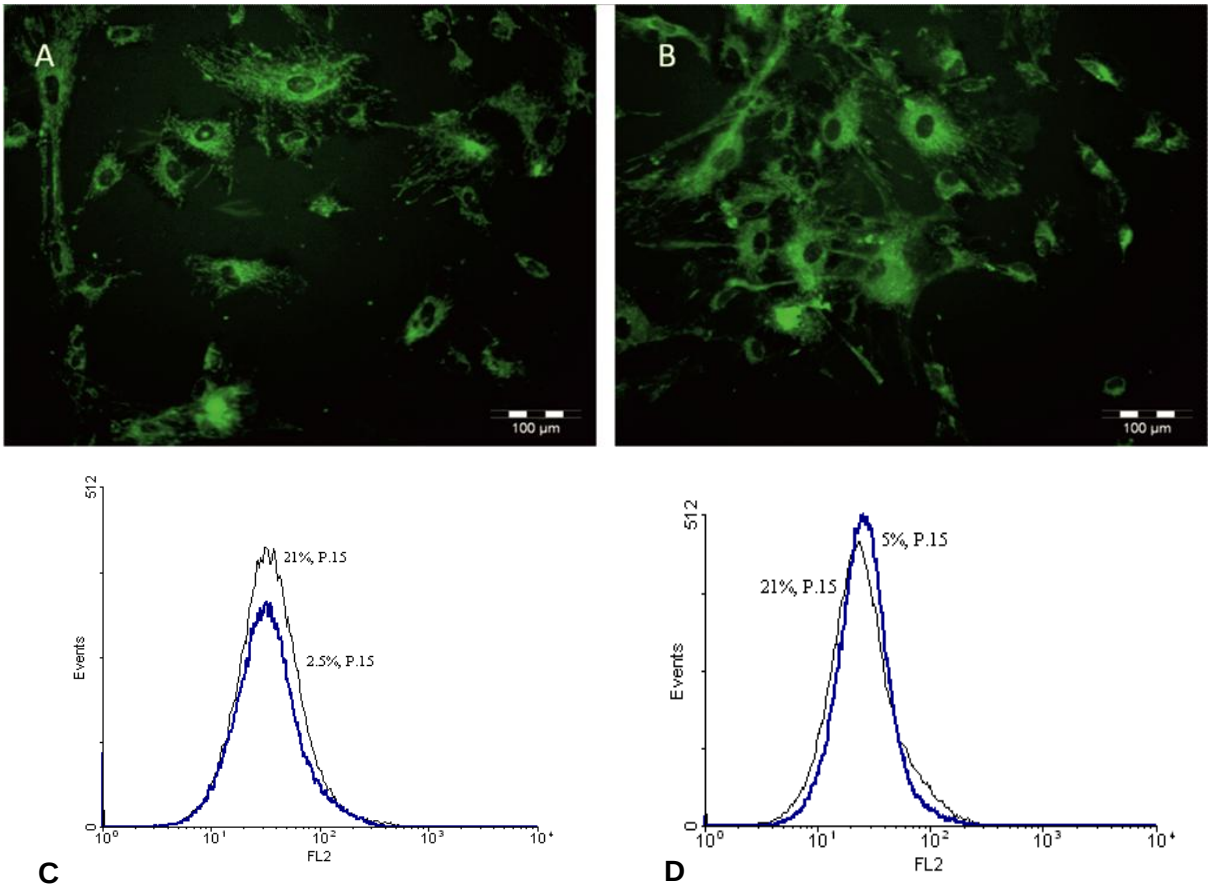

Figure 27: The effect of hypoxia on mitochondrial biogenesis in UC-MSC long-term culture. Cells from three donors were cultivated over 15 passages under 21%, 2.5% and 5% O_2 and stained with mitotracker green. Representative micrograph of UC-MSC from 21% (A) and 2.5% O_2 (B) and flow-cytometric measurements (characterization) of mitochondrial biomass from cells cultivated in 2.5% (blue line) versus 21% O_2 (C) and 5% (blue line) versus 21% O_2 (D) revealed no difference between hypoxic and normoxic cultures

There are many theories how mitochondrial biogenesis is regulated in MSC. It has been suggested that undifferentiated MSC contain less mitochondria than differentiated ones

and the number of mitochondria can be taken as a characteristic of cell stemness [214]. The localization of mitochondria in the cell is different in differentiated and undifferentiated cells [215]. Another explanation of lower mitochondria numbers in undifferentiated cells is a metabolic shift. MSC, like cancer cells, also exhibit the Warburg effect, which is anaerobic glycolytic activity in the presence of sufficient oxygen molecules (aerobic glycolysis). It has been speculated that this effect helps actively dividing progenitor and cancer cells to avoid DNA damage by mitochondrial ROS. Mitochondrial activity is regulated by hypoxia via HIFs and it was shown that in ESC, iPSC and MSC hypoxia is an "enhancer of stemness" [216]. On the other hand, oxygen deficiency can lead to metabolic starvation and cause mitochondrial autophagy under hypoxia [217]. To check if hypoxia causes alteration in mitochondrial mass, UC-MSC cultivated over 15 passages in hypoxia and normoxia were stained with mitotracker green and microscopy, as well as flow cytometry were performed (fig. 27). Mitotracker green binds irreversibly to the mitochondrial membrane and its binding is independent on mitochondrial transmembrane potential. Staining of UC-MSC from hypoxic and normoxic cell cultures revealed no difference in the mitochondrial biomass by microscopic visualization (fig. 27A, B) and flow-cytometric characterization (fig. 27C, D). These findings are not in agreement with data published by Basciano et al., who showed decreased mitochondria biomass in hypoxic culture of BM-MSC [196]. The authors, however, made a wrong conclusion, since the reagent used in their case- mitotracker orange, shows staining intensity dependent on the mitochondrial transmembrane potential, but not on the mitochondrial biomass itself. Moreover, another working group demonstrated in primary human fibroblasts that mitochondrial changes under hypoxia are functional, but not structural and the quantity of mitochondria per cell is not altered at lower oxygen concentration [164].

4.1.13 Differentiation potential after long-term cultivation in hypoxic and normoxic conditions

The ability of MSC to respond to external differentiation factors is an important property of these cells. Expanded *in vitro* over several passages, MSC can lose their differentiation capacity. This phenomenon is called *in vitro* cell aging. It was demonstrated that the differentiation potential of BM-MSC to adipocyte and osteocyte diminished with successive passages [198]. Bork et al. demonstrated changes in the DNA methylation pattern

after long-term cultivation of BM-MSC [218]. Cultivation of the cells in a physiological microenvironment could help to overcome this problem. To investigate the differentiation capacity of UC-MSC during long-term expansion, cells were cultivated under 2.5%, 5% and 21% O_2 over 15 passages and differentiation toward chodrocytes, osteocytes and adipocytes was induced with differentiation media. After 23 days of differentiation in 21% O_2, cells were fixed and stained with von Kossa and calceine staining for osteogenic differentiation, BODIPY staining for adipogenic differentiation and Alcian Blue staining for chondrogenic differentiation.

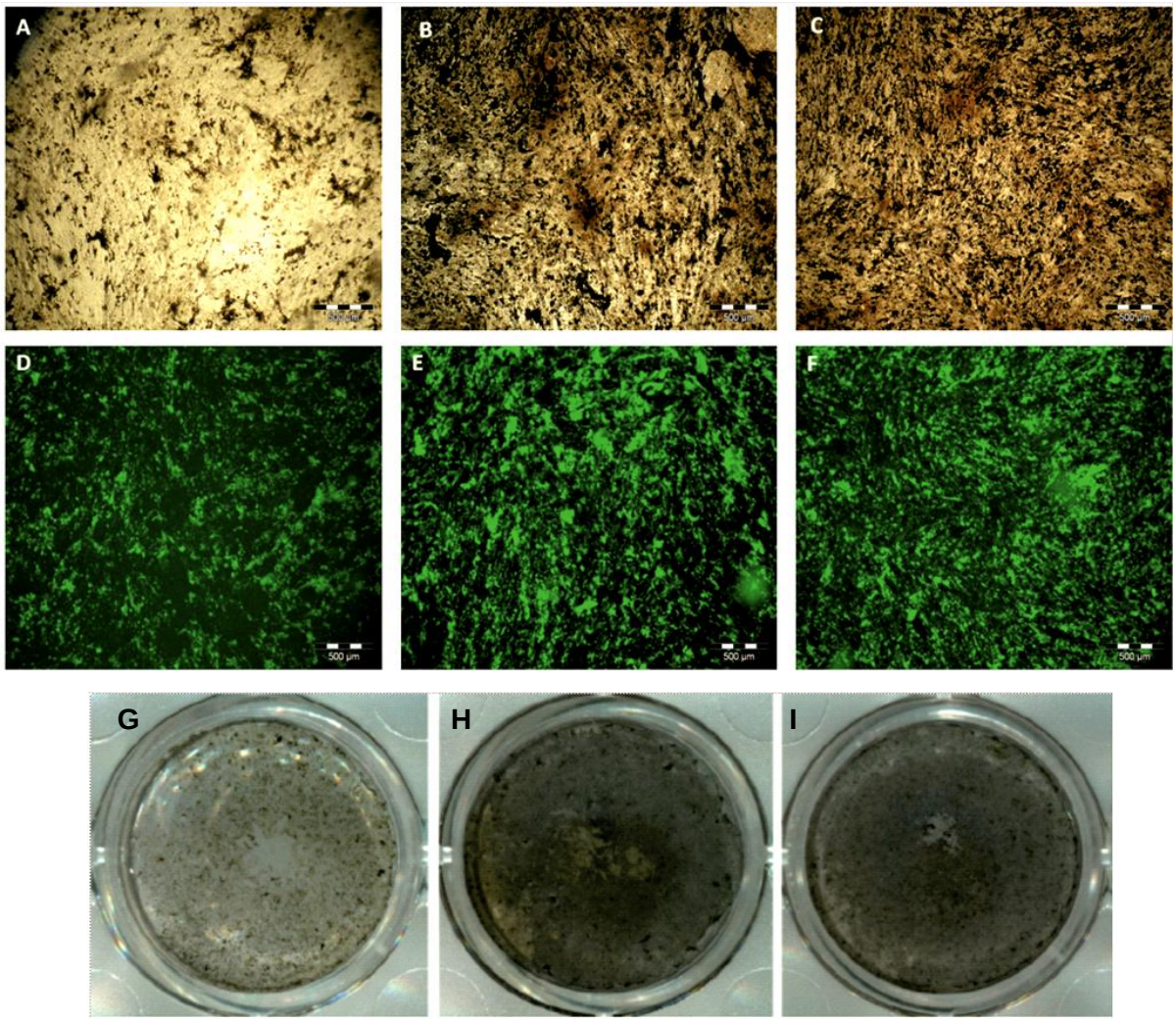

Figure 28: The effect of hypoxia on the osteogenic differentiation potential of UC-MSC after long-term cultivation under 2.5% O_2 (B, E, H) and 5% O_2 (C, F, I) in comparison to 21% O_2 controls (A, D, G). A, B, C – von Kossa staining; D, E, F – calcein staining; G, H, I – von Kossa staining, wells overview

The results of osteogenic differentiation are presented in figure 28. It is clearly seen that cells cultivated in hypoxic conditions had higher degree of differentiation towards

osteocytes, namely a higher calcium deposition. Both, calcein and von Kossa staining were stronger for cells cultivated in 2.5% and 5% oxygen concentration. Indeed, previous studies with BM-MSC showed that expansion of BM-MSC under low oxygen tension (5% [155] and 3% [219]) enhanced subsequent osteogenesis.

Similar results were obtained for adipogenic differentiation (fig. 29). UC-MSC cultivated in 2.5% (fig. 29B) and 5% (fig. 29C) oxygen tension exhibited more lipid droplets when compared to the control at 21% O_2 (fig. 29A).

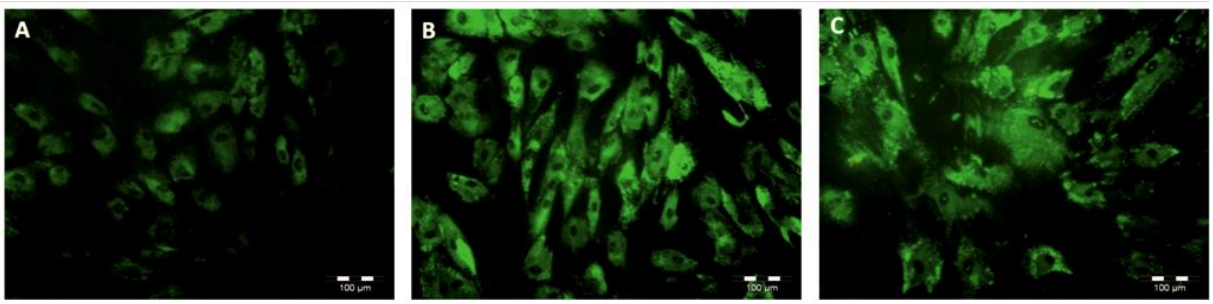

Figure 29: The effect of hypoxia on the adipogenic differentiation potential of UC-MSC after long-term cultivation under 2.5% (B) and 5% O_2 (C) as compared to 21% O_2 control (A). BODIPY staining

In the chondrogenic differentiation experiment, cells cultivated in 2.5% oxygen demonstrated the best results (fig. 30, B) – Alcian Blue staining of acidic proteoglycans was more intense than in cells cultivated in 5% (fig. 30, C) or 21% O_2 (fig. 30, A).

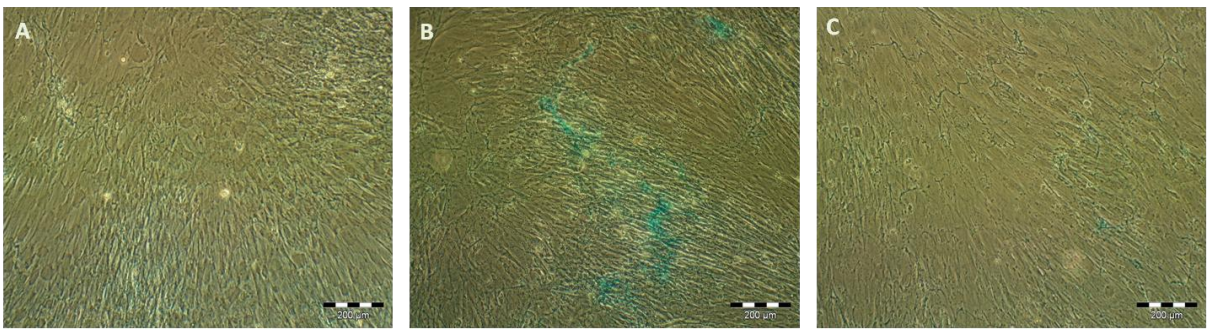

Figure 30: The effect of hypoxia on the chondrogenic differentiation potential of UC-MSC after long-term cultivation under 2.5% O_2 (B) and 5% O_2 (C) as compared to 21% O_2 (A); Alcian Blue staining

Cartilage is an avascular tissue and thus resides in a microenvironment with reduced oxygen concentration. Oxygen concentration in articular cartilage is between 1% and 5% O_2 [220]. It was demonstrated by numerous working groups that hypoxic conditions promote

chondrogenesis of MSC [152-155]. Proliferation under lower oxygen concentration before differentiation can stimulate the expression of transcriptional factors that direct cell fate towards chondrogenesis.

All together, these results demonstrate that lower oxygen tensions seem to be beneficial for the cells in the long-term cultivation and help UC-MSC to retain their ability to differentiate into chondrocytes, adipocytes and osteocytes at late passages (here passage 15).

4.2 Dynamic cultivation

4.2.1 Expansion of UC-MSC in the Z®RP 2000 H bioreactor

Safety requirements and the necessity to obtain high cell numbers without frequent subcultivation of cells raised the question of the possibility of expanding UC-MSC in one-way (single-use) disposable bioreactors. Dynamic cultivation conditions have several advantages in comparison to static cell expansion. First of all, cultivation in a closed system without the need to change the culture medium in a clean bench significantly reduces the risk of possible contamination. Second, the programmed control of all parameters of cultivation together with continuous documentation makes it possible to assure the quality of cells and to avoid human errors. Third, dynamic cultivation systems like bioreactors provide active mass transfer, supplying MSC with gases and nutrients while removing toxic metabolites. Last but not least, there is the argument of production costs - which can be a major obstacle to the spread of MSC clinical applications. In this part of the work, UC-MSC were expanded over 5 days without subcultivation in the Z®RP 2000 H bioreactor (fig. 31) at 21% oxygen tension, and the yield and quality of the expanded cells was studied.

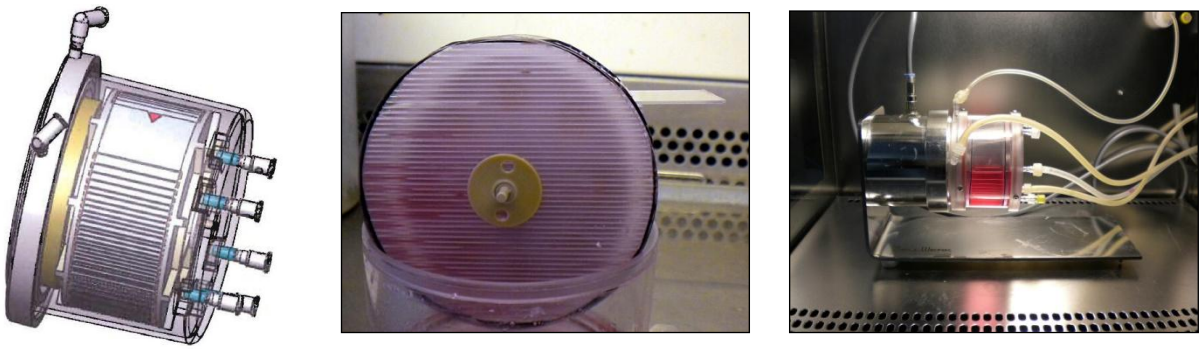

A B C

Figure 31: Disposable bioreactor Z®RP 2000 H (Zellwerk GmbH, Oberkrämer) (A, C) with rotating bed consisted of polycarbonate cell carrier slides (B), total surface area 2000 cm^2 (reactor size 8.8 x 4.6 cm)

4.2.1.1 Cell growth in the Z®RP 2000 H bioreactor

For expansion in the bioreactor, UC-MSC were seeded at a cell density of 1500 cells/cm^2. Since the total surface area of the bioreactor is 2000 cm^2, the entire cell number resulted in 3 x 10^6 cells. Cells were seeded on both sides of the polycarbonate cell carrier slides with 24 hours attaching time for each side. After the attaching phase, dynamic cultivation was started and cells were expanded over 5 days in a rotating system. After 5 days, cells were trypsinized and total cell numbers were estimated with a haemocytometer. The total cell number at the end of the dynamic cultivation was 25 x 10^6 cells for the first cultivation, 22.1 x 10^6 cells for the second cultivation and 26.9 x 10^6 cells for the third cultivation, giving together a mean value of 24.6 ± 2.4 x 10^6 cells and 8.2 ± 0.8-fold expansion. Population doubling time was 39.6 ± 1.8 hours (in static cultivation 31 hours) and the total population doublings were 3.03 ± 0.14.

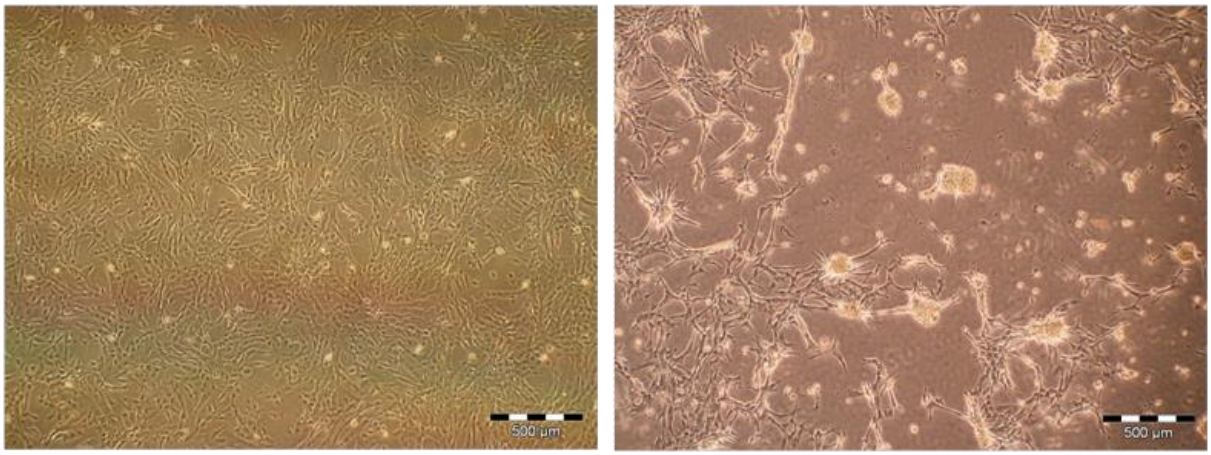

Figure 32: Cell growth on the polycarbonate cell carrier slides after 5 days of cultivation: (A) after static cultivation and (B) after dynamic cultivation

Microscopic imaging of UC-MSC cell growth on the polycarbonate cell carrier slides after 5 days of cultivation demonstrated that under static conditions cells were growing in a monolayer, reaching 90-95% of confluence. In the bioreactor, cells were partially growing in micromass formations composing 3D structures (fig. 32). It was, however, possible to separate the cells with the accutase. Collected UC-MSC also retained their differentiation capacity towards chondrogenic, adipogenic and osteogenic lineages (data are not shown).

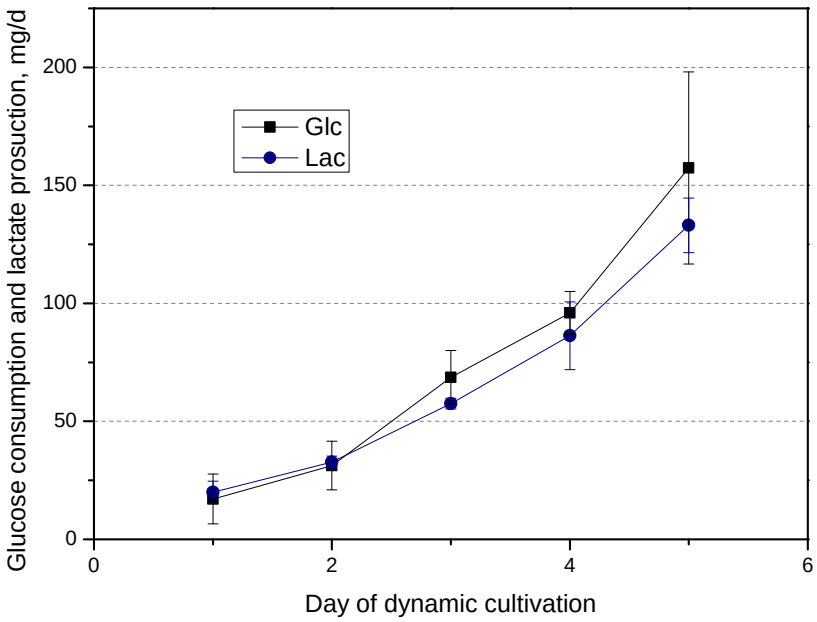

Figure 33: Total glucose consumption and lactate production of UC-MSC cultivated in the Z®RP 2000 H bioreactor

Total glucose consumption and lactate production was increasing during cultivation, reaching 157.3 ± 40.7 mg per day for glucose and 133.0 ± 11.6 mg per day for lactate at day 5 (fig. 33).

4.2.1.2 Cellular senescence after expansion in Z®RP 2000 H bioreactor

While in a long-term UC-MSC cultivation cellular senescence is a desirable outcome, the appearance of senescence during short-term expansion is a sign of non-optimal culture conditions, since senescence is also one of the responses of the cells to stress (stress-induced premature senescence) [221]. To check if the dynamic cultivation of UC-MSC can lead to stress-induced premature senescence, cells were harvested and seeded after expansion in Z®RP 2000 H at a density of 6000 cells/cm^2 in 6-well plates. After 48 hours the cells were fixed and the expression level of senescence-associated β-galactosidase was studied by the Cell Senescence Kit. No expression of β-galactosidase and, consequently, no cellular senescence was detected. Moreover, high proportions of cells undergoing cell division (arrows) could be observed, indicating that UC-MSC expanded in the bioreactor did not lose their mitotic activity (fig. 34).

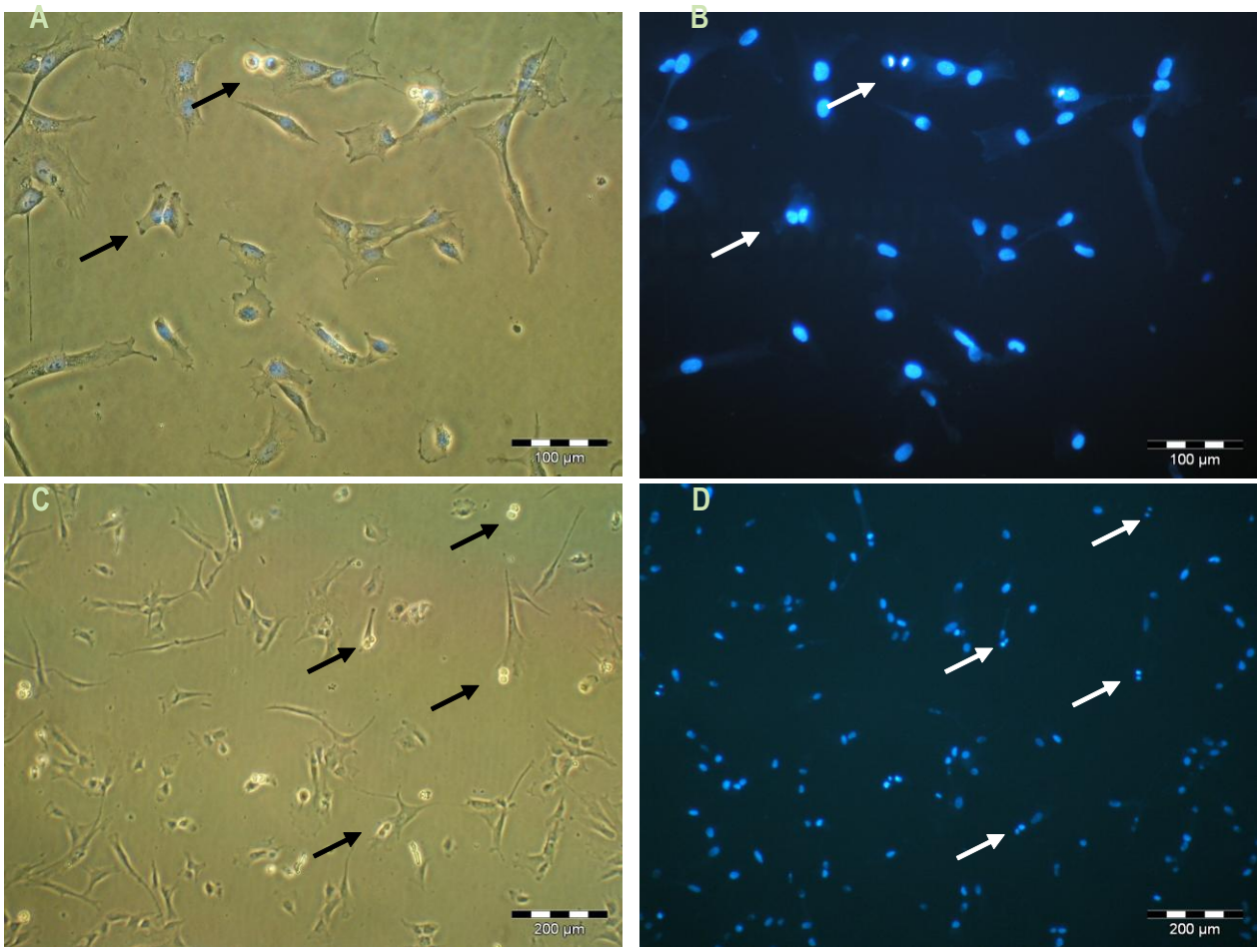

Figure 34: Senescence-associated β-galactosidase staining of UC-MSC cultivated in the Z®RP 2000 H bioreactor: (A) β-galactosidase and (B) DAPI-staining, magnification x50; (C) β-galactosidase and (D) DAPI-staining, magnification x20

4.2.1.3 Surface immunophenotype characterization of UC-MSC after expansion in the Z®RP 2000 H bioreactor

After expansion in the Z®RP 2000 H bioreactor, UC-MSC were harvested and analyzed by flow cytometry after staining with FITC- or PE-conjugated antibodies against CD31, CD34, CD44, CD45, CD73, CD90, CD105 and isotype control immunoglobulins. Flow cytometric analysis of UC-MSC showed that they were negative for hematopoietic (CD34, CD45) and endothelial (CD31) markers and were strongly positive for specific immunophenotypic MSC markers (CD44, CD73, CD90 and CD105) (fig. 35)

Marker	Expression, %
CD31	0.0 %
CD34	0.3 %
CD44	98.3 %
CD45	0.3 %
CD73	99.9 %
CD90	98.1 %
CD105	99.8 %

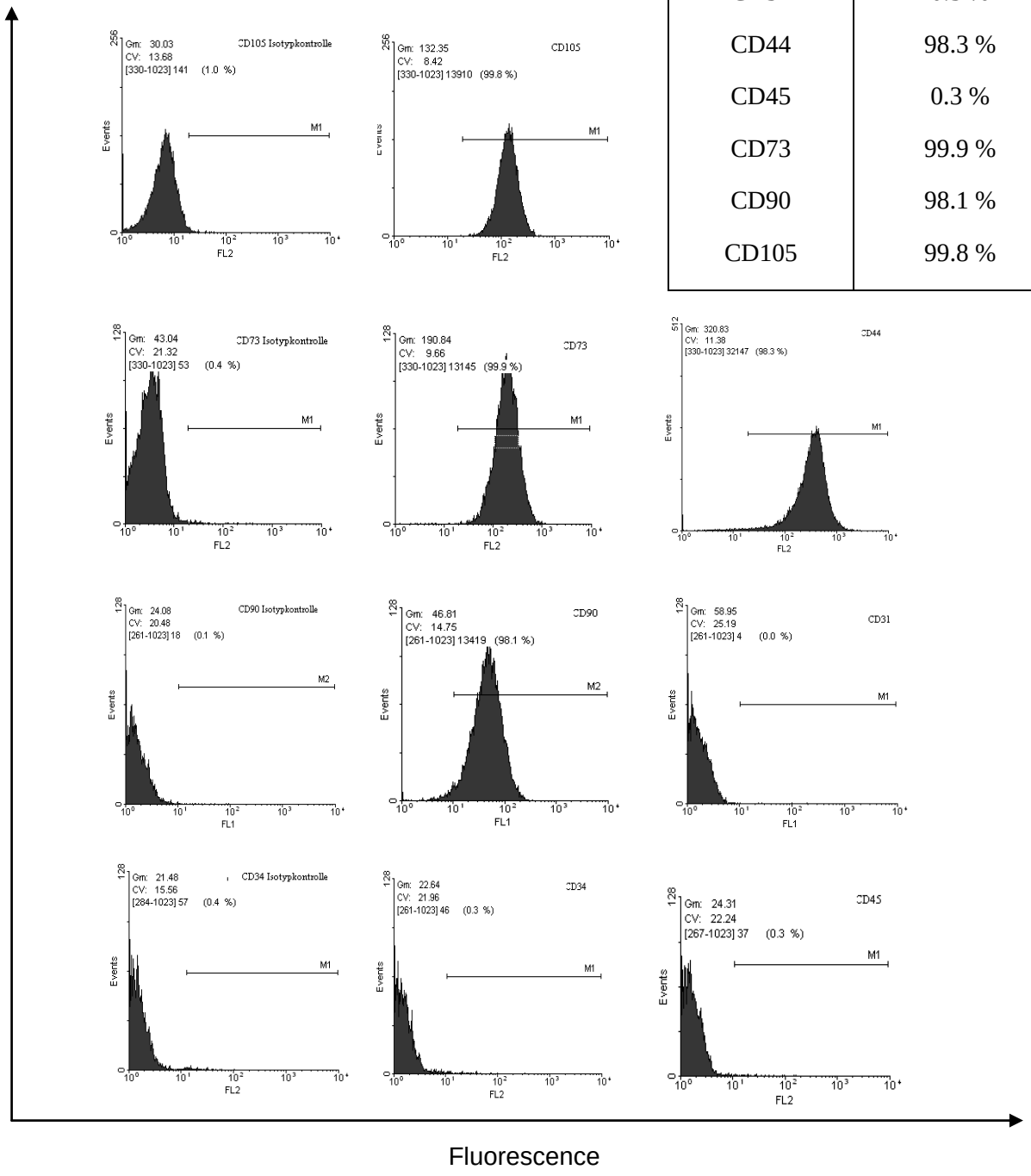

Figure 35: Flow-cytometric analysis of UC-MSC expanded in the Z®RP 2000 H bioreactor.

Taken together, the results of the dynamic cultivation show that this system is suitable for UC-MSC expansion. Moreover, newly developed reactors with a higher volume and

surface area (Z®RP 6000 H with 6000 cm^2) will make it possible to obtain higher cell numbers in one reactor run without passaging. Another development would be dynamic cell expansion under hypoxic conditions, which could be useful to obtain a higher yield of cell numbers within a shorter period of time (like in a static cultivation). To perform such a cultivation, however, all components of the system must be gas-tight, including connection tubes. Unfortunately, there are no clinically approved gas-tight tubes available on the market currently, but since interest in hypoxia is rising, it may soon result in the development of such a product.

5 Conclusions and outlook

Two different strategies were investigated in this work in order to optimize the yield and quality of *in vitro* expanded UC-MSC. In the first approach, the influence of oxygen concentration on the static cultivation of UC-MSC was explored. The second method involved dynamic cultivations in a disposable Z®RP 2000 H bioreactor.

Short-term cultivation under hypoxia (1.5%, 2.5% and 5% O_2) revealed that at an oxygen concentration of 2.5% UC-MSC significantly increased their proliferative capacity, while no changes in proliferation at 1.5% O_2 were observed. There was only a minor increase in proliferative capacity at 5% O_2 when compared to the control (21% O_2). Cultivation of UC-derived human MSC at 1.5% O_2 revealed little if any increase in apoptosis and no increase in necrosis. This means that UC-MSC can survive and proliferate at oxygen concentrations approaching pathological hypoxia. The results from the present study reveal that UC-derived stem cells adapt their oxygen consumption and the accompanying energy metabolism according to available oxygen concentrations. 300 genes were differently expressed under hypoxia (2.5% O_2) when compared to 21% oxygen concentration. Gene expression analysis of selected cytokines revealed an up-regulation of IGFBP3, IGFBP6, SCF-R and VEGF mRNA expression. HBEGF was significantly down-regulated. On the protein level, expression of 35 cytokines and receptors was analyzed and among them 17 proteins could be quantified. Almost all analysed proteins were up-regulated, but up-regulation was statistically significant in only five proteins (IGFBP6, IGFBP2, FGF-7, VEGF-R2 and SCF-R). These data suggest that under hypoxia (2.5%) paracrine and autocrine activities of UC-MSC are increased when compared to the normoxic (21%) control. UC-MSC also increased their migratory activity at 2.5% oxygen concentration. Taken together, these data demonstrate that MSC adapt to the microenvironmental conditions and even short-term (3 days) cultivation under hypoxia changes their metabolic and paracrine activity.

Long-term cultivation (over 25 passages within 3 months) demonstrated that higher cell numbers can be obtained at hypoxic conditions (2.5% and 5% O_2) if compared to 21% oxygen concentration. After 25 passages cells underwent a replicative senescence and stopped to divide, both in hypoxic and normoxic conditions. This finding is important, since replicative senescence is a significant *in vivo* anti-cancer mechanism and UC-MSC expanded *ex vivo* can be applied in patients with less risk of neoplastic MSC-transformation. It is unlikely that UC-MSC will be expanded for clinical use *in vitro* for more than 10 passages,

since expansion over 10 passages already yields up to a 1000-fold increase in cell numbers. UC-MSC cultivated over 10 passages were studied for their oncogene expression profiles. No expression of hTERT was observed after UC-MSC cultivation over 10 passages, both in hypoxic (2.5% and 5% O_2) and normoxic (21% O_2) conditions. Expression profiles of p53, H-RAS and C-MYC remained unchanged. Surface marker expression was also unaltered during long-term expansion in 2.5%, 5% and 21% oxygen concentrations. Also, cultivation under hypoxia did not influence mitochondrial biogenesis. UC-MSC cultivated under hypoxia showed better retention of their adipogenic and osteogenic differentiation capacities after 15 passages. Chondrogenic differentiation capacity was maintained only by UC-MSC cultivated at 2.5% oxygen concentration. Taken together, these data demonstrate that hypoxic conditions are beneficial for UC-MSC expansion. Moreover, long-term cultivation under hypoxia did not lead to spontaneous differentiation and neoplastic transformation.

In the last part of this work, UC-MSC were expanded over 5 days without subcultivation in the Z®RP 2000 H bioreactor under 21% oxygen concentration. Dynamic cultivation in disposable bioreactors has several advantages in comparison to traditional static cultivation in cell culture flasks. The improved documentation process, the fully-automated control and the lower risk of cross-contamination makes this technique very attractive for future GMP-conform MSC expansion. Partial medium exchange helps in maintaining the homeostatic *in vitro* microenvironment, e.g. signal molecules and cytokines produced by the UC-MSC. Cultivation of UC-MSC in the bioreactor over 5 days resulted in their 8-fold expansion. Although the UC-MSC in the bioreactor were partially growing in micromass-formations composing 3D structures, it was possible to separate the cells with accutase treatment. Moreover, the cells retained their MSC-properties with regard to immunophenotype surface marker expression, differentiational and proliferational capacities.

This study demonstrated for the first time that expansion of UC-MSC in hypoxic conditions can be beneficial for the cells and does not lead to their spontaneous *in vitro* transformation. The cultivation of MSC in hypoxic conditions is a new, fast-developing field in basic research, as well as in applied biotechnology. Since current cultivation techniques, chemicals and analytics were developed for atmospheric oxygen concentrations, new methods and protocols should be introduced for MSC cultivation under hypoxia. One example of such a new approach is the indirect cell proliferation analysis, since the majority of existing kits and methods are based on cell metabolic activities and cannot be used in unequal reduction-oxidation states.

It is feasible to expand MSC under dynamic conditions in a Z®RP 2000 H bioreactor, making it possible to obtain high yield of UC-MSC without their subcultivation. Combination of hypoxic and dynamic cultivation in the future can lead to the improvement of the UC-MSC yield and quality during *in vitro* UC-MSC expansion, and can improve cell survival after transplantation.

6 References

1. Prockop DJ: **Marrow stromal cells as stem cells for nonhematopoietic tissues.** *Science* 1997, **276:**71-74.

2. Friedenstein AJ, Chailakhjan RK, Lalykina KS: **The development of fibroblast colonies in monolayer cultures of guinea-pig bone marrow and spleen cells.** *Cell Tissue Kinet* 1970, **3:**393-403.

3. Dominici M, Le Blanc K, Mueller I, Slaper-Cortenbach I, Marini F, Krause D, Deans R, Keating A, Prockop D, Horwitz E: **Minimal criteria for defining multipotent mesenchymal stromal cells. The International Society for Cellular Therapy position statement.** *Cytotherapy* 2006, **8:**315-317.

4. Tuan RS, Boland G, Tuli R: **Adult mesenchymal stem cells and cell-based tissue engineering.** *Arthritis Res Ther* 2003, **5:**32-45.

5. Baglioni S, Francalanci M, Squecco R, Lombardi A, Cantini G, Angeli R, Gelmini S, Guasti D, Benvenuti S, Annunziato F, et al: **Characterization of human adult stem-cell populations isolated from visceral and subcutaneous adipose tissue.** *FASEB J* 2009, **23:**3494-3505.

6. Alsalameh S, Amin R, Gemba T, Lotz M: **Identification of mesenchymal progenitor cells in normal and osteoarthritic human articular cartilage.** *Arthritis Rheum* 2004, **50:**1522-1532.

7. Huang AH, Chen YK, Chan AW, Shieh TY, Lin LM: **Isolation and characterization of human dental pulp stem/stromal cells from nonextracted crown-fractured teeth requiring root canal therapy.** *J Endod* 2009, **35:**673-681.

8. Patki S, Kadam S, Chandra V, Bhonde R: **Human breast milk is a rich source of multipotent mesenchymal stem cells.** *Hum Cell* 2010, **23:**35-40.

9. Zvaifler NJ, Marinova-Mutafchieva L, Adams G, Edwards CJ, Moss J, Burger JA, Maini RN: **Mesenchymal precursor cells in the blood of normal individuals.** *Arthritis Res* 2000, **2:**477-488.

10. Gang EJ, Hong SH, Jeong JA, Hwang SH, Kim SW, Yang IH, Ahn C, Han H, Kim H: **In vitro mesengenic potential of human umbilical cord blood-derived mesenchymal stem cells.** *Biochem Biophys Res Commun* 2004, **321:**102-108.

11. Tang XP, Zhang M, Yang X, Chen LM, Zeng Y: **Differentiation of human umbilical cord blood stem cells into hepatocytes in vivo and in vitro.** *World J Gastroenterol* 2006, **12:**4014-4019.

12. Jazedje T, Secco M, Vieira NM, Zucconi E, Gollop TR, Vainzof M, Zatz M: **Stem cells from umbilical cord blood do have myogenic potential, with and without differentiation induction in vitro.** *J Transl Med* 2009, **7:**6.

13. Berger MJ, Adams SD, Tigges BM, Sprague SL, Wang XJ, Collins DP, McKenna DH: **Differentiation of umbilical cord blood-derived multilineage progenitor cells into respiratory epithelial cells.** *Cytotherapy* 2006, **8:**480-487.

14. Zhang Y, McNeill E, Tian H, Soker S, Andersson KE, Yoo JJ, Atala A: **Urine derived cells are a potential source for urological tissue reconstruction.** *J Urol* 2008, **180:**2226-2233.

15. Witkowska-Zimny M, Wrobel E: **Perinatal sources of mesenchymal stem cells: Wharton's jelly, amnion and chorion.** *Cell Mol Biol Lett,* **16:**493-514.

16. Moretti P, Hatlapatka T, Marten D, Lavrentieva A, Majore I, Hass R, Kasper C: **Mesenchymal stromal cells derived from human umbilical cord tissues: primitive cells with potential for clinical and tissue engineering applications.** *Adv Biochem Eng Biotechnol* 2010, **123:**29-54.

17. Majore I, Moretti P, Stahl F, Hass R, Kasper C: **Growth and differentiation properties of mesenchymal stromal cell populations derived from whole human umbilical cord.** *Stem Cell Rev* 2011, **7:**17-31.

18. Le Blanc K, Tammik L, Sundberg B, Haynesworth SE, Ringden O: **Mesenchymal stem cells inhibit and stimulate mixed lymphocyte cultures and mitogenic responses independently of the major histocompatibility complex.** *Scandinavian Journal of Immunology* 2003, **57:**11-20.

19. Zuk PA, Zhu M, Ashjian P, De Ugarte DA, Huang JI, Mizuno H, Alfonso ZC, Fraser JK, Benhaim P, Hedrick MH: **Human adipose tissue is a source of multipotent stem cells.** *Molecular Biology of the Cell* 2002, **13:**4279-4295.

20. Kern S, Eichler H, Stoeve J, Kluter H, Bieback K: **Comparative analysis of mesenchymal stem cells from bone marrow, umbilical cord blood, or adipose tissue.** *Stem Cells* 2006, **24:**1294-1301.

21. Di Nicola M, Carlo-Stella C, Magni M, Milanesi M, Longoni PD, Matteucci P, Grisanti S, Gianni AM: **Human bone marrow stromal cells suppress T-lymphocyte proliferation induced by cellular or nonspecific mitogenic stimuli.** *Blood* 2002, **99:**3838-3843.

22. Selmani Z, Naji A, Zidi I, Favier B, Gaiffe E, Obert L, Borg C, Saas P, Tiberghien P, Rouas-Freiss N, et al: **Human leukocyte antigen-G5 secretion by human mesenchymal stem cells is required to suppress T lymphocyte and natural killer function and to induce CD4+CD25highFOXP3+ regulatory T cells.** *Stem Cells* 2008, **26:**212-222.

23. Jiang XX, Zhang Y, Liu B, Zhang SX, Wu Y, Yu XD, Mao N: **Human mesenchymal stem cells inhibit differentiation and function of monocyte-derived dendritic cells.** *Blood* 2005, **105:**4120-4126.

24. Corcione A, Benvenuto F, Ferretti E, Giunti D, Cappiello V, Cazzanti F, Risso M, Gualandi F, Mancardi GL, Pistoia V, Uccelli A: **Human mesenchymal stem cells modulate B-cell functions.** *Blood* 2006, **107:**367-372.

25. Lund RD, Wang S, Lu B, Girman S, Holmes T, Sauve Y, Messina DJ, Harris IR, Kihm AJ, Harmon AM, et al: **Cells isolated from umbilical cord tissue rescue photoreceptors and visual functions in a rodent model of retinal disease.** *Stem Cells* 2007, **25:**602-611.

26. Jones J, Jaramillo-Merchan J, Bueno C, Pastor D, Viso-Leon M, Martinez S: **Mesenchymal stem cells rescue Purkinje cells and improve motor functions in a mouse model of cerebellar ataxia.** *Neurobiol Dis* 2010, **40:**415-423.

27. Morigi M, Imberti B, Zoja C, Corna D, Tomasoni S, Abbate M, Rottoli D, Angioletti S, Benigni A, Perico N, et al: **Mesenchymal stem cells are renotropic, helping to repair the kidney and improve function in acute renal failure.** *J Am Soc Nephrol* 2004, **15:**1794-1804.

28. Lin YT, Chern Y, Shen CK, Wen HL, Chang YC, Li H, Cheng TH, Hsieh-Li HM: **Human mesenchymal stem cells prolong survival and ameliorate motor deficit through trophic support in Huntington's disease mouse models.** *PLoS One* 2011, **6:**e22924.

29. Tate CC, Fonck C, McGrogan M, Case CC: **Human mesenchymal stromal cells and their derivative, SB623 cells, rescue neural cells via trophic support following in vitro ischemia.** *Cell Transplant* 2010, **19:**973-984.

30. Walter MN, Wright KT, Fuller HR, MacNeil S, Johnson WE: **Mesenchymal stem cell-conditioned medium accelerates skin wound healing: an in vitro study of fibroblast and keratinocyte scratch assays.** *Exp Cell Res* 2010, **316:**1271-1281.

31. Angoulvant D, Ivanes F, Ferrera R, Matthews PG, Nataf S, Ovize M: **Mesenchymal stem cell conditioned media attenuates in vitro and ex vivo myocardial reperfusion injury.** *J Heart Lung Transplant* 2011, **30:**95-102.

32. Neuhuber B, Timothy Himes B, Shumsky JS, Gallo G, Fischer I: **Axon growth and recovery of function supported by human bone marrow stromal cells in the injured spinal cord exhibit donor variations.** *Brain Res* 2005, **1035:**73-85.

33. Wilkins A, Kemp K, Ginty M, Hares K, Mallam E, Scolding N: **Human bone marrow-derived mesenchymal stem cells secrete brain-derived neurotrophic factor which promotes neuronal survival in vitro.** *Stem Cell Res* 2009.

34. Sordi V: **Mesenchymal stem cell homing capacity.** *Transplantation* 2009, **87:**S42-45.

35. Lu D, Mahmood A, Wang L, Li Y, Lu M, Chopp M: **Adult bone marrow stromal cells administered intravenously to rats after traumatic brain injury migrate into brain and improve neurological outcome.** *Neuroreport* 2001, **12:**559-563.

36. Lu D, Li Y, Wang L, Chen J, Mahmood A, Chopp M: **Intraarterial administration of marrow stromal cells in a rat model of traumatic brain injury.** *J Neurotrauma* 2001, **18:**813-819.

37. Chen J, Li Y, Wang L, Lu M, Zhang X, Chopp M: **Therapeutic benefit of intracerebral transplantation of bone marrow stromal cells after cerebral ischemia in rats.** *J Neurol Sci* 2001, **189:**49-57.

38. Askari AT, Unzek S, Popovic ZB, Goldman CK, Forudi F, Kiedrowski M, Rovner A, Ellis SG, Thomas JD, DiCorleto PE, et al: **Effect of stromal-cell-derived factor 1 on stem-cell homing and tissue regeneration in ischaemic cardiomyopathy.** *Lancet* 2003, **362:**697-703.

39. Wang Y, Johnsen HE, Mortensen S, Bindslev L, Ripa RS, Haack-Sorensen M, Jorgensen E, Fang W, Kastrup J: **Changes in circulating mesenchymal stem cells, stem cell homing factor, and vascular growth factors in patients with acute ST elevation myocardial infarction treated with primary percutaneous coronary intervention.** *Heart* 2006, **92:**768-774.

40. Mansilla E, Marin GH, Drago H, Sturla F, Salas E, Gardiner C, Bossi S, Lamonega R, Guzman A, Nunez A, et al: **Bloodstream cells phenotypically identical to human mesenchymal bone marrow stem cells circulate in large amounts under the influence of acute large skin damage: new evidence for their use in regenerative medicine.** *Transplant Proc* 2006, **38:**967-969.

41. Majore I, Moretti P, Hass R, Kasper C: **Identification of subpopulations in mesenchymal stem cell-like cultures from human umbilical cord.** *Cell Commun Signal* 2009, **7:**6.

42. Fong CY, Richards M, Manasi N, Biswas A, Bongso A: **Comparative growth behaviour and characterization of stem cells from human Wharton's jelly.** *Reproductive Biomedicine Online* 2007, **15:**708-718.

43. Bongso A, Fong CY, Gauthaman K: **Taking Stem Cells to the Clinic: Major Challenges.** *Journal of Cellular Biochemistry* 2008, **105:**1352-1360.

44. Weiss ML, Medicetty S, Bledsoe AR, Rachakatla RS, Choi M, Merchav S, Luo Y, Rao MS, Velagaleti G, Troyer D: **Human umbilical cord matrix stem cells: preliminary characterization and effect of transplantation in a rodent model of Parkinson's disease.** *Stem Cells* 2006, **24:**781-792.

45. Jomura S, Uy M, Mitchell K, Dallasen R, Bode CJ, Xu Y: **Potential treatment of cerebral global ischemia with Oct-4+ umbilical cord matrix cells.** *Stem Cells* 2007, **25:**98-106.

46. Hu SL, Lu PG, Zhang LJ, Li F, Chen Z, Wu N, Meng H, Lin JK, Feng H: **In vivo magnetic resonance imaging tracking of SPIO-labeled human umbilical cord mesenchymal stem cells.** *J Cell Biochem* 2012, **113:**1005-1012.

47. Ferrara JL, Levine JE, Reddy P, Holler E: **Graft-versus-host disease.** *Lancet* 2009, **373:**1550-1561.

48. Ringden O, Uzunel M, Rasmusson I, Remberger M, Sundberg B, Lonnies H, Marschall HU, Dlugosz A, Szakos A, Hassan Z, et al: **Mesenchymal stem cells for treatment of therapy-resistant graft-versus-host disease.** *Transplantation* 2006, **81:**1390-1397.

49. Lin Y, Hogan WJ: **Clinical Application of Mesenchymal Stem Cells in the Treatment and Prevention of Graft-versus-Host Disease.** *Adv Hematol* 2011, **2011:**427863.

50. Britten MB, Abolmaali ND, Assmus B, Lehmann R, Honold J, Schmitt J, Vogl TJ, Martin H, Schachinger V, Dimmeler S, Zeiher AM: **Infarct remodeling after intracoronary progenitor cell treatment in patients with acute myocardial infarction (TOPCARE-AMI): mechanistic insights from serial contrast-enhanced magnetic resonance imaging.** *Circulation* 2003, **108:**2212-2218.

51. Leistner DM, Fischer-Rasokat U, Honold J, Seeger FH, Schachinger V, Lehmann R, Martin H, Burck I, Urbich C, Dimmeler S, et al: **Transplantation of progenitor cells and regeneration enhancement in acute myocardial infarction (TOPCARE-AMI): final 5-year results suggest long-term safety and efficacy.** *Clin Res Cardiol* 2011, **100:**925-934.

52. Assmus B, Fischer-Rasokat U, Honold J, Seeger FH, Fichtlscherer S, Tonn T, Seifried E, Schachinger V, Dimmeler S, Zeiher AM: **Transcoronary transplantation of functionally competent BMCs is associated with a decrease in natriuretic peptide serum levels and improved survival of patients with chronic postinfarction heart failure: results of the TOPCARE-CHD Registry.** *Circ Res* 2007, **100:**1234-1241.

53. Holinski S, Schmeck B, Claus B, Radtke H, Elgeti T, Holzhausen M, Konertz W: **Encouraging experience with intracardiac transplantation of unselected autologous bone marrow cells concomitant with coronary artery bypass surgery after myocardial infarction.** *Ann Thorac Cardiovasc Surg* 2011, **17:**383-389.

54. Wong RS: **Mesenchymal stem cells: angels or demons?** *J Biomed Biotechnol* 2011, **2011:**459510.

55. Mohseny AB, Hogendoorn PC: **Concise review: mesenchymal tumors: when stem cells go mad.** *Stem Cells* 2011, **29:**397-403.

56. Lazennec G, Jorgensen C: **Concise review: adult multipotent stromal cells and cancer: risk or benefit?** *Stem Cells* 2008, **26:**1387-1394.

57. Amariglio N, Hirshberg A, Scheithauer BW, Cohen Y, Loewenthal R, Trakhtenbrot L, Paz N, Koren-Michowitz M, Waldman D, Leider-Trejo L, et al: **Donor-derived brain tumor following neural stem cell transplantation in an ataxia telangiectasia patient.** *PLoS Med* 2009, **6:**e1000029.

58. Rosland GV, Svendsen A, Torsvik A, Sobala E, McCormack E, Immervoll H, Mysliwietz J, Tonn JC, Goldbrunner R, Lonning PE, et al: **Long-term cultures of bone marrow-derived human mesenchymal stem cells frequently undergo spontaneous malignant transformation.** *Cancer Res* 2009, **69:**5331-5339.

59. Bernardo ME, Zaffaroni N, Novara F, Cometa AM, Avanzini MA, Moretta A, Montagna D, Maccario R, Villa R, Daidone MG, et al: **Human bone marrow derived mesenchymal stem cells do not undergo transformation after long-term in vitro culture and do not exhibit telomere maintenance mechanisms.** *Cancer Res* 2007, **67:**9142-9149.

60. Rubio D, Garcia-Castro J, Martin MC, de la Fuente R, Cigudosa JC, Lloyd AC, Bernad A: **Spontaneous human adult stem cell transformation.** *Cancer Res* 2005, **65:**3035-3039.

61. **Identity crisis.** *Nature* 2009, **457:**935-936.

62. Torsvik A, Rosland GV, Svendsen A, Molven A, Immervoll H, McCormack E, Lonning PE, Primon M, Sobala E, Tonn JC, et al: **Spontaneous malignant transformation of human mesenchymal stem cells reflects cross-contamination: putting the research field on track - letter.** *Cancer Res* 2010, **70:**6393-6396.

63. Garcia S, Bernad A, Martin MC, Cigudosa JC, Garcia-Castro J, de la Fuente R: **Pitfalls in spontaneous in vitro transformation of human mesenchymal stem cells.** *Exp Cell Res* 2010, **316:**1648-1650.

64. Sharpless NE, DePinho RA: **Telomeres, stem cells, senescence, and cancer.** *J Clin Invest* 2004, **113:**160-168.

65. Shiras A, Chettiar ST, Shepal V, Rajendran G, Prasad GR, Shastry P: **Spontaneous transformation of human adult nontumorigenic stem cells to cancer stem cells is driven by genomic instability in a human model of glioblastoma.** *Stem Cells* 2007, **25:**1478-1489.

66. Miura M, Miura Y, Padilla-Nash HM, Molinolo AA, Fu B, Patel V, Seo BM, Sonoyama W, Zheng JJ, Baker CC, et al: **Accumulated chromosomal instability in murine bone marrow mesenchymal stem cells leads to malignant transformation.** *Stem Cells* 2006, **24:**1095-1103.

67. Burns JS, Abdallah BM, Guldberg P, Rygaard J, Schroder HD, Kassem M: **Tumorigenic heterogeneity in cancer stem cells evolved from long-term cultures of telomerase-immortalized human mesenchymal stem cells.** *Cancer Res* 2005, **65:**3126-3135.

68. Rodriguez R, Rubio R, Masip M, Catalina P, Nieto A, de la Cueva T, Arriero M, San Martin N, de la Cueva E, Balomenos D, et al: **Loss of p53 induces tumorigenesis in p21-deficient mesenchymal stem cells.** *Neoplasia* 2009, **11:**397-407.

69. Spaeth E, Klopp A, Dembinski J, Andreeff M, Marini F: **Inflammation and tumor microenvironments: defining the migratory itinerary of mesenchymal stem cells.** *Gene Ther* 2008, **15:**730-738.

70. Dvorak HF: **Tumors: wounds that do not heal. Similarities between tumor stroma generation and wound healing.** *N Engl J Med* 1986, **315:**1650-1659.

71. Loebinger MR, Kyrtatos PG, Turmaine M, Price AN, Pankhurst Q, Lythgoe MF, Janes SM: **Magnetic resonance imaging of mesenchymal stem cells homing to pulmonary metastases using biocompatible magnetic nanoparticles.** *Cancer Res* 2009, **69:**8862-8867.

72. Sasportas LS, Kasmieh R, Wakimoto H, Hingtgen S, van de Water JA, Mohapatra G, Figueiredo JL, Martuza RL, Weissleder R, Shah K: **Assessment of therapeutic efficacy and fate of engineered human mesenchymal stem cells for cancer therapy.** *Proc Natl Acad Sci U S A* 2009, **106:**4822-4827.

73. Yang B, Wu X, Mao Y, Bao W, Gao L, Zhou P, Xie R, Zhou L, Zhu J: **Dual-targeted antitumor effects against brainstem glioma by intravenous delivery of tumor necrosis factor-related, apoptosis-inducing, ligand-engineered human mesenchymal stem cells.** *Neurosurgery* 2009, **65:**610-624; discussion 624.

74. Patel SA, Meyer JR, Greco SJ, Corcoran KE, Bryan M, Rameshwar P: **Mesenchymal stem cells protect breast cancer cells through regulatory T cells: role of mesenchymal stem cell-derived TGF-beta.** *J Immunol* 2010, **184:**5885-5894.

75. Menon LG, Picinich S, Koneru R, Gao H, Lin SY, Koneru M, Mayer-Kuckuk P, Glod J, Banerjee D: **Differential gene expression associated with migration of mesenchymal stem cells to conditioned medium from tumor cells or bone marrow cells.** *Stem Cells* 2007, **25:**520-528.

76. Kidd S, Caldwell L, Dietrich M, Samudio I, Spaeth EL, Watson K, Shi Y, Abbruzzese J, Konopleva M, Andreeff M, Marini FC: **Mesenchymal stromal cells alone or expressing interferon-beta suppress pancreatic tumors in vivo, an effect countered by anti-inflammatory treatment.** *Cytotherapy* 2010, **12:**615-625.

77. Suzuki K, Sun R, Origuchi M, Kanehira M, Takahata T, Itoh J, Umezawa A, Kijima H, Fukuda S, Saijo Y: **Mesenchymal stromal cells promote tumor growth through the enhancement of neovascularization.** *Mol Med* 2011, **17:**579-587.

78. Tian LL, Yue W, Zhu F, Li S, Li W: **Human mesenchymal stem cells play a dual role on tumor cell growth in vitro and in vivo.** *J Cell Physiol* 2011, **226:**1860-1867.

79. Konopleva M, Konoplev S, Hu W, Zaritskey AY, Afanasiev BV, Andreeff M: **Stromal cells prevent apoptosis of AML cells by up-regulation of anti-apoptotic proteins.** *Leukemia* 2002, **16:**1713-1724.

80. Karnoub AE, Dash AB, Vo AP, Sullivan A, Brooks MW, Bell GW, Richardson AL, Polyak K, Tubo R, Weinberg RA: **Mesenchymal stem cells within tumour stroma promote breast cancer metastasis.** *Nature* 2007, **449:**557-563.

81. Lin YM, Zhang GZ, Leng ZX, Lu ZX, Bu LS, Gao S, Yang SJ: **Study on the bone marrow mesenchymal stem cells induced drug resistance in the U937 cells and its mechanism.** *Chin Med J (Engl)* 2006, **119:**905-910.

82. Zhu Y, Sun Z, Han Q, Liao L, Wang J, Bian C, Li J, Yan X, Liu Y, Shao C, Zhao RC: **Human mesenchymal stem cells inhibit cancer cell proliferation by secreting DKK-1.** *Leukemia* 2009, **23:**925-933.

83. Ohlsson LB, Varas L, Kjellman C, Edvardsen K, Lindvall M: **Mesenchymal progenitor cell-mediated inhibition of tumor growth in vivo and in vitro in gelatin matrix.** *Exp Mol Pathol* 2003, **75:**248-255.

84. Khakoo AY, Pati S, Anderson SA, Reid W, Elshal MF, Rovira, II, Nguyen AT, Malide D, Combs CA, Hall G, et al: **Human mesenchymal stem cells exert potent antitumorigenic effects in a model of Kaposi's sarcoma.** *J Exp Med* 2006, **203:**1235-1247.

85. Maestroni GJ, Hertens E, Galli P: **Factor(s) from nonmacrophage bone marrow stromal cells inhibit Lewis lung carcinoma and B16 melanoma growth in mice.** *Cell Mol Life Sci* 1999, **55:**663-667.

86. Secchiero P, Zorzet S, Tripodo C, Corallini F, Melloni E, Caruso L, Bosco R, Ingrao S, Zavan B, Zauli G: **Human bone marrow mesenchymal stem cells display anti-cancer activity in SCID mice bearing disseminated non-Hodgkin's lymphoma xenografts.** *PLoS One* 2010, **5:**e11140.

87. Klopp AH, Gupta A, Spaeth E, Andreeff M, Marini F, 3rd: **Concise review: Dissecting a discrepancy in the literature: do mesenchymal stem cells support or suppress tumor growth?** *Stem Cells* 2011, **29:**11-19.

88. Cousin B, Ravet E, Poglio S, De Toni F, Bertuzzi M, Lulka H, Touil I, Andre M, Grolleau JL, Peron JM, et al: **Adult stromal cells derived from human adipose tissue provoke pancreatic cancer cell death both in vitro and in vivo.** *PLoS One* 2009, **4:**e6278.

89. Dasari VR, Velpula KK, Kaur K, Fassett D, Klopfenstein JD, Dinh DH, Gujrati M, Rao JS: **Cord blood stem cell-mediated induction of apoptosis in glioma downregulates X-linked inhibitor of apoptosis protein (XIAP).** *PLoS One* 2010, **5:**e11813.

90. Dasari VR, Kaur K, Velpula KK, Gujrati M, Fassett D, Klopfenstein JD, Dinh DH, Rao JS: **Upregulation of PTEN in glioma cells by cord blood mesenchymal stem cells inhibits migration via downregulation of the PI3K/Akt pathway.** *PLoS One* 2010, **5:**e10350.

91. Gondi CS, Gogineni VR, Chetty C, Dasari VR, Gorantla B, Gujrati M, Dinh DH, Rao JS: **Induction of apoptosis in glioma cells requires cell-to-cell contact with human umbilical cord blood stem cells.** *Int J Oncol* 2010, **36:**1165-1173.

92. Ganta C, Chiyo D, Ayuzawa R, Rachakatla R, Pyle M, Andrews G, Weiss M, Tamura M, Troyer D: **Rat umbilical cord stem cells completely abolish rat mammary carcinomas with no evidence of metastasis or recurrence 100 days post-tumor cell inoculation.** *Cancer Res* 2009, **69:**1815-1820.

93. Grisendi G, Bussolari R, Veronesi E, Piccinno S, Burns JS, De Santis G, Loschi P, Pignatti M, Di Benedetto F, Ballarin R, et al: **Understanding tumor-stroma interplays for targeted therapies by armed mesenchymal stromal progenitors: the Mesenkillers.** *Am J Cancer Res* 2011, **1:**787-805.

94. van Wezel AL: **Growth of cell-strains and primary cells on micro-carriers in homogeneous culture.** *Nature* 1967, **216:**64-65.

95. van Hemert P, Kilburn DG, van Wezel AL: **Homogeneous cultivation of animal cells for the production of virus and virus products.** *Biotechnol Bioeng* 1969, **11:**875-885.

96. Martin Y, Eldardiri M, Lawrence-Watt DJ, Sharpe JR: **Microcarriers and Their Potential in Tissue Regeneration.** *Tissue Eng Part B Rev*.

97. Frauenschuh S, Reichmann E, Ibold Y, Goetz PM, Sittinger M, Ringe J: **A microcarrier-based cultivation system for expansion of primary mesenchymal stem cells.** *Biotechnol Prog* 2007, **23:**187-193.

98. Sart S, Schneider YJ, Agathos SN: **Influence of culture parameters on ear mesenchymal stem cells expanded on microcarriers.** *J Biotechnol*, **150:**149-160.

99. Schop D, van Dijkhuizen-Radersma R, Borgart E, Janssen FW, Rozemuller H, Prins HJ, de Bruijn JD: **Expansion of human mesenchymal stromal cells on microcarriers: growth and metabolism.** *J Tissue Eng Regen Med*, **4:**131-140.

100. Gao H, Ayyaswamy PS, Ducheyne P: **Dynamics of a microcarrier particle in the simulated microgravity environment of a rotating-wall vessel.** *Microgravity Sci Technol* 1997, **10:**154-165.

101. Sheyn D, Pelled G, Netanely D, Domany E, Gazit D: **The effect of simulated microgravity on human mesenchymal stem cells cultured in an osteogenic differentiation system: a bioinformatics study.** *Tissue Eng Part A* 2010, **16:**3403-3412.

102. Heilkenbrinker A: **Etablierung eines disposablen Bioreaktors zur Expansion mesenchymaler Stammzellen aus Nabelschnurgewebe.** Gottfried Wilhelm Leibniz Universität Hannover, Institut für Technische Chemie; 2011.

103. Keith B, Simon MC: **Hypoxia-inducible factors, stem cells, and cancer.** *Cell* 2007, **129:**465-472.

104. Semenza GL: **Hypoxia-inducible factor 1: oxygen homeostasis and disease pathophysiology.** *Trends Mol Med* 2001, **7:**345-350.

105. Gaber T, Dziurla R, Tripmacher R, Burmester GR, Buttgereit F: **Hypoxia inducible factor (HIF) in rheumatology: low O2! See what HIF can do!** *Ann Rheum Dis* 2005, **64:**971-980.

106. Kotch LE, Iyer NV, Laughner E, Semenza GL: **Defective vascularization of HIF-1alpha-null embryos is not associated with VEGF deficiency but with mesenchymal cell death.** *Dev Biol* 1999, **209:**254-267.

107. Iyer NV, Kotch LE, Agani F, Leung SW, Laughner E, Wenger RH, Gassmann M, Gearhart JD, Lawler AM, Yu AY, Semenza GL: **Cellular and developmental control of O2 homeostasis by hypoxia-inducible factor 1 alpha.** *Genes Dev* 1998, **12:**149-162.

108. Wenger RH: **Cellular adaptation to hypoxia: O2-sensing protein hydroxylases, hypoxia-inducible transcription factors, and O2-regulated gene expression.** *FASEB J* 2002, **16:**1151-1162.

109. Papandreou I, Cairns RA, Fontana L, Lim AL, Denko NC: **HIF-1 mediates adaptation to hypoxia by actively downregulating mitochondrial oxygen consumption.** *Cell Metabolism* 2006, **3:**187-197.

110. Warburg O: **On the origin of cancer cells.** *Science* 1956, **123:**309-314.

111. Vander Heiden MG, Cantley LC, Thompson CB: **Understanding the Warburg effect: the metabolic requirements of cell proliferation.** *Science* 2009, **324:**1029-1033.

112. Dos Santos F, Andrade PZ, Boura JS, Abecasis MM, da Silva CL, Cabral JM: **Ex vivo expansion of human mesenchymal stem cells: a more effective cell proliferation kinetics and metabolism under hypoxia.** *J Cell Physiol* 2010, **223:**27-35.

113. Kondoh H, Lleonart ME, Nakashima Y, Yokode M, Tanaka M, Bernard D, Gil J, Beach D: **A high glycolytic flux supports the proliferative potential of murine embryonic stem cells.** *Antioxid Redox Signal* 2007, **9:**293-299.

114. Semenza GL: **Life with oxygen.** *Science* 2007, **318:**62-64.

115. Tuttle SW, Maity A, Oprysko PR, Kachur AV, Ayene IS, Biaglow JE, Koch CJ: **Detection of reactive oxygen species via endogenous oxidative pentose phosphate cycle activity in response to oxygen concentration: implications for the mechanism of HIF-1alpha stabilization under moderate hypoxia.** *J Biol Chem* 2007, **282:**36790-36796.

116. Gupte SA, Arshad M, Viola S, Kaminski PM, Ungvari Z, Rabbani G, Koller A, Wolin MS: **Pentose phosphate pathway coordinates multiple redox-controlled relaxing mechanisms in bovine coronary arteries.** *Am J Physiol Heart Circ Physiol* 2003, **285:**H2316-2326.

117. Zhou F, Bi J, Zeng AP, Yuan J: **A macrokinetic model for myeloma cell culture based on stoichiometric balance.** *Biotechnol Appl Biochem* 2007, **46:**85-95.

118. Fernandes TG, Diogo MM, Fernandes-Platzgummer A, da Silva CL, Cabral JM: **Different stages of pluripotency determine distinct patterns of proliferation, metabolism, and lineage commitment of embryonic stem cells under hypoxia.** *Stem Cell Res* 2010, **5:**76-89.

119. Ahmad S, White CW, Chang LY, Schneider BK, Allen CB: **Glutamine protects mitochondrial structure and function in oxygen toxicity.** *Am J Physiol Lung Cell Mol Physiol* 2001, **280:**L779-791.

120. Chow DC, Wenning LA, Miller WM, Papoutsakis ET: **Modeling pO(2) distributions in the bone marrow hematopoietic compartment. I. Krogh's model.** *Biophysical Journal* 2001, **81:**675-684.

121. Bizzarri A, Koehler H, Cajlakovic M, Pasic A, Schaupp L, Klimant I, Ribitsch V: **Continuous oxygen monitoring in subcutaneous adipose tissue using microdialysis.** *Analytica Chimica Acta* 2006, **573:**48-56.

122. Harrison JS, Rameshwar P, Chang V, Bandari P: **Oxygen saturation in the bone marrow of healthy volunteers.** *Blood* 2002, **99:**394-394.

123. Silver IA: **Measurement of pH and ionic composition of pericellular sites.** *Philos Trans R Soc Lond B Biol Sci* 1975, **271:**261-272.

124. Fermor B, Christensen SE, Youn I, Cernanec JM, Davies CM, Weinberg JB: **Oxygen, nitric oxide and articular cartilage.** *Eur Cell Mater* 2007, **13:**56-65; discussion 65.

125. Panchision DM: **The role of oxygen in regulating neural stem cells in development and disease.** *J Cell Physiol* 2009, **220:**562-568.

126. Dollery CT, Bulpitt CJ, Kohner EM: **Oxygen supply to the retina from the retinal and choroidal circulations at normal and increased arterial oxygen tensions.** *Invest Ophthalmol* 1969, **8:**588-594.

127. Masamoto K, Tanishita K: **Oxygen transport in brain tissue.** *J Biomech Eng* 2009, **131:**074002.

128. Zhang K, Zhu L, Fan M: **Oxygen, a Key Factor Regulating Cell Behavior during Neurogenesis and Cerebral Diseases.** *Front Mol Neurosci* 2011, **4:**5.

129. Fischer B, Bavister BD: **Oxygen-Tension in the Oviduct and Uterus of Rhesus-Monkeys, Hamsters and Rabbits.** *Journal of Reproduction and Fertility* 1993, **99:**673-679.

130. Ma T, Grayson WL, Frohlich M, Vunjak-Novakovic G: **Hypoxia and Stem Cell-Based Engineering of Mesenchymal Tissues.** *Biotechnology Progress* 2009, **25:**32-42.

131. Eskes TK, Jongsma HW, Houx PC: **Percentiles for gas values in human umbilical cord blood.** *Eur J Obstet Gynecol Reprod Biol* 1983, **14:**341-346.

132. Yeomans ER, Hauth JC, Gilstrap LC, 3rd, Strickland DM: **Umbilical cord pH, PCO2, and bicarbonate following uncomplicated term vaginal deliveries.** *Am J Obstet Gynecol* 1985, **151:**798-800.

133. Rurak D, Selke P, Fisher M, Taylor S, Wittmann B: **Fetal oxygen extraction: comparison of the human and sheep.** *Am J Obstet Gynecol* 1987, **156:**360-366.

134. Ivanovic Z: **Hypoxia or in situ normoxia: The stem cell paradigm.** *J Cell Physiol* 2009, **219:**271-275.

135. Zhu W, Chen J, Cong X, Hu S, Chen X: **Hypoxia and serum deprivation-induced apoptosis in mesenchymal stem cells.** *Stem Cells* 2006, **24:**416-425.

136. Rosova I, Dao M, Capoccia B, Link D, Nolta JA: **Hypoxic preconditioning results in increased motility and improved therapeutic potential of human mesenchymal stem cells.** *Stem Cells* 2008, **26:**2173-2182.

137. Grayson WL, Zhao F, Izadpanah R, Bunnell B, Ma T: **Effects of hypoxia on human mesenchymal stem cell expansion and plasticity in 3D constructs.** *Journal of Cellular Physiology* 2006, **207:**331-339.

138. Nekanti U, Dastidar S, Venugopal P, Totey S, Ta M: **Increased proliferation and analysis of differential gene expression in human Wharton's jelly-derived mesenchymal stromal cells under hypoxia.** *Int J Biol Sci* 2010, **6:**499-512.

139. Nekanti U, Rao VB, Bahirvani AG, Jan M, Totey S, Ta M: **Long-term expansion and pluripotent marker array analysis of Wharton's jelly-derived mesenchymal stem cells.** *Stem Cells Dev* 2010, **19:**117-130.

140. Malladi P, Xu Y, Chiou M, Giaccia AJ, Longaker MT: **Effect of reduced oxygen tension on chondrogenesis and osteogenesis in adipose-derived mesenchymal cells.** *Am J Physiol Cell Physiol* 2006, **290:**C1139-1146.

141. Lennon DP, Edmison JM, Caplan AI: **Cultivation of rat marrow-derived mesenchymal stem cells in reduced oxygen tension: effects on in vitro and in vivo osteochondrogenesis.** *J Cell Physiol* 2001, **187:**345-355.

142. Huang J, Deng F, Wang L, Xiang XR, Zhou WW, Hu N, Xu L: **Hypoxia induces osteogenesis-related activities and expression of core binding factor alpha1 in mesenchymal stem cells.** *Tohoku J Exp Med*, **224:**7-12.

143. Potier E, Ferreira E, Andriamanalijaona R, Pujol JP, Oudina K, Logeart-Avramoglou D, Petite H: **Hypoxia affects mesenchymal stromal cell osteogenic differentiation and angiogenic factor expression.** *Bone* 2007, **40:**1078-1087.

144. Yang DC, Yang MH, Tsai CC, Huang TF, Chen YH, Hung SC: **Hypoxia inhibits osteogenesis in human mesenchymal stem cells through direct regulation of RUNX2 by TWIST.** *PLoS One*, **6:**e23965.

145. Holzwarth C, Vaegler M, Gieseke F, Pfister SM, Handgretinger R, Kerst G, Muller I: **Low physiologic oxygen tensions reduce proliferation and differentiation of human multipotent mesenchymal stromal cells.** *BMC Cell Biol*, **11:**11.

146. Grayson WL, Zhao F, Izadpanah R, Bunnell B, Ma T: **Effects of hypoxia on human mesenchymal stem cell expansion and plasticity in 3D constructs.** *J Cell Physiol* 2006, **207:**331-339.

147. Nekanti U, Dastidar S, Venugopal P, Totey S, Ta M: **Increased proliferation and analysis of differential gene expression in human Wharton's jelly-derived mesenchymal stromal cells under hypoxia.** *Int J Biol Sci*, **6:**499-512.

148. D'Ippolito G, Diabira S, Howard GA, Roos BA, Schiller PC: **Low oxygen tension inhibits osteogenic differentiation and enhances stemness of human MIAMI cells.** *Bone* 2006, **39:**513-522.

149. Wang DW, Fermor B, Gimble JM, Awad HA, Guilak F: **Influence of oxygen on the proliferation and metabolism of adipose derived adult stem cells.** *J Cell Physiol* 2005, **204:**184-191.

150. Merceron C, Vinatier C, Portron S, Masson M, Amiaud J, Guigand L, Cherel Y, Weiss P, Guicheux J: **Differential effects of hypoxia on osteochondrogenic potential of human adipose-derived stem cells.** *Am J Physiol Cell Physiol*, **298:**C355-364.

151. Hirao M, Tamai N, Tsumaki N, Yoshikawa H, Myoui A: **Oxygen tension regulates chondrocyte differentiation and function during endochondral ossification.** *J Biol Chem* 2006, **281:**31079-31092.

152. Scherer K, Schunke M, Sellckau R, Hassenpflug J, Kurz B: **The influence of oxygen and hydrostatic pressure on articular chondrocytes and adherent bone marrow cells in vitro.** *Biorheology* 2004, **41:**323-333.

153. Krinner A, Zscharnack M, Bader A, Drasdo D, Galle J: **Impact of oxygen environment on mesenchymal stem cell expansion and chondrogenic differentiation.** *Cell Prolif* 2009, **42:**471-484.

154. Robins JC, Akeno N, Mukherjee A, Dalal RR, Aronow BJ, Koopman P, Clemens TL: **Hypoxia induces chondrocyte-specific gene expression in mesenchymal cells in association with transcriptional activation of Sox9.** *Bone* 2005, **37:**313-322.

155. Sheehy EJ, Buckley CT, Kelly DJ: **Oxygen tension regulates the osteogenic, chondrogenic and endochondral phenotype of bone marrow derived mesenchymal stem cells.** *Biochem Biophys Res Commun*.

156. Meyer EG, Buckley CT, Thorpe SD, Kelly DJ: **Low oxygen tension is a more potent promoter of chondrogenic differentiation than dynamic compression.** *J Biomech*, **43:**2516-2523.

157. Annabi B, Lee YT, Turcotte S, Naud E, Desrosiers RR, Champagne M, Eliopoulos N, Galipeau J, Beliveau R: **Hypoxia promotes murine bone-marrow-derived stromal cell migration and tube formation.** *Stem Cells* 2003, **21:**337-347.

158. Rosova I, Dao M, Capoccia B, Link D, Nolta JA: **Hypoxic preconditioning results in increased motility and improved therapeutic potential of human mesenchymal stem cells.** *Stem Cells* 2008, **26:**2173-2182.

159. Volkmer E, Kallukalam BC, Maertz J, Otto S, Drosse I, Polzer H, Bocker W, Stengele M, Docheva D, Mutschler W, Schieker M: **Hypoxic preconditioning of human mesenchymal stem cells overcomes hypoxia-induced inhibition of osteogenic differentiation.** *Tissue Eng Part A* 2010, **16:**153-164.

160. Peterson KM, Aly A, Lerman A, Lerman LO, Rodriguez-Porcel M: **Improved survival of mesenchymal stromal cell after hypoxia preconditioning: role of oxidative stress.** *Life Sci* 2011, **88:**65-73.

161. Eliasson P, Jonsson JI: **The Hematopoietic Stem Cell Niche: Low in Oxygen but a Nice Place to be.** *Journal of Cellular Physiology* 2010, **222:**17-22.

162. Ivanovic Z: **Hypoxia or In Situ Normoxia: The Stem Coll Paradigm.** *Journal of Cellular Physiology* 2009, **219:**271-275.

163. Lavrentieva A, Majore I, Kasper C, Hass R: **Effects of hypoxic culture conditions on umbilical cord-derived human mesenchymal stem cells.** *Cell Commun Signal* 2010, **8:**18.

164. Papandreou I, Cairns RA, Fontana L, Lim AL, Denko NC: **HIF-1 mediates adaptation to hypoxia by actively downregulating mitochondrial oxygen consumption.** *Cell Metab* 2006, **3:**187-197.

165. Subczynski WK, Hopwood LE, Hyde JS: **Is the mammalian cell plasma membrane a barrier to oxygen transport?** *J Gen Physiol* 1992, **100:**69-87.

166. Golstein P, Kroemer G: **Cell death by necrosis: towards a molecular definition.** *Trends in Biochemical Sciences* 2007, **32:**37-43.

167. Dos Santos F, Andrade PZ, Boura JS, Abecasis MM, da Silva CL, Cabral JM: **Ex vivo expansion of human mesenchymal stem cells: a more effective cell proliferation kinetics and metabolism under hypoxia.** *J Cell Physiol*, **223:**27-35.

168. Schop D, Janssen FW, van Rijn LD, Fernandes H, Bloem RM, de Bruijn JD, van Dijkhuizen-Radersma R: **Growth, metabolism, and growth inhibitors of mesenchymal stem cells.** *Tissue Eng Part A* 2009, **15:**1877-1886.

169. Miller WM, Wilke CR, Blanch HW: **Effects of Dissolved-Oxygen Concentration on Hybridoma Growth and Metabolism in Continuous Culture.** *Journal of Cellular Physiology* 1987, **132:**524-530.

170. Thomas PD, Kejariwal A, Campbell MJ, Mi H, Diemer K, Guo N, Ladunga I, Ulitsky-Lazareva B, Muruganujan A, Rabkin S, et al: **PANTHER: a browsable database of gene products organized by biological function, using curated protein family and subfamily classification.** *Nucleic Acids Res* 2003, **31:**334-341.

171. Mi H, Dong Q, Muruganujan A, Gaudet P, Lewis S, Thomas PD: **PANTHER version 7: improved phylogenetic trees, orthologs and collaboration with the Gene Ontology Consortium.** *Nucleic Acids Res* 2010, **38:**D204-210.

172. Heidbreder M, Frohlich F, Johren O, Dendorfer A, Qadri F, Dominiak P: **Hypoxia rapidly activates HIF-3alpha mRNA expression.** *FASEB J* 2003, **17:**1541-1543.

173. Lee JW, Bae SH, Jeong JW, Kim SH, Kim KW: **Hypoxia-inducible factor (HIF-1)alpha: its protein stability and biological functions.** *Exp Mol Med* 2004, **36:**1-12.

174. Yu AY, Frid MG, Shimoda LA, Wiener CM, Stenmark K, Semenza GL: **Temporal, spatial, and oxygen-regulated expression of hypoxia-inducible factor-1 in the lung.** *Am J Physiol* 1998, **275:**L818-826.

175. Huang LE, Arany Z, Livingston DM, Bunn HF: **Activation of hypoxia-inducible transcription factor depends primarily upon redox-sensitive stabilization of its alpha subunit.** *J Biol Chem* 1996, **271:**32253-32259.

176. Hwa V, Oh Y, Rosenfeld RG: **The insulin-like growth factor-binding protein (IGFBP) superfamily.** *Endocr Rev* 1999, **20:**761-787.

177. Chen L, Jiang W, Huang J, He BC, Zuo GW, Zhang W, Luo Q, Shi Q, Zhang BQ, Wagner ER, et al: **Insulin-like growth factor 2 (IGF-2) potentiates BMP-9-induced osteogenic differentiation and bone formation.** *J Bone Miner Res* 2010, **25:**2447-2459.

178. Kuo YS, Tang YB, Lu TY, Wu HC, Lin CT: **IGFBP-6 plays a role as an oncosuppressor gene in NPC pathogenesis through regulating EGR-1 expression.** *J Pathol* 2010, **222:**299-309.

179. Jaques G, Noll K, Wegmann B, Witten S, Kogan E, Radulescu RT, Havemann K: **Nuclear localization of insulin-like growth factor binding protein 3 in a lung cancer cell line.** *Endocrinology* 1997, **138:**1767-1770.

180. Paharkova-Vatchkova V, Lee KW: **Nuclear export and mitochondrial and endoplasmic reticulum localization of IGF-binding protein 3 regulate its apoptotic properties.** *Endocr Relat Cancer* 2010, **17:**293-302.

181. Radulescu RT: **From insulin, retinoblastoma protein and the insulin receptor to a new model on growth factor specificity: the nucleocrine pathway.** *J Endocrinol* 1995, **146:**365-368.

182. Gieseke F, Schutt B, Viebahn S, Koscielniak E, Friedrich W, Handgretinger R, Muller I: **Human multipotent mesenchymal stromal cells inhibit proliferation of PBMCs independently of IFNgammaR1 signaling and IDO expression.** *Blood* 2007, **110:**2197-2200.

183. Crivellato E: **The role of angiogenic growth factors in organogenesis.** *Int J Dev Biol* 2011, **55:**365-375.

184. Chung HM, Won CH, Sung JH: **Responses of adipose-derived stem cells during hypoxia: enhanced skin-regenerative potential.** *Expert Opin Biol Ther* 2009, **9:**1499-1508.

185. Crisostomo PR, Wang Y, Markel TA, Wang M, Lahm T, Meldrum DR: **Human mesenchymal stem cells stimulated by TNF-alpha, LPS, or hypoxia produce growth factors by an NF kappa B- but not JNK-dependent mechanism.** *Am J Physiol Cell Physiol* 2008, **294:**C675-682.

186. Rongo C: **Epidermal Growth Factor and aging: a signaling molecule reveals a new eye opening function.** *Aging (Albany NY)* 2011, **3:**896-905.

187. Bae KS, Park JB, Kim HS, Kim DS, Park DJ, Kang SJ: **Neuron-like differentiation of bone marrow-derived mesenchymal stem cells.** *Yonsei Med J* 2011, **52:**401-412.

188. Kuhn MA, Xia G, Mehta VB, Glenn S, Michalsky MP, Besner GE: **Heparin-binding EGF-like growth factor (HB-EGF) decreases oxygen free radical production in vitro and in vivo.** *Antioxid Redox Signal* 2002, **4:**639-646.

189. Lakshmipathy U, Hart RP: **Concise review: MicroRNA expression in multipotent mesenchymal stromal cells.** *Stem Cells* 2008, **26:**356-363.

190. Tsai SM, Wang WP: **Expression and function of fibroblast growth factor (FGF) 7 during liver regeneration.** *Cell Physiol Biochem* 2011, **27:**641-652.

191. Niu J, Chang Z, Peng B, Xia Q, Lu W, Huang P, Tsao MS, Chiao PJ: **Keratinocyte growth factor/fibroblast growth factor-7-regulated cell migration and invasion through activation of NF-kappaB transcription factors.** *J Biol Chem* 2007, **282:**6001-6011.

192. Rodriguez LG, Wu X, Guan JL: **Wound-healing assay.** *Methods Mol Biol* 2005, **294:**23-29.

193. Hu X, Yu SP, Fraser JL, Lu Z, Ogle ME, Wang JA, Wei L: **Transplantation of hypoxia-preconditioned mesenchymal stem cells improves infarcted heart function via enhanced survival of implanted cells and angiogenesis.** *J Thorac Cardiovasc Surg* 2008, **135:**799-808.

194. Leroux L, Descamps B, Tojais NF, Seguy B, Oses P, Moreau C, Daret D, Ivanovic Z, Boiron JM, Lamaziere JM, et al: **Hypoxia preconditioned mesenchymal stem cells improve vascular and skeletal muscle fiber regeneration after ischemia through a Wnt4-dependent pathway.** *Mol Ther* 2010, **18:**1545-1552.

195. Wang JA, Chen TL, Jiang J, Shi H, Gui C, Luo RH, Xie XJ, Xiang MX, Zhang X: **Hypoxic preconditioning attenuates hypoxia/reoxygenation-induced apoptosis in mesenchymal stem cells.** *Acta Pharmacol Sin* 2008, **29:**74-82.

196. Basciano L, Nemos C, Foliguet B, de Isla N, de Carvalho M, Tran N, Dalloul A: **Long term culture of mesenchymal stem cells in hypoxia promotes a genetic program maintaining their undifferentiated and multipotent status.** *BMC Cell Biol* 2011, **12:**12.

197. Hayflick L, Moorhead PS: **The serial cultivation of human diploid cell strains.** *Exp Cell Res* 1961, **25:**585-621.

198. Bonab MM, Alimoghaddam K, Talebian F, Ghaffari SH, Ghavamzadeh A, Nikbin B: **Aging of mesenchymal stem cell in vitro.** *BMC Cell Biol* 2006, **7:**14.

199. Campisi J: **Cellular senescence as a tumor-suppressor mechanism.** *Trends Cell Biol* 2001, **11:**S27-31.

200. Chen Z, Trotman LC, Shaffer D, Lin HK, Dotan ZA, Niki M, Koutcher JA, Scher HI, Ludwig T, Gerald W, et al: **Crucial role of p53-dependent cellular senescence in suppression of Pten-deficient tumorigenesis.** *Nature* 2005, **436:**725-730.

201. Vousden KH, Prives C: **Blinded by the Light: The Growing Complexity of p53.** *Cell* 2009, **137:**413-431.

202. Riley T, Sontag E, Chen P, Levine A: **Transcriptional control of human p53-regulated genes.** *Nat Rev Mol Cell Biol* 2008, **9:**402-412.

203. Moll UM, Wolff S, Speidel D, Deppert W: **Transcription-independent pro-apoptotic functions of p53.** *Curr Opin Cell Biol* 2005, **17:**631-636.

204. Armesilla-Diaz A, Elvira G, Silva A: **p53 regulates the proliferation, differentiation and spontaneous transformation of mesenchymal stem cells.** *Exp Cell Res* 2009, **315:**3598-3610.

205. Madan E, Gogna R, Bhatt M, Pati U, Kuppusamy P, Mahdi AA: **Regulation of glucose metabolism by p53: Emerging new roles for the tumor suppressor.** *Oncotarget* 2011, **2:**948-957.

206. Sermeus A, Michiels C: **Reciprocal influence of the p53 and the hypoxic pathways.** *Cell Death Dis* 2011, **2:**e164.

207. van den Bos C, Silverstetter S, Murphy M, Connolly T: **p21(cip1) rescues human mesenchymal stem cells from apoptosis induced by low-density culture.** *Cell Tissue Res* 1998, **293:**463-470.

208. Blackburn EH: **Structure and function of telomeres.** *Nature* 1991, **350:**569-573.

209. Zaffaroni N, Villa R, Pastorino U, Cirincione R, Incarbone M, Alloisio M, Curto M, Pilotti S, Daidone MG: **Lack of telomerase activity in lung carcinoids is dependent on human telomerase reverse transcriptase transcription and alternative splicing and is associated with long telomeres.** *Clin Cancer Res* 2005, **11:**2832-2839.

210. Vaziri H, Benchimol S: **Reconstitution of telomerase activity in normal human cells leads to elongation of telomeres and extended replicative life span.** *Curr Biol* 1998, **8:**279-282.

211. Kim NW, Piatyszek MA, Prowse KR, Harley CB, West MD, Ho PL, Coviello GM, Wright WE, Weinrich SL, Shay JW: **Specific association of human telomerase activity with immortal cells and cancer.** *Science* 1994, **266:**2011-2015.

212. Yeh E, Cunningham M, Arnold H, Chasse D, Monteith T, Ivaldi G, Hahn WC, Stukenberg PT, Shenolikar S, Uchida T, et al: **A signalling pathway controlling c-Myc degradation that impacts oncogenic transformation of human cells.** *Nat Cell Biol* 2004, **6:**308-318.

213. Green DR, Reed JC: **Mitochondria and apoptosis.** *Science* 1998, **281:**1309-1312.

214. Chen CT, Shih YR, Kuo TK, Lee OK, Wei YH: **Coordinated changes of mitochondrial biogenesis and antioxidant enzymes during osteogenic differentiation of human mesenchymal stem cells.** *Stem Cells* 2008, **26:**960-968.

215. Lonergan T, Brenner C, Bavister B: **Differentiation-related changes in mitochondrial properties as indicators of stem cell competence.** *J Cell Physiol* 2006, **208:**149-153.

216. Rehman J: **Empowering self-renewal and differentiation: the role of mitochondria in stem cells.** *J Mol Med (Berl)* 2010, **88:**981-986.

217. Zhang H, Bosch-Marce M, Shimoda LA, Tan YS, Baek JH, Wesley JB, Gonzalez FJ, Semenza GL: **Mitochondrial autophagy is an HIF-1-dependent adaptive metabolic response to hypoxia.** *J Biol Chem* 2008, **283:**10892-10903.

218. Bork S, Pfister S, Witt H, Horn P, Korn B, Ho AD, Wagner W: **DNA methylation pattern changes upon long-term culture and aging of human mesenchymal stromal cells.** *Aging Cell* 2010, **9:**54-63.

219. Fehrer C, Brunauer R, Laschober G, Unterluggauer H, Reitinger S, Kloss F, Gully C, Gassner R, Lepperdinger G: **Reduced oxygen tension attenuates differentiation capacity of human mesenchymal stem cells and prolongs their lifespan.** *Aging Cell* 2007, **6:**745-757.

220. Lafont JE: **Lack of oxygen in articular cartilage: consequences for chondrocyte biology.** *Int J Exp Pathol*, **91:**99-106.

221. Toussaint O, Dumont P, Remacle J, Dierick JF, Pascal T, Frippiat C, Magalhaes JP, Zdanov S, Chainiaux F: **Stress-induced premature senescence or stress-induced senescence-like phenotype: one in vivo reality, two possible definitions?** *ScientificWorldJournal* 2002, **2:**230-247.

222. Repenning C: **Statistische Auswertung von Microarray-Daten.** Gottfried Leibniz University Hanover, Instut for Technical Chemistry; 2010.

223. Lönne M: **Gen- und Proteinexpression mesenchymaler Stammzellen unter hypoxischen Bedingungen.** Gottfried Leibniz University Hanover, Institut for Technical Chemistry; 2011.

224. Moretti P: **Establishment of recombinant cell lines and characterization of primary cells for stem cell technology applications.** Gottfried Leibniz University Hanover, Institut of Technical Chemistry; 2010.

7 Materials

7.1 Materials

Material	Manufacturer
Latex gloves, Diamond Grip Plus	Microflex, Reno, USA
Nitril gloves, Rotiprotect Nitril	Carl Roth GmbH & Co KG, Karlsruhe
Serologic Pipetts (5, 25, 50, 100 ml)	Sarstedt AG & Co, Numbrecht
Syringes	Becton Dickinson GmbH, Heidelberg
Needles	B. Braun Melsungen AG, Melsungen
Cryo Pure Tubes	Sarstedt AG & Co, Numbrecht
PCR Tubes, 0.2 ml	Kisker Biotech GmbH & Co. KG, Steinfurt
PCR Plates	Fisher Scienctific GmbH, Schwerte
Reaction tubes (1.5 ml, 2 ml)	Sarstedt AG & Co, Numbrecht
Lab flasks (100 ml, 250 ml,1 l)	VWR International GmbH, Darmstadt
Multichannel pipette tips RAININ 200 µl	Mettler Toledo GmbH, Giesen
Syringe filter, Minisart NY25, 0.25 µl	Sartorius AG, Gottingen
Pipette tips (20, 200,1000 µl)	Brand GmbH & CO KG, Wertheim
Cell culture flasks (T25, T75, T175)	Sarstedt AG & Co, Numbrecht
Cell culture plates (6-, 12-, 24-, 96-Wells)	Sarstedt AG & Co, Numbrecht
Cell culture plates BD BioCoat, fibronectin	BD Biosciences, Bedford, USA
Cell scraper, 13 mm	Klinge, Sarstedt AG & Co, Numbrecht
Conical tubes (15 ml, 50 ml)	Greiner Bio-One GmbH, Frickenhausen

7.2 Equipment

Equipment	Manufacturer
Analytic balances ED 224S	Sartorius AG, Gottingen
Fluoroscan Ascent microplate reader	Thermo Scientific GmbH, Langenselbold
Flow cytometer Epics XL/MCL	Beckman Coulter, Krefeld
YSI 2700 SELECT analyzer	YSI Incorporated Life Sciences, Yellow Springs, USA
Incubator Heracell 240i	Thermo Scientific GmbH, Langenselbold
lectrophoresis chamber Classic	Thermo Fisher Scienctific, Bonn
HPLC Fluorescence Detector RF-10AXL	Shimadzu, Japan
Microarray Scanner GenePix 4000B	Molecular Devices Germany GmbH, Ismaning
Gel iX Imager	Intas Science Imaging Instruments GmbH, Gottingen
SFR-Shake Flask Reader	Presens GmbH, Regensburg, Germany
Magnetic stirrer MSH Basic	IKA-Werke GmbH & CO KG, Staufen
Multichannel pipette	Pipet-Lite 12-chanel, Mettler Toledo GmbH, Giesen
PCR-Thermocycler	Doppio, VWR International GmbH, Darmstadt
Microscope	IX 50, Olympus Europa Holding GmbH, Hamburg
Pipetting aid	Easypet, Eppendorf AG, Hamburg
Pump	Laboport, Knf-Lab Trenton, USA
Pipette tips	VWR International GmbH, Darmstadt
Real-Time-PCR-Station	iQ5, Bio-Rad Laboratories GmbH, Munchen
Lab rocker	Stuart Mini Gyro-Rocker, Bibby Scientific Limited, Stone, GB
Clean bench	Technoflow 2F150-II GS, Integra Biosciences AG, Zurich

Thermomixer	Thermomixer Comfort, Eppendorf AG, Hamburg
Centrifuge	Carl Roth GmbH & Co KG, Karlsruhe
UV/Vis-Spectralphotometer	Nanodrop ND-1000, PeqLab-Biotechnologie GmbH, Erlangen
Vortex	VWR International GmbH, Darmstadt
Ultra pure water system	Arium 611, Sartorius AG, Gottingen
Water bath	WNB, Memmert GmbH & Co KG, Schwabach
Mini-centrifuge	MiniSpin, Eppendorf AG, Hamburg
Centrifuge for conical tubes	Centrifuge 5702, Eppendorf AG, Hamburg

7.3 Chemicals

Chemicals	**Manufacturer**
Accutase	PAA Laboratories GmbH, Pasching
Acetic acid	AppliChem GmbH, Darmstadt
Agarose	ABGene, Hamburg
α-Minimum Essential Medium (MEM)	GIBCO Invitrogen GmbH, Darmstadt
Alcianblue 8G Solution	Sigma Aldrich Chemie GmbH, München
BODIPY	Invitrogen GmbH, Darmstadt
BSA	Sigma Aldrich Chemie GmbH, München
Bromphenol Blue	Fluka Chemie AG, Buchs
Cell lysis buffer	RayBiotech, Inc, Norcross, USA
Calcein	Sigma Aldrich Chemie GmbH, München
Calcein-AM	Promega GmbH, Mannheim

DAPI	Roth GmbH + Co. KG, Karlsruhe
Dithiothreitol (DTT)	Invitrogen GmbH, Darmstadt
DMSO	Sigma Aldrich Chemie GmbH, München
DNA-Polymerase GoTaq	Promega GmbH, Mannheim
dNTPs	Fermentas GmbH, St. Leon-Rot
EDTA	AppliChem GmbH, Darmstadt
Ethanol	Carl Roth GmbH & Co KG, Karlsruhe
Reaction tubes, 1.5 ml, 2 ml	Sarstedt AG & Co, Numbrecht
Ethidium bromide (EtBr)	Sigma Aldrich Chemie GmbH, München
Formamide	Carl Roth GmbH & Co KG, Karlsruhe
GeneRuler 100 bp DNA-Ladder	Fermentas GmbH, St. Leon-Rot
Gentamicin	PAA Laboratories GmbH, Pasching
Human serum	Institut fur Transfusionsmedizin, Medizinische Hochschule Hannover
Isopropanol	Merck KGaA, Darmstadt
KCl	Honeywell Specialty Chemicals GmbH, Seelze
Loading buffer	Fermentas GmbH, St. Leon-Rot
KH_2PO_4	AppliChem GmbH, Darmstadt
NaCl	Sigma Aldrich Chemie GmbH, München
Protease inhibitor „Plus“	Carl Roth GmbH & Co KG, Karlsruhe
$Na_2HPO4 \bullet 2\ H_2O$	Honeywell Specialty Chemicals GmbH, Seelze
$Na_2S_2O_3$-Solution	Sigma Aldrich Chemie GmbH, München
SDS	Sigma Aldrich Chemie GmbH, München
β-Mercaptoethanol	Gibco, Karlsruhe
Nitrogen	Linde Gas Deutschland, Pullach
Paraformaldehyde	Sigma Aldrich Chemie GmbH, München

Propidium iodide	Sigma Aldrich Chemie GmbH, München
Silver nitrate solution	Sigma Aldrich Chemie GmbH, München
Tris-Base	Sigma Aldrich Chemie GmbH, München
Trypan blue	Sigma Aldrich Chemie GmbH, München
Xylene cyanol FF	AppliChem GmbH, Darmstadt
Reverse Transkriptase Superscript III	Invitrogen GmbH, Darmstadt
DNA-Polymerase iQ Supermix	Bio-Rad Laboratories GmbH, Munchen

7.4 Solutions and buffers

Solutions	**Formation**
Agarose gel	TAE running buffer with 2 % Agarose + 0.002 % Ethidium bromide
BODIPY stock solution	10 mM in DMSO (10 mg BODIPY-powder in 3.815 ml DMSO)
BODIPY working solution	1 µl BODIPY-Stock solution in 2 ml PBS
Blocking buffer	2% FCS in PBS
Calcein stock solution	200 µg/ml Calcein in ddH_2O
Calcein working solution	2.5 mL Calcein-Stock solution + 97.5 mL ddH_2O
Cell disruption solution	Cell lysis buffer + 1% Proteases inhibitor
Cryomedium	α-MEM Medium + 10 % Human serum + 10 % DMSO
Agarose gelelectrophoresis loading buffer (2x)	95 % Formamide; 0.025 % SDS; 0.025 % Bromphenol blue; 0.025 % Xylene cyanol FF; 0.025 % EtBr; 0.5 mM EDTA
PBS	137 mM NaCl; 2.7 mM KCl; 8.1 mM $Na_2HPO_4 \cdot 2\ H_2O$; 1.8 mM KH_2PO_4; pH 7.4
Primer solutions	1 pmol/µl forward primer + 1/µl pmol reverse primer in ddH_2O
SSC (20x)	175.3 g NaCl; 88.3 g Trinatriumcitrate-dihydrate; in 1000 ml ddH_2O, pH 7
TAE Running buffer	40 mM Tris Base; 20 mM Acetic acid; 1 mM EDTA; in ddH_2O; pH 8

TNT-buffer	0.1M TrisHCl; 0.15M NaCl; 0.05% Tween 20; in ddH_2O; pH 7.5
Von Kossa $AgNO_3$ solution	5% $AgNO_3$ in ddH_2O
Von Kossa formaldehyde solution	5%Na_2CO_3 + 0.2% formaldehyde in ddH_2O
Fixation solution	4% paraformaldehyde in PBS

7.5 Kits

Kit	Manufacturer
CellTiter-Blue® Cell Viability Assay	Promega BioScience, San Luis Obispo, USA
Quantibody Human Growth Factor Array 1	RayBiotech, Inc, Norcross, USA
RNA-Isolation RNeasy Mini Kit Plus	Qiagen GmbH, Hilden
NEN TSA Labeling and Detection Kit	PerkinElmer Life and Analytical Sciences, Inc, Rodgau
ApoOne® Homogeneous Caspase-3/7 Assay	Promega BioScience, San Luis Obispo, USA
CytoTox-ONE™ Assay	Promega BioScience, San Luis Obispo, USA
β-Galactosidase Staining kit	Cell Signalling Technologies, Danvers, USA

7.6 Differentiation Media

Differentiation	Medium	Manufacturer
Osteogenic	NH OsteoDiff Medium	Miltenyi Biotec GmbH, Bergisch Gladbach

Chondrogenic	NH ChondroDiff Medium	Miltenyi Biotec GmbH, Bergisch Gladbach
Adipogenic	NH AdipoDiff Medium	Miltenyi Biotec GmbH, Bergisch Gladbach
Control	DMEM + 5% human serum	Sigma Aldrich Chemie GmbH, München

7.7 Primers

Gene	NCBI accession number	Forward sequence	Reverse sequence	Melting temperature, °C	Product length, bp
HPRT1	NM_000194.2	AAGCTTGCTG GTGAAAAGGA	AAGCAGATGG CCACAGAACT	59.9/59.8	267
LDHA	NM_005566.3	ACGTCAGCAA GAGGGAGAAA	CGCTTCCAATA ACACGGTTT	59.9/60.0	191
PDK1	NM_002610.3	CACGCTGGGT AATGAGGATT	ACTGCATCTGT CCCGTAACC	59.9/60.0	243
GLUT1	NM_006516.2	CTTCACTGTC GTGTCGCTGT	TGAAGAGTTCA GCCACGATG	60.1/59.9	230
G6PD	NM_000402.3	GAGGCCGTGT ACACCAAGAT	AATATAGGGG ATGGGCTTGG	60.0/60.0	258
VEGFA	NM_001171624.1	TGAGGAGTCC AACATCACCA	TTTCTTGCGC TTTCGTTTTT	60.1/60.0	181
PGF	NM_002632.4	GTTCAGCCCA TCCTGTGTCT	CTTCATCTTC TCCCGCAGAG	59.4/59.4	199
bFGF	NM_002006.4	CCGTTACCTG GCTATGAAGG	TGTGGCCATTA AAATCAGCTC	59.4/55.9	243
VEGF-R	NM_002019.4	GGCTCTGTGG AAAGTTCAGC	GCTCACACTG CTCATCCAAA	60.0/59.9	223

p39	NM_002228.3	CAGGTGGCAC AGCTTAAACA	TTTTTCTCTCC GTCGCAACT	59.9/59.9	180
p53	NM_000546.4	GTTCCGAGAG CTGAATGAGG	TCTGAGTCAG GCCCTTCTGT	59.9/59.9	159
H-RAS	NM_001130442.1	CCAGCTGATC CAGAACCATT	ATGGCAAACA CACACAGGAA	60.0/60.0	189
hTERT	NM_001193376.1	AGGAGCTGAC GTGGAAGATG	TTGCAACTTG CTCCAGACAC	60.4/60.0	239
SCF-R	NM_000222.2	TCATGGTCGG ATCACAAAGA	AGGGGCTGCT TCCTAAAGAG	60.0/59.9	206
IGFBP6	NM_002178.2	GCTGTTGCAG AGGAGAATCC	TCACAATTGG GCACGTAGAG	59.9/59.7	242
C-MYC	NM_002467.4	CCTACCCTCT CAACGACAGC	CTCTGACCTT TTGCCAGGAG	59.8/59.9	248
HBEGF	NM_001945.2	GCTCTTTCTG GCTGCAGTTC	GCTTGTGGCT TGGAGGATAA	59.4/57.3	216
TGFβ3	NM_003239.2	GGAATGAGCA GAGGATCGAG	ATTGGGCTGAA AGGTGTGAC	59.4/57.3	218
IGFBP3	NM_000598.4	GTCCCTGCCG TAGAGAAATG	AGGCTGCCCA TACTTATCCA	59.4/57.3	182

8 Methods

8.1 Cell culture

Human MSC were isolated from the umbilical cords of 12 different term-deliveries (38-40 weeks) by Cesarean section. All patients have delivered their informed consent, as approved by the Institutional Review Board, project #3037 on 17th June, 2006 and in an extended permission #443 on 26th February, 2009. The isolated populations have been

extensively characterized as mesenchymal stem cells by surface marker analysis and functional properties. MSC were expanded and cryopreserved until the start of the experiment as described. After thawing, the cells were expanded over two passages. At about 80% of confluency the MSCs were harvested by accutase treatment and plated at a density of 3000 cells/cm^2 in 25cm^2 cell culture flasks and in 6-well plates, respectively. Experiments were performed with cells of passages 3 to 7. Cells were cultivated in αMEM containing 1 g/l glucose, 2mM L-glutamine , 10% human serum and 50 µg/ml gentamicin in a humidified atmosphere containing 5% CO_2 and 21% O_2 at 37°C.

8.2 Hypoxic cell culture

For the short-term cultivation under hypoxic conditions, cells were first plated at atmospheric oxygen concentrations. Twenty four hours after seeding, all non-adherent cells were removed by media changes and for the following 72 h the MSC were incubated at 37° C in a humidified atmosphere (Incubator Heracell 240i, Thermo Fisher Scientific) containing 5% CO_2 and various oxygen concentrations (1.5%, 2.5%, 5% or 21%). Desired oxygen concentrations were established by introduction of N_2 into the incubator culturing system. In the present work, oxygen concentrations are expressed as volumetric percentage. The corresponding partial pressure (mmHg) values and concentrations are presented in the following table:

% Vol	mmHg	Concentration
21%	160	0.220 mmol O_2/l
5%	38	0.050 mmol O_2/l
2.5%	19	0.025 mmol O_2/l
1.5%	11.4	0.015 mmol O_2/l

For long-term expansion under low oxygen tension, cells were isolated from the same cords as normoxic controls and cultivated over all passages under 2.5% or 5% O_2. Cells were subcultivated 2 times per week with a seeding density of 2000 cells/cm^2.

8.3 Cell thawing

After removal from the liquid nitrogen, the cryopreservation vial was transferred immediately into a 37° C water bath and agitated until the medium was thawed (approximately 2 minutes). Under a clean bench, 1 ml of cold (room temperature) medium was added. After 2 minutes, the cell suspension was added to 6 ml medium in a 15 ml conical tube (8 ml total) and centrifuged for 5 min at 300 x g. The supernatant was discarded and the pellet was re-suspended in 1 ml medium. Cell number was estimated in a haemocytometer. After the addition of 5 ml warm (37°C) medium, the cell suspension was transferred into a 175-cm^2 culture flask. Another 15 ml of warm (37°C) medium were added (αMEM with 10% human serum and 0.5% gentamicin) and the flask was placed in the incubator. Once the cells have been attached (overnight), the culture medium was renewed.

8.4 Cell number, apoptosis and necrosis

At the end of cultivation, cells were washed with PBS, detached by accutase treatment, sedimented by centrifugation for 5 min at 200 x g and counted using a haemocytometer following re-suspension in 1 ml culture medium. Cell viability was determined by trypan blue exclusion (n=4). Occurrence of apoptosis was measured with the ApoOne® Homogeneous Caspase-3/7 Assay by the amount of the fluorescent product Rhodamine 110 (Ex_{355}/Em_{460}) cleaved by caspase-3/7 from the non-fluorescent substrate Z-DEVD-R110 after cell lysis following a 6 h incubation at 37 °C. Cell damage or cell necrosis was evaluated by measuring lactate dehydrogenase (LDH) activity in the cell culture supernatant (30 min incubation time, 25 °C) using the CytoTox-ONE™ assay, by the amount of enzymatically reduced resorufin according to manufacturer's instructions and by measuring its fluorescence intensity (Ex_{355}/Em_{460}). All fluorescence measurements were performed using the Fluoroscan Ascent microplate reader.

Normoxic (21% O_2) cultures of the same passage were used as control cell population and the results of each oxygen concentration were presented as percentage of change to the normoxic controls.

8.5 Cumulative cell population doublings

During long-term cultivation, cells were cultured over 25 passages every 3-4 days when a confluence of 60-80% was reached. At each passage, the cells were counted with a haemocytometer and the population doublings were calculated according to the following formula:

$$Nd = \frac{\ln\left(\frac{x}{x_0}\right)}{\ln 2}$$

where ***Nd*** isthe number of population doublings during a Δt period of time, x_0 is the number of living cells at time t = 0, and ***x*** is the number of living cells at time t. Population doubling time ***Td*** was calculated with the following formula:

$$Td = \frac{\Delta t}{Nd}$$

Cumulative cell population doublings were calculated as a sum of all population doublings from the beginning of the experiment until the time point *t*.

8.6 O_2 and pH measurements

Dissolved oxygen concentration (in µmol/l) and pH values in the cell culture supernatant were recorded online in 25 cm^2 cell culture flasks every 10-20 minutes by using a

SFR-Shake Flask Reader with optical sensors integrated and pre-calibrated by PreSens GmbH. These measurements are based on the luminescence lifetime of the sensor dye, which depends on the oxygen partial pressure and the pH of the sample, respectively. The luminescence lifetime was detected non-invasively through the transparent flask bottom and represents oxygen equivalents and pH values according to the company's software. Culture flasks with the same amount of medium (6 ml) without cells were used as a control. Oxygen consumption was calculated as the difference of dissolved oxygen concentration in the medium with and without cells, divided by the number of living cells. For each oxygen concentration UC-MSC from 4 donors were measured in duplets.

8.7 RNA isolation and cDNA synthesis

Total RNA from cells incubated at different oxygen conditions was isolated by using the RNeasy Mini Plus Kit (Qiagen GmbH, Hilden) according to the manufacturer's instructions. The RNA concentration was measured with a Nanodrop 1000 (PeqLab-Biotechnologie GmbH, Erlangen). Thereafter, 1 µg of total RNA was transcribed into cDNA using Reverse Transcriptase and a mixture of oligo(dT) primers (Roth GmbH) according to the manufacturer's instructions.

8.8 RT-PCR and qRT- PCR

Primers for glucose transporter-1 (GLUT-1), lactate dehydrogenase A (LDHA), glucose-6-phosphate dehydrogenase (G6PD), pyruvate dehydrogenase kinase-1 (PDK-1), vascular endothelial growth factor A (VEGFA), vascular endothelial growth factor receptor (VEGF-R,) hypoxanthine phosphoribosyltransferase-1 (HPRT1), placental growth factor (PGF), basic fibroblast growth factor (bFGF), tumor protein p53 (p53), v-Ha-ras Harvey rat sarcoma viral oncogene homolog (H-RAS), telomerase reverse transcriptase (hTERT), stem cell factor receptor (SCF-R), insulin-like growth factor binding protein 6 (IGFBP6), v-myc myelocytomatosis viral oncogene homolog (C-MYC), heparin-binding EGF-like growth factor (HBEGF), transforming growth factor beta 3 (TGFβ3) and insulin-like growth factor binding protein 3 (IGFBP3) genes were designed using OligoPerfect™ Designer Software (Invitrogen). Designed primers were synthesised by MWG Operon (Ebersberg, Germany).

8.8.1 RT-PCR

The PCR amplifications were performed in a 50-µl reaction mix containing ~ 25 ng of cDNA, 1.25 units Taq DNA polymerase (Fermentas), 160 µM of each dNTP (Fermentas), 10 pM of each gene specific primer (MWG), 1x GreenGo Taq Buffer (Promega GmbH) and 35.75 µl of RNase-free water in iCycler (BioRad) with the following program:

1. 5 min 95 °C
2. 40× 0.5 min 95 °C
   0.5 min 59 °C
   0.5 min 72 °C
3. 7 min 72 °C
4. 4 °C

PCR products (amplicons) were analyzed using agarose-gel electrophoresis. DNA-fragments were separated in TAE running buffer at 100 V for 30-40 min and amplicon-bands were visualized in ultraviolet light using the Gel iX Imager (INTAS Science Imaging Instruments GmbH, Gottingen).

8.8.2 q RT-PCR

Quantitative RT-PCR was performed using IQ™SYBR®Green Supermix and the IQTM5 real-time PCR Detection System. The HPRT1 gene was used as an internal control and a non-template control was used as a negative control. The dissociation curves were run for all completed SYBR Green reactions to rule out non-specific amplifications and primer-dimers. Data were analyzed using the comparative Ct (ΔΔCT) method:

$$\Delta C_T = C_{T(Target\ gene)} - C_{T(Housekeeping\ gene)}$$

$$\Delta\Delta C_T = \Delta C_{T(Experiment)} - \Delta C_{T(Control)}$$

$$Expression\ ratio = 2^{-\Delta\Delta C_T}$$

where C_T is the threshold cycle of a single PCR reaction.

For each sample triplicate measurements were performed.

8.9 Glucose and L-glutamine consumption, lactate and glutamate production (metabolic analysis)

At the end of each cultivation, the concentration of glucose and lactate in the medium was measured using an YSI 2700 SELECT analyzer. L-glutamine and L-glutamate concentrations were measured using a gradient HPLC (column: Waters Resolve C18, 5µm, 3.9x150mm, 30°C, flow: 1 ml/min) with a Fluorescence Detector RF-10AXL (Shimadzu, Japan).

Specific metabolite consumption rates (*qmet*) were calculated using the following equation:

$$qmet = \frac{\mu}{Cx(0)} \times \frac{C_{met}(t) - C_{met}(0)}{e^{\mu t} - 1}$$

with

$$\mu = \frac{\ln\left[Cx(t) / Cx(0)\right]}{\Delta t}$$

whereby *Cx(0)* and *Cx(t)* represent the cell numbers and *Cmet(0)* and *Cmet(t)* the amount of metabolite at the start (0) and the end (t) of the exponential growth phase, respectively, *t* the time (h) and μ the specific growth rate (h^{-1}).

8.10 Quantitative cytokine expression analysis

The intracellular concentration of cytokines at different oxygen concentrations was measured with the help of *Quantibody Human Growth Factor Array I*. For the quantitative cytokine expression analysis, UC-MSC from 3 donors were seeded into 6-wells plates at a density of 3000 cells/cm^2. Twenty four hours after seeding, all non-adherent cells were

removed by media changes and for the following 72 hours the MSC were incubated either at 2.5% or at 21% oxygen concentration. At the end of cultivation, cells were washed with PBS, immediately disrupted with lysis buffer and collected with a cell scraper. Cell lysates were homogenised via pipetting and centrifugated 5 minutes at $13.5x10^3$ g. Total protein concentration in the supernatant was measured with a photometer. Using the sample diluent provided by the kit, all samples were diluted to the final concentration of 500 µg/ml of total protein. Diluted cell lysates were incubated overnight at 4°C on the chip.

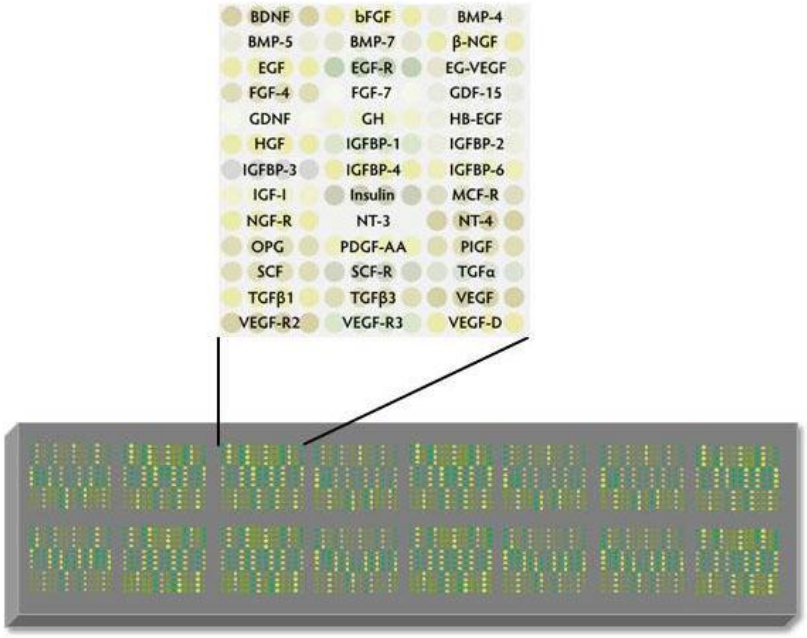

Figure 36: Schematic representation of the *Quantibody Human Growth Factor Array I* slide

The used microarray glass slide was spotted with 16 wells of identical cytokine antibody arrays. Each array consists of 168 spots, where every 4 spots represent identical capture antibodies, which detect the same cytokine. Along with positive controls, 40 different cytokines could be measured in one array (fig. 36). According to the manufacturer's instructions, serial dilutions of cytokine standards were prepared and incubated on the 8 arrays parallel to the experiment samples. After incubation, the glass slide was washed with the washing buffer, incubated with the detection antibody cocktail, washed again, incubated with the Cy3 fluorescence equivalent fluorescent dye, washed and dried with compressed air. Afterwards, the chip was scanned with a laser scanner at 532 nm. Multiple scans were

performed with a higher photo-multiplier tube (PMT) for low-signal cytokines and low PMT for high-signal cytokines.

8.11 Whole-genome DNA-microarray

The gene expression profile of UC-MSC cultivated at 21% and 2.5% oxygen concentration was detected using the DNA Microarray Human One Array (Phalanx Biotech Group, USA). After 72h of cultivation, cells were disrupted and RNA was isolated as described earlier (see chapter 7.6). Total RNA from each sample was reverse-transcribed in two different ways - one part with Cy3-labeling and another part with Cy5-labeling (dye-swap experiment). cDNA from the 2.5% O_2 sample marked with Cy5 was hybridized on the microarray-slide together with Cy3-labeled cDNA from the 21% O_2 sample and *vice versa*. The cDNA was labelled with biotin or fluorescein (Tyramide Signal Amplification (TSA)-labelling) and labelled cDNA was hybridized on the microarray slide with horseradish peroxidise-conjugated streptavidin or anti-fluorescein antibodies. Horseradish peroxidase converts fluoroconjugates (Cy3-tyramid, Cy5-tyramid) performing fluorescent staining of cDNA.

cDNA synthesis

• mix
  6‑8 µg RNA
  2 µl dNTPs
  1 µl Biotin- or Fluorescein nucleotides
  1 µl Hexamer primers
  1 µl Oligo-dT-primers
  ad 15 µL H_2O
• incubate for 10 min at 65°C, then add
  3 µl DTT
  5 µl RT buffer (5×) Superscript III
  2 µl Superscript III Reverse Transkriptase (200 U/µl)

• incubate for 2 hours at 42°C, cool for 5 min on ice
• add 2.5 µl 0.5 M EDTA (pH 8.0) and 2.5 µl 1 N NaOH
• incubate for 30 min at 65°C, cool for 5 min on ice
• add 6.5 µl 1 M Tris-HCl (pH 7.5)

Hybridization and detection

cDNA from 21 % O_2 and 2.5 % O_2 samples was mixed with hybridization buffer, denatured for 5 min at 95°C, then 10 % of Top-Block was added and cooled on ice for 1 min.

cDNA was transferred on the microarray slide and hybridized overnight at 42°C. For detection, the following steps were performed:

• wash 5 min with 2xSSC, 0.1 % SDS
• wash 5 min with 1x SSC
• wash 5 min with 0.5 x SSC

• incubate 10 min with 300 µl TNB-G blocking buffer
• wash 1 min in TNT-Buffer
• incubate 10 min with 200 µl Anti-Fl-HRP conjugate solution
• wash 3×1 min in TNT-Buffer
• incubate 10 min with 250 µl Cyanine-3 Tyramide solution
• wash 3×5 min in TNT-Buffer
• incubate 10 min with 200 µl HRP inactivation solution
• wash 3×1 min in TNT-buffer
• incubate 10 min with 200 µl Streptavidin-HRP conjugate solution
• wash 3×1 min in TNT-buffer
• incubate 10 min with 250 µl Cyanine-5 Tyramide solution
• wash 2×5 min in TNT-buffer
• wash 5 min in washing buffer 2 (1x SSC, 42° C)
• wash 1 min in 0.05x SSC
• dry slides by centrifugation for 2 min
• scan slides

Primary analysis and normalization

The microarrays were scanned at the wavelengths 532 nm (Cy3-channel) and 635 nm (Cy5-channel) in a Microarray Scanner GenePix 4000B. The single spots were detected and analyzed by Genepix Pro Software and signal intensities as well as intensity of the background were calculated. With the help of the software, developed in the Institute for Technical Chemistry [222], saturation effects were removed, gene replicates signal intensities were averaged and a quality analysis of the obtained data was performed. Spots with low signal to noise ratio, as well as high in variety between gene replicates, were eliminated. For the rest of the data average values of the background intensity were subtracted from the signal intensities and the results were logarithmized. The obtained values were defined as "spot intensity". Scanning-dependent variability was also compensated. Staining-dependent variability was removed with the help of a Loess-regression. Finally, all spot intensities of the dye-swap experiment for each gene were used to calculate the relative gene expression and its significance.

Functional analysis

To perform a functional analysis of the gene expression in different oxygen concentrations, PANTHER (**P**rotein **AN**alysis **TH**rough **E**volutionary **R**elationships) software was used. It is a system that classifies genes by their functions, using published scientific experimental evidence and evolutionary relationships to predict function even in the absence of direct experimental evidence. PANTHER biological function analysis tool classifies genes into 17 categories according to the role the proteins, which are encoded for by these genes play [170, 171]. The list of genes which are regulated differently under hypoxia when compared to normoxia can be found in table 9.1 of the supplementary materials. For more detailed information of the microarray analysis see [223].

8.12 Cell differentiation

To evaluate cell differentiation capacities, cells were seeded into fibronectin-coated 12-well cell culture plates at a density of 3000 cells/cm^2. After seeding, cells were cultivated for 72-96 hours (until full confluence) in αMEM containing 10% human serum and 50 µg/ml gentamicin in a humidified atmosphere containing 5% CO_2 and 21% O_2 at 37°C. Afterwards, the cell culture medium was changed to the osteogenic, chondrogenic or adipogenic differentiation medium, respectively. Differentiation and control media were supplemented with 50 µg/ml gentamicin. Medium exchange was performed every 3-4 days. Cells were cultured for the next 23 days and then fixed for 40 minutes in 4°C with 4% paraformaldehyde for staining.

8.13 Staining procedures

8.13.1 Von Kossa staining

To estimate cell differentiation towards the osteogenic lineage, von Kossa staining was performed. Fixed cell cultures were washed once with cold PBS, followed by washing twice with cold ddH_2O. 500 µl $AgNO_3$ solution was added in each well and cells were incubated in

this solution for 30 minutes in the dark. After incubation, cells were washed three times with ddH_2O and 500 µl formaldehyde solution was added to each well. After 1-2 minutes reaction, formaldehyde was removed and the cells were washed three times with PBS, after which they were examined under a microscope.

8.13.2 Calcein staining

Calcium accumulation in the extracellular matrix was detected by calcein fluorescent stain, which has a high affinity to Ca^{2+}. The fixed cell layer was washed twice with PBS, and covered with 1 ml of calcein solution (5 µg/ml in H_2O). Samples were incubated overnight at 4°C and thereafter washed extensively with distilled water. The fluorescence of the bounded calcein was detected at an excitation wavelength of 480 nm and an emission wavelength of 530 nm.

8.13.3 BODIPY staining

The intracellular accumulation of lipid droplets was visualised using BODIPY 493/503 (4,4-difluoro-1,3,5,7,8-pentamethyl-4-bora-3a,4a-diaza-s-indacene) stain. The BODIPY binds specifically to the triglycerides of lipid droplets without unspecific binding to the cell membrane lipids. The fixed cell layer was washed twice with PBS, 600 µl of BODIPY working solution (5 µM in PBS) was added per well and incubated in the dark for 5 minutes at room temperature. After incubation, the cell layer was washed twice with PBS and the fluorescence of the bounded BODIPY was detected at an excitation wavelength of 480 nm and an emission wavelength of 530 nm.

8.13.4 Alcian Blue staining

The accumulation of proteoglycans in the extracellular matrix was visualized by using Alcian Blue staining. Fixed cell layers were washed twice with PBS, incubated for 3 minutes in 3% acetic acid at room temperature, followed by 30 minutes incubation in Alcian Blue solution (1% Alcian Blue 8GX in 3% acetic acid) at room temperature. After incubation, the

cell layer was washed several times with 3% acetic acid and presence of the bounded Alcian Blue stain was detected with a microscope.

8.13.5 Mitochondria staining

For an evaluation of the mitochondria biomass in UC-MSC with flow cytometric analysis, cells were trypsinized, washed with PBS, centrifuged and incubated for 30 min at 37°C in 300 nM Mitotracker Green FM (Molecular Probes, Leiden, The Netherlands) diluted in αMEM without serum supplement. After the staining was complete, the cell suspension was re-pelleted by centrifugation and re-suspended in PBS. The flow cytometric analysis was performed using a FL-2 Filter (BP 560-590 nm) with at least 100,000 counted events. For microscopy, adherent cells were washed with warm PBS (37°C), incubated for 30 min at 37°C in 300 nM Mitotracker Green FM diluted in αMEM without serum supplement, washed with PBS and photographed using the fluorescent microscope Olympus IX50.

8.13.6 Senescence-associated β-galactosidase staining

Cell senescence was estimated with the use of the Senescence β-Galactosidase Staining Kit (Cell Signaling Technology, Danvers, USA) in accordance to the manufacturers' instructions. For the staining, cells were seeded at a density of 6,000 cells/cm^2 for 48 h, then washed with PBS, fixed with the fixation solution from the kit. Senescence-associated β-galactosidase (SA-β-gal) staining was performed overnight at 37°C.

8.14 Cell migration assay (wound healing assay)

For the cell migration assay, MSC were seeded on the 24-well plates with a density of 3000 cells/cm^2 48 hours before assay start. At the beginning of the assay (0 hours) the cell monolayer was manually scraped with a 200 µl pipette tip and the medium was exchanged. Eight hours after starting the assay, cells were photographed under a microscope using phase contrast or a fluorescent filter after calcein- acetoxymethyl ester (calcein-AM) staining.

8.15 Flow cytometric analysis of surface antigen expression

UC-MSC were harvested by accutase treatment, washed twice in a cold blocking buffer and re-suspended to a concentration of 10^6 cells per ml. Specific antibody-staining was performed by adding 20 µl of pre-diluted staining solution to 100 µl of cell suspension as described earlier [224]. Cells stained with matched isotype control antibodies served as a negative control. After 20 minutes incubation at room temperature in the dark, 400 µl of blocking buffer were added and cells were analyzed in an EPICS XL/MCL flow cytometer. At least, 10000 gated events were acquired on a LOG fluorescence scale. Generated data were analyzed using the program WinMDI 2.8.

Antibody	**Manufacturer**	**Antibody concentration per test, µg/120 µl**
Anti CD34-PE-Cy5	BD Bioscience	0.01
Anti CD45-PE-Cy5	BD Bioscience	0.01
BD mouse IgG1, k-PE-Cy5	BD Bioscience	0.01
Anti CD44-PE	BD Bioscience	0.03
Anti CD73-PE	BD Bioscience	0.03
BD mouse IgG1, k-PE	BD Bioscience	0.03
Anti CD105-PE	Invitrogen	0.05
Invitrogen mouse IgG1-R-PE	Invitrogen	0.05
Anti CD90-FITC	BD Bioscience	0.10
Anti CD31-FITC	BD Bioscience	0.10
BD mouse IgG1, k-FITC	BD Bioscience	0.10

8.16 Cell expansion in the Z®RP 2000 H bioreactor.

Before seeding, the tubing system, the bioreactor and all sensors were sterilized (in an autoclave or in 70% ethanol) according to the manufacturer's instructions. After sterilization, the tubing system was connected to the reactor, feed-flask, waste-flask and sensors according to the manufacturer's piping diagram (fig. 37). After installation, the system was filled with

αMEM and a 24 hours-sterile run was performed. To check sterility of the system, a cell culture media sample was taken from the reactor after 24 hours, glucose and lactate concentrations were measured and a microscopic observation was performed inspecting the presence of bacterial or fungal contamination.

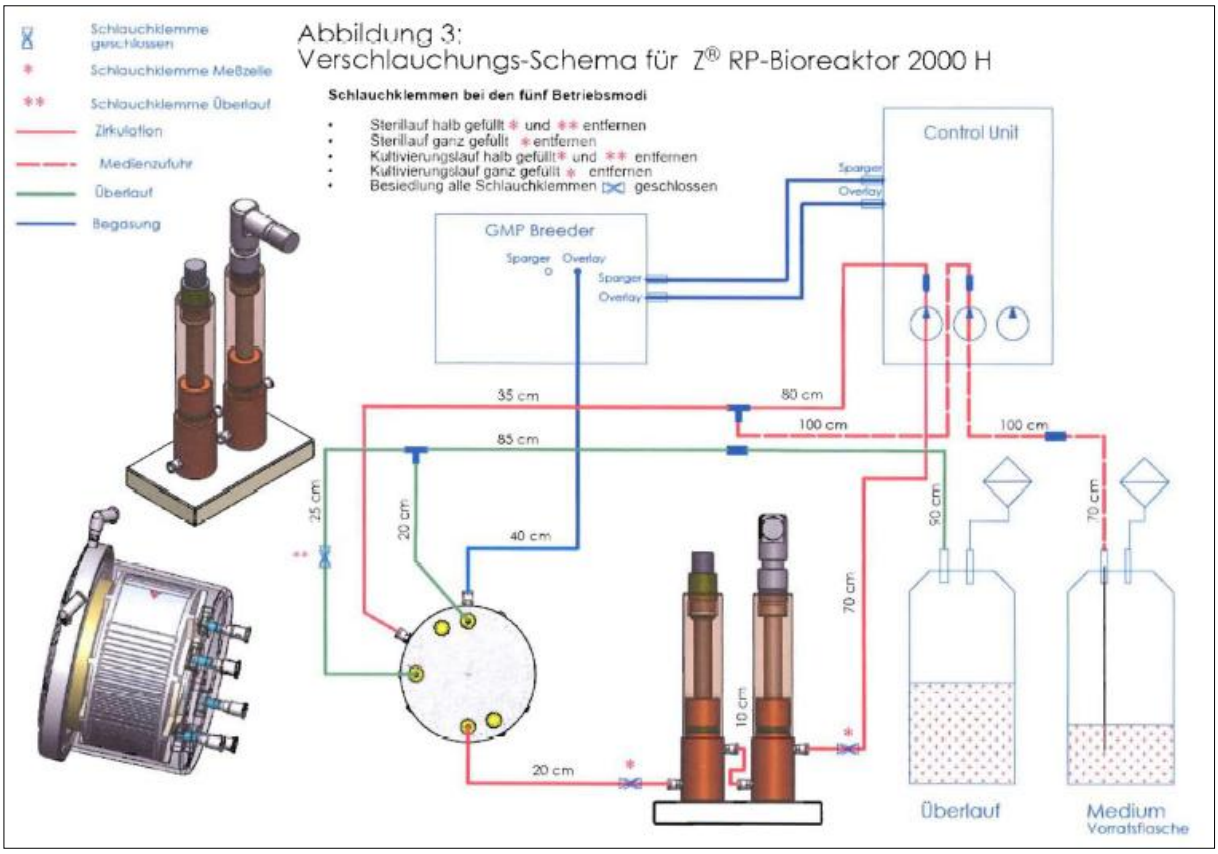

Figure 37: Piping and instrumentation diagram of the Z®RP 2000 H bioreactor system

For the expansion in the Z®RP 2000 H bioreactor, frozen UC-MSC were first revitalized, cultivated over 2 passages and seeded at a cell density of 1500 cells/cm^2 (total cell number 3 x 10^6 cells). Cells were seeded on both sides of the polycarbonate cell carrier slides with 24 hours attaching time for each side. For each seeding, the rotation bed was stopped so that the carrier slides were situated parallel to the ground. Afterwards, the bioreactor was filled with the cell suspension in 125 ml αMEM, supplemented with 10% human serum and 0.5% gentamicin (37°C). After attachment on both sides of the slides, bed rotation and

medium circulation were started. Cell culture media from the bioreactor was sampled once a day with the help of a syringe via a membrane installed on the bioreactor.

Figure 38: Z®RP 2000 H bioreactor system with breeder and control tower

Medium circulation was set on 0.1 ml/min, bed rotation – on 0.1 rpm, feeding rate with fresh cell culture medium was set on the intermitted mode (started with 2%) and increased each day depending on glucose consumption and lactate production. Breeder temperature was set on 37°C. The overlay gas mixture consisted of 95% air and 5% CO_2.

After 5 days of expansion, cells were harvested by treatment with accutase. First of all, the cell culture medium was removed from the bioreactor with the help of the pump, then the bioreactor was filled with warm (37°C) PBS, bed rotation was switched on and cells were washed for 5 minutes. After washing, PBS was removed, the bioreactor was filled with 80 ml accutase (37°C) and bed rotation was switched on for the next 20 minutes. After incubation with accutase, the harvested cells were collected in falcon-tubes and centrifuged for 15 minutes at 300 x g. Cell pellets were re-suspended in fresh αMEM and cell numbers were estimated by counting in a haemocytometer.

8.17 Statistical analysis

Data are represented as mean ± SD for triplicate measurements/counts for each sample. Statistical significance was defined as p value of 0.05 or less. Statistic was performed using one way ANOVA.

9 Supplementary materials

9.1 Functional analysis of genes, differently expressed under hypoxia (2.5% O_2)

Table 9.1. The list of genes, which were differently expressed in UC-MSC cultured for 72 hours in 2.5% O_2 if compared to 21% O_2.

Biological function	Number of genes	*List of genes*			
Apoptosis	13	*BOK* *CAPN1* *CASP10* *CASP9* *DPF2* *FKBP10* *IL10RA*	*ILF3* *LOX* *RELA* *STAU1* *TESK2* *TNFRSF10D*		
Cell adhesion	23	*AUP1* *BMP1* *CD63* *CD81* *COL1A2* *COL4A1* *COL5A1* *COL6A2* *COL6A3* *CRELD2* *DSC1* *EMR4P*	*FBLN2* *FURIN* *GPC1* *IGFBP3* *LEPREL2* *LOX* *ODZ4* *PLOD2* *PLOD3* *SIPA1* *SMAP2*		
Cell communication	62	*ANXA5* *ARL4C* *AUP1* *BMP1* *CAMTA2* *CAPN1* *CD63* *CD81* *CDC42EP1* *CLIC3* *COL1A2* *COL4A1* *COL5A1* *COL6A2* *COL6A3* *CREB3L3* *CRELD2* *DSC1*	*FABP5L3* *FBLN2* *FKBP10* *FOXP4* *FURIN* *GJA1* *GNB2* *GRK5* *IFT140* *IGFBP3* *IL10RA* *IQGAP1* *JUN* *KIR3DP1L* *CN1* *LEPREL2* *LOX* *LPAR1*	*NENF* *ODZ4* *PLXND1* *RAGE* *RAN* *RCAN3* *RELA* *S100A16* *S100A6* *SAG* *SHANK1* *SMAP2* *SPPL2B* *SSTR5* *SYT5* *TAS1R2* *TESK2* *TH*	*TNNC1* *TRIM23* *WNK4*

		EMR4P	*LRRC1*	*TNFRSF10*
		ERRFI1	*MYO19*	*D*
Cell cycle	20	*CCNB1*	*JUN*	
		DAZAP1	*MYO19*	
		DPF2	*PTP4A2*	
		DYNC1I2	*RAGE*	
		FBXL7	*RAN*	
		FKBP10	*RELA*	
		FOXP4	*S100A16*	
		HMGA1	*S100A6*	
		ILF3	*STAU1*	
		IQGAP1	*TESK2*	
Cellular component organization	19	*BRD2*	*HIST3H2BB*	
		COL1A2	*INO80*	
		COL4A1	*MIER2*	
		COL5A1	*MYO19*	
		COL6A2	*NF2*	
		COL6A3	*PLP1*	
		DYNC1I2	*TESK2*	
		FHL1	*TIMM17B*	
		FOXP4	*TJP2*	
		H2AFY2		
Cellular process	88	*ANXA5*	*FKBP10*	*PLP1*
		ARL4C	*FOXP4*	*PLXND1*
		ARPC5	*FURIN*	*PTP4A2*
		AUP1	*GJA1*	*RAGE*
		BMP1	*GNB2*	*RAN*
		BRD2	*GPC1*	*RCAN3*
		CAMTA2	*GRK5*	*RELA*
		CAPN1	*H2AFY2*	*S100A16*
		CCNB1	*HIST3H2BB*	*S100A6*
		CD63	*HMGA1*	*SAG*
		CD81	*IFT140*	*SHANK1*
		CDC42EP1	*IGFBP3*	*SIPA1*
		CLIC3	*IL10RA*	*SMAP2*
		COL1A2	*ILF3*	*SPPL2B*
		COL4A1	*INF2*	*SSTR5*
		COL5A1	*INO80*	*STAU1*
		COL6A2	*IQGAP1*	*SYT5*
		COL6A3	*JUN*	*TAS1R2*
		CREB3L3	*KIR3DP1*	*TESK2*
		CRELD2	*LCN1*	*TH*
		DAZAP1	*LEPREL2*	*TIMM17B*
		DPF2	*LOX*	*TJP2*
		DSC1	*LPAR1*	*TNFRSF10*
		DYNC1I2	*LRRC1*	*D*
		EMR4P	*MIER2*	*TNNC1*
		ENC1	*MYO19*	*TRIM23*
		ERRFI1	*NENF*	*WNK4*
		FABP5L3	*NF2*	

		FBLN2	*ODZ4*			
		FBXL7	*PLOD2*			
		FHL1	*PLOD3*			
Developmental process	36	*BMP1*	*ENC1*	*PLP1*		
		COL1A2	*FABP5L3*	*POGZ*		
		COL4A1	*FBLN2*	*RAGE*		
		COL5A1	*FHL1*	*RCAN3*		
		COL6A2	*FOXP4*	*SFXN4*		
		COL6A3	*FURIN*	*SMPD1*		
		CREB3L3	*HAND2*	*SMPDL3B*		
		CRELD2	*ILF3MAPK*	*STAU1*		
		DAZAP1	*BP1*	*TJP2*		
		DDAH1	*MIER2*	*TNFRSF10*		
		DLX1	*MYO19*	*D*		
		DYNC1I2	*NF2*			
		EMR4P	*NPAS4*			
Generation of precursor metabolites and energy	4	*ATPIF1*				
		COX6B1				
		L2HGDH				
		TAS1R2				
Homeostatic process	2	*COL1A2*				
		COL6A3				
Immune system processes	39	*ABHD11*	*FBXL7*	*S100A16*		
		B2M	*FHL1*	*S100A6*		
		BMP1	*FKBP10*	*SLC11A1*		
		CCDC8	*GLIPR2*	*STAU1*		
		CD63	*HSP90AA1*	*TAPBP*		
		CD81	*HSPA13*	*TESK2*		
		CLIC3	*HSPA2*	*TNFRSF10*		
		COL1A2	*IL10RA*	*D*		
		COL4A1	*ILF3*	*WFIKKN2*		
		COL5A1	*LCN1*			
		COL6A2	*LRRC1*			
		COL6A3	*NFE2L1*			
		CREB3L3	*PPIB PXDN*			
		EMR4P	*RAGE*			
		FBLN2	*RELA*			
Localization (RNA+Proteins)	4	*DYNC1I2*				
		MAPKBP1				
		RAN				
		STAU1				
Metabolic process	138	*ABHD11*	*DAZAP1*	*HSPA2*	*PLD4*	*SLC5A5*
		ACOT7	*DENR*	*ILF3*	*PLOD2*	*SMPD1*
		ACYP2	*DHX9*	*IMPDH2*	*PLOD3*	*SMPDL3B*
		AHCY	*DIO3*	*INO80*	*PLXND1*	*SRPR*

		ALG9	*DLX1*	*JUN*	*POGZ*	*ST3GAL1*
		ANXA5	*DPF2*	*L2HGDH*	*POLR3GL*	*ST6GALNA*
		APEX2	*DYNC1I2*	*LAMP1*	*PPA1*	*C4*
		ATP5O	*EEF1B2*	*LCN1*	*PPIB*	*STAU1*
		ATPIF1	*EIF3G*	*LOX*	*PRDM12*	*TAF11*
		BAHCC1	*EIF4E*	*LRRC1*	*PSAP*	*TAF15*
		BMP1	*FABP5L3*	*MAP2K3*	*PSMA2*	*TARS*
		BRD2	*FBLN2*	*MAPKBP1*	*PSMB1*	*TAS1R2*
		CAMTA2	*FBXL7*	*MIER2*	*PSMB4*	*TBP*
		CAPN1	*FHL1*	*MPDU1*	*PTP4A2*	*TERT*
		CARM1	*FKBP10*	*MRPL37*	*PXDN*	*TESK2*
		CASP10	*FOXP4*	*NANS*	*RABGGTB*	*TFEB*
		CASP9	*FURIN*	*NFE2L1*	*RAGE*	*TGM2*
		CHSY1	*G6PD*	*NHP2L1*	*RAN*	*TIMP3*
		CLIC3	*GLTPD2*	*NPAS4*	*RELA*	*TTLL12*
		CLPP	*GPAA1*	*NRBP1*	*RPL26*	*UTP14A*
		COL1A2	*GRK5*	*NT5DC2*	*RPL5*	*VWA5B1*
		COL4A1	*H2AFY2*	*NUBP2*	*RPS11*	*WFIKKN2*
		COL5A1	*HAND2*	*ODZ4*	*RPS12*	*WNK4*
		COL6A2	*HIST3H2BB*	*OTUD7B*	*RPS4Y2*	*ZBTB11*
		COL6A3	*HMGA1*	*PABPN1*	*RRM1*	*ZBTB7A*
		CPT1A	*HNRNPH1*	*PECI*	*SERPINE2*	*ZNF444*
		CREB3L3	*HSP90AA1*	*PFKL*	*SF3B3*	*ZNF692*
		CRELD2	*HSPA13*	*PGD*	*SLC38A10*	
Reproduction	7	*CD63*				
		CD81				
		DAZAP1				
		ILF3				
		LCN1				
		STAU1				
		TESK2				
Response to stimulus	34	*ABHD11*	*STAU1*			
		B2M	*TAPBP*			
		BMP1	*TAS1R2*			
		CD63	*TESK2*			
		CD81	*TNFRSF10D*			
		CLIC3	*WFIKKN2*			
		COL1A2	*IL10RA*			
		COL4A1	*KIR3DP1*			
		COL5A1	*LCN1*			
		COL6A2	*LOX*			
		COL6A3	*NFE2L1*			
		CREB3L3	*RAGE*			
		EMR4P	*RELA*			
		FHL1	*S100A16*			
		FKBP10	*S100A6*			
		HSP90AA1	*SLC11A1*			
		HSPA13				
		HSPA2				
System process	31	*BMP1*	*KCNK18*			
		CD63	*LCN1*			
		CD81	*LOX*			

		CNN1	*LPAR1*	
		COL1A2	*MOBP*	
		COL6A3	*MYO19*	
		CREB3L3	*PLP1*	
		CRELD2	*SAG*	
		DAZAP1	*SSTR5*	
		EMR4P	*STAU1*	
		FBLN2	*SYT5*	
		FKBP10	*TAF15TAS1*	
		FOXP4	*R2*	
		GNB2	*TNNC1*	
		GRK5	*WNK4*	
		ILF3		
Transport	43	*ANXA5*	*EMR4P*	*RAN*
		AP2A1	*FABP5L3*	*RHCE*
		ARL4C	*GLTPD2*	*SAG*
		ATP5O	*IFT140*	*SFXN4*
		BMP1	*ILF3*	*SLC11A1*
		CLIC3	*KCNK18*	*SLC38A10*
		CLTB	*LAMP1*	*SLC5A5*
		COL1A2	*LCN1*	*SNX32*
		COL4A1	*LOX*	*SRPR*
		COL5A1	*MOBP*	*SSR2*
		COL6A2	*MYO19*	*TIMM17B*
		COL6A3	*NRBP1*	*TRIM23*
		COPA	*ODZ4PIGU*	
		CRELD2	*PPIB*	
		DYNC1I2	*PSAP*	
Regulation of bilogical processes	0			

Table 8.1. The list of ratios of significanlely up- or down-regulated genes under hypoxia (2.5% O_2)

Phalanx_id	Gene_symbol	Description	Entrez_gene	RefSeq	Regulation significa	E1 2,5 % O2 gegen 21 % O2 Ratio 1-3 : 11-13	Regulation	SE
PH_hs_0033270	HIST1H4H|HIST1H4E	histone cluster 1, H4h	8365|8367	NM_003543.3|NM_00	2	-9,1645	-3	8,6032
PH_hs_0044010	LOC100130856	hypothetical LOC100:	100130856	XR_078853.1,XR_079	2	-9,1512	-3	11,4531
PH_hs_0023822	OTUD7B	OTU domain containir	56957	NM_020205.2	2	-7,1337	-3	8,9546
PH_hs_0029966	RPS12	ribosomal protein S12	6206	NM_001016.3	2	-5,5584	-3	5,8872
PH_hs_0015581	ZBTB11	zinc finger and BTB d	27107	NM_014415.3	2	-5,36	-3	5,1097
PH_hs_0044626	POGZ	pogo transposable ele	23126	NM_145796.2	2	-5,2745	-3	7,3565
PH_hs_0030515	KRTAP20-2	keratin associated pr	337976	NM_181616.1	2	-5,1938	-3	4,1255
PH_hs_0008886	CDC42EP1	CDC42 effector protei	11135	NM_152243.2	2	-4,9926	-2	6,1905
PH_hs_0019545	AUP1	ancient ubiquitous pr	550	NM_181575.3	2	-4,8547	-2	5,1556
PH_hs_0025386	POMGNT1	protein O-linked mant	55624	NM_017739.3,NR_02	2	-4,5375	-2	4,0007
PH_hs_0000093	TRIM23	tripartite motif-contain	373	NM_001656.3	2	-4,3531	-2	4,0087
PH_hs_0047862	RANGAP1	Ran GTPase activatin	5905	NM_002883.2	2	-4,2901	-2	5,0343
PH_hs_0027023	INO80	INO80 homolog (S. ce	54617	NM_017553.1	2	-4,1268	-2	5,8089
PH_hs_0034181	IL10RA	interleukin 10 recepto	3587	NM_001558.3,NR_02	2	-3,9788	-2	4,6161
PH_hs_0019363	DLX1	distal-less homeobox	1745	NM_001038493.1,NM	2	-3,5662	-2	3,6707
PH_hs_0042710	GLTPD2	glycolipid transfer pro	388323	NM_001014985.1	2	-3,4732	-2	2,4873
PH_hs_0027566	S100A16	S100 calcium binding	140576	NM_080388.1	2	-3,4619	-2	3,4025
PH_hs_0042033	RPL26	ribosomal protein L26	6154	NM_000987.3	2	-3,4398	-2	4,0003
PH_hs_0002463	EIF3G	eukaryotic translation	8666	NM_003755.3	2	-3,3835	-2	0,63848
PH_hs_0042155	SHANK1	SH3 and multiple ank	50944	NM_016148.2	2	-3,3242	-2	2,5584
PH_hs_0029923	DHX9	DEAH (Asp-Glu-Ala-H	1660	NM_001357.4,NR_03	2	-3,2277	-2	2,9983
PH_hs_0040143	VWA5B1	von Willebrand factor	127731	NM_001039500.2	2	-3,2111	-2	4,471
PH_hs_0000440	ST6GALNAC4	ST6 (alpha-N-acetyl-n	27090	NM_175039.3,NM_17	2	-3,1976	-2	2,6202
PH_hs_0026052	CD63	CD63 molecule	967	NM_001780.4,NM_00	2	-3,1238	-2	3,9282
PH_hs_0030503	RPL5	ribosomal protein L5	6125	NM_000969.3	2	-3,1023	-2	2,9992
PH_hs_0027643	FPGT	fucose-1-phosphate g	8790	NM_003838.2	2	-2,9345	-2	2,6158
PH_hs_0029874	HNRNPA1|LOC64569	heterogeneous nuclea	3178|644037|645691	NM_002136.2,NM_03	2	-2,903	-2	2,6201
PH_hs_0046469	TLX1NB	TLX1 neighbor	100038246	NM_001085398.1	2	-2,9014	-2	2,4083
PH_hs_0010680	MAP2K3	mitogen-activated pro	5606	NM_002756.4,NM_14	2	-2,8565	-2	2,1965
PH_hs_0043029	KBTBD13	kelch repeat and BTB	390594	NM_001101362.2	2	-2,8391	-2	3,4595
PH_hs_0043883	RELA	v-rel reticuloendotheli	5970	NM_021975.3,NM_00	2	-2,7973	-2	1,9772
PH_hs_0043221	GNB2	guanine nucleotide bi	2783	NM_005273.3	2	-2,7729	-2	2,9468
PH_hs_0035877	MYADM	myeloid-associated d	91663	NM_001020821.1,NM	2	-2,74	-2	2,8555
PH_hs_0003564	CD81	CD81 molecule	975	NM_004356.3	2	-2,6982	-2	2,8326
PH_hs_0002191	INF2	inverted formin, FH2 a	64423	NM_001031714.3,NM	2	-2,6897	-2	2,7639
PH_hs_0024458	HAND2	heart and neural crest	9464	NM_021973.2	2	-2,6873	-2	3,0247
PH_hs_0026265	KCNK18	potassium channel, s	338567	NM_181840.1	2	-2,6385	-2	2,6809
PH_hs_0035093	LOC440031	hypothetical LOC440(	440031	XR_040618.2,XR_017	2	-2,6003	-2	2,0774
PH_hs_0010296	TROAP	trophinin associated p	10024	NM_005480.3	2	-2,5713	-2	1,7952
PH_hs_0036873	PCDHB19P|CABP4	protocadherin beta 19	84054|57010	NR_001282.2|NM_14	2	-2,5553	-2	3,269
PH_hs_0026842	L2HGDH	L-2-hydroxyglutarate d	79944	NM_024884.2	2	-2,5535	-2	1,7566
PH_hs_0023824	CASP9	caspase 9, apoptosis	842	NM_032996.1,NM_00	2	-2,5035	-2	2,2004
PH_hs_0023994	CAPN1	calpain 1, (mu/I) large	823	NM_005186.2	2	-2,4907	-2	1,6949
PH_hs_0004749	TAF11	TAF11 RNA polymera	6882	NM_005643.2	3	-2,4876	-2	0,2272
PH_hs_0043105	RAN	RAN, member RAS o	5901	NM_006325.3	2	-2,4872	-2	1,3927
PH_hs_0018539	CLTB	clathrin, light chain B	1212	NM_001834.2,NM_00	2	-2,4835	-2	1,5781
PH_hs_0026471	POU5F2	POU domain class 5,	134187	NM_153216.1	2	-2,4824	-2	1,1267
PH_hs_0007549	KCAN3	KCAN family member	11123	NM_013441.2	2	-2,3897	-2	1,6885
PH_hs_0005962	CAMTA2	calmodulin binding tra	23125	NM_015099.3,NM_00	2	-2,2909	-2	2,1399
PH_hs_0044118	SMPDL3B	sphingomyelin phospl	27293	NM_001009568.1,NM	2	-2,2819	-2	2,2647
PH_hs_0042750	OR6C70	olfactory receptor, fan	390327	NM_001005499.1	3	-2,2749	-2	0,21695
PH_hs_0049587	CTAG1A|CTAG1B|CT	cancer/testis antigen	1485|30848|246100	NM_139250.1|NM_00	2	-2,2639	-2	1,2678
PH_hs_0026823	TGM2	transglutaminase 2 (C	7052	NM_004613.2	2	-2,2615	-2	2,9251
PH_hs_0030181	RPS11	ribosomal protein S11	6205	NM_001015.3	2	-2,2564	-2	0,85018
PH_hs_0046433	NCRNA00164	non-protein coding RN	554226	NR_027020.2	2	-2,2539	-2	2,4937
PH_hs_0043566	FAM54A	family with sequence	113115	NM_001099286.1,NM	2	-2,2462	-2	1,7536
PH_hs_0023944	SLC38A10	solute carrier family 3	124565	NM_138570.2	2	-2,243	-2	1,6636
PH_hs_0032312	POU2F3|POU3F1|PO	POU class 2 homeob	5455|5453|25833	NM_014352.2|NM_00	2	-2,2173	-2	1,8436
PH_hs_0044633	PTP4A2	protein tyrosine phosp	8073	NM_080392.2,NM_08	2	-2,2136	-2	2,2532
PH_hs_0042367	TNNC1	troponin C type 1 (slo	7134	NM_003280.2	2	-2,2071	-2	1,0404
PH_hs_0049694	H3F3B|H3F3C	H3 histone, family 3B	440093|3021	NM_005324.3|NM_00	2	-2,2068	-2	1,4385
PH_hs_0042321	OR1I1	olfactory receptor, fan	126370	NM_001004713.1	2	-2,2048	-2	1,9684
PH_hs_0029772	SMCR8	Smith-Magenis syndr	140775	NM_144775.2	2	-2,1918	-2	3,0898
PH_hs_0028920	HMGA1	high mobility group A1	3159	NM_145905.2,NM_14	2	-2,18625	-2	1,448945
PH_hs_0023823	GPC1	glypican 1	2817	NM_002081.2	2	-2,1591	-2	1,5715
PH_hs_0026852	ARHGAP39	Rho GTPase activatin	80728	NM_025251.1	2	-2,1586	-2	1,2192
PH_hs_0028357	COBRA1	cofactor of BRCA1	25920	NM_015456.3	2	-2,1526	-2	1,2751
PH_hs_0000462	MRPL37	mitochondrial ribosom	51253	NM_016491.3	2	-2,138	-2	1,9504
PH_hs_0023074	WFIKKN2	WAP, follistatin/kazal	124857	NM_175575.5	2	-2,1355	-2	1,0159
PH_hs_0046596	LOC100294360	hypothetical protein L	100294360	XM_002347180.1	2	-2,1348	-2	2,1244
PH_hs_0013495	ILF3	interleukin enhancer b	3609	NM_017620.2,NM_01	2	-2,1266	-2	1,5713
PH_hs_0047850	GPAA1	glycosylphosphatidyli	8733	NM_003801.3	2	-2,1247	-2	2,1018
PH_hs_0032896	PFKL	phosphofructokinase,	5211	NM_002626.4,NR_02	2	-2,1133	-2	1,9808
PH_hs_0047518	FAM26E	family with sequence	254228	NM_153711.2	3	-2,0919	-2	0,28982
PH_hs_0003807	FURIN	furin (paired basic am	5045	NM_002569.2	2	-2,0901	-2	2,3143
PH_hs_0027539	LCN1	lipocalin 1 (tear prealt	3933	NM_002297.2	2	-2,0791	-2	1,6456
PH_hs_0025939	SRPR	signal recognition par	6734	NM_003139.3,NM_00	2	-2,0764	-2	1,8669
PH_hs_0024266	MAPKBP1	mitogen-activated pro	23005	NM_001128608.1,NM	2	-2,068	-2	2,8887
PH_hs_0043374	B2M	beta-2-microglobulin	567	NM_004048.2	2	-2,056	-2	2,1876
PH_hs_0039500	ST3GAL1	ST3 beta-galactoside	6482	NM_003033.3,NM_17	2	-2,0434	-2	1,7175
PH_hs_0022607	ANXA5	annexin A5	308	NM_001154.3	2	-2,0256	-2	0,8271
PH_hs_0045469	LOC100129984	similar to LOC642031	100129984	XR_078962.1,XR_079	2	-2,02	-2	0,8028
PH_hs_0043389	SNX32	sorting nexin 32	254122	NM_152760.2	2	-2,0157	-2	2,631
PH_hs_0035739	S100A6	S100 calcium binding	6277	NM_014624.3	2	-2,0125	-2	0,65654
PH_hs_0000699	C16orf61	chromosome 16 open	56942	NM_020188.3	2	-2,0062	-2	1,8346
PH_hs_0035507	MIER2	mesoderm induction e	54531	NM_017550.1	2	-2,0032	-2	0,69624
PH_hs_0043313	ROMO1	reactive oxygen speci	140823	NM_080748.2	2	-2,0017	-2	1,8318
PH_hs_0025350	INO80E	INO80 complex subur	283899	NM_173618.1	2	2,0009	2	0,40449
PH_hs_0005831	ENC1	ectodermal-neural cor	8507	NM_003633.2	2	2,0046	2	0,53724
PH_hs_0018551	DDAH1	dimethylarginine dime	23576	NM_012137.3,NM_00	2	2,0146	2	0,48873
PH_hs_0023170	COL6A3	collagen, type VI, alpl	1293	NM_057167.3,NM_00	2	2,0148	2	0,3297
PH_hs_0015263	BOK	BCL2-related ovarian	666	NM_032515.3	3	2,0163	2	0,093989
PH_hs_0032984	HIST3H2BB	histone cluster 3, H2b	128312	NM_175055.2	2	2,0171	2	0,30748
PH_hs_0001955	DENR	density-regulated prot	8562	NM_003677.3	3	2,0217	2	0,19596
PH_hs_0033638	FABP5L3	fatty acid binding prot	220832	NR_002935.1	2	2,0218	2	0,58445
PH_hs_0006559	PXDN	peroxidasin homolog	7837	NM_012293.1	2	2,0287	2	0,39388
PH_hs_0040555	ZNF860	zinc finger protein 86(	344787	NM_001137674.1	2	2,029	2	0,36303

PH_hs_0022427	LRRC1	leucine rich repeat co	55227	NM_018214.4	3	2,0452	2	0,087192
PH_hs_0031355	LOC649395|LOC4409	tyrosine 3-monooxyg	7531|440917|649395	NR_029404.1|XR_041	3	2,0456	2	0,21523
PH_hs_0045793	NHP2L1	NHP2 non-histone ch	4809	NM_005008.2,NM_0C	2	2,0544	2	0,43634
PH_hs_0005933	FAM5C	family with sequence	339479	NM_199051.1	3	2,0587	2	0,26729
PH_hs_0000946	TESK2	testis-specific kinase	10420	NM_007170.2	2	2,0603	2	0,31078
PH_hs_0011521	C1orf107	chromosome 1 open	27042	NM_014388.5	2	2,0729	2	0,57438
PH_hs_0000798	SMAP2	small ArfGAP2	64744	NM_022733.1	3	2,0735	2	0,26563
PH_hs_0043523	WDR83	WD repeat domain 83	84292	NR_029375.1,NM_03	3	2,0742	2	0,27602
PH_hs_0042334	MT4	metallothionein 4	84560	NM_032935.2	3	2,092	2	0,193
PH_hs_0001029	CCM2	cerebral cavernous m	83605	NM_001167934.1,NM	3	2,0938	2	0,29822
PH_hs_0001423	PECI	peroxisomal D3,D2-er	10455	NM_001166010.1,NM	2	2,0965	2	0,43702
PH_hs_0045059	CPT1A	carnitine palmitoyltrar	1374	NM_001876.3	2	2,1001	2	0,48934
PH_hs_0029645	COTL1	coactosin-like 1 (Dict	23406	NM_021149.2	2	2,1002	2	0,3978
PH_hs_0042749	APOB48R	apolipoprotein B48 re	55911	NM_018690.2	3	2,1015	2	0,29307
PH_hs_0015252	PRR14	proline rich 14	78994	NM_024031.2	2	2,1015	2	0,48074
PH_hs_0009351	HNRNPUL1	heterogeneous nuclea	11100	NM_144732.2,NM_0C	2	2,1067	2	0,50926
PH_hs_0028935	CCDC85B	coiled-coil domain co	11007	NM_006848.2	2	2,1108	2	0,41616
PH_hs_0005949	RBM17	RNA binding motif pro	84991	NM_001145547.1,NM	3	2,1142	2	0,28675
PH_hs_0037874	C16orf46	chromosome 16 open	123775	NM_001100873.1	3	2,1186	2	0,23213
PH_hs_0042240	PSMB1	proteasome (prosome	5689	NM_002793.3	2	2,1187	2	0,40597
PH_hs_0049655	RHCE	Rh blood group, CcE	6006	NM_020485.3,NM_13	3	2,1207	2	0,20736
PH_hs_0029021	TARS	threonyl-tRNA synthe	6897	NM_152295.3	2	2,1502	2	0,4065
PH_hs_0045945	UTP14A	UTP14, U3 small nuc	10813	NM_001166221.1,NM	2	2,1563	2	0,36883
PH_hs_0028149	BCL7C	B-cell CLL/lymphoma	9274	NM_004765.2	3	2,157	2	0,097649
PH_hs_0045570	TAPBP	TAP binding protein (t	6892	NM_172208.2	3	2,1575	2	0,15425
PH_hs_0022878	SFXN4	sideroflexin 4	119559	NM_213649.1	3	2,1625	2	0,28302
PH_hs_0025276	PGBD2	piggyBac transposabl	267002	NM_001017434.1,NM	2	2,1688	2	0,31983
PH_hs_0027589	TIMM17B	translocase of inner n	10245	NM_001167947.1,NM	3	2,1726	2	0,20548
PH_hs_0045836	SIPA1	signal-induced prolifer	6494	NM_153253.29,NM_0	2	2,1754	2	0,31016
PH_hs_0000238	IQGAP1	IQ motif containing G	8826	NM_003870.3	3	2,1786	2	0,19003
PH_hs_0048360	ARL4C	ADP-ribosylation fact	10123	NM_005737.3	2	2,1799	2	0,33279
PH_hs_0032808	HSPA13	heat shock protein 70	6782	NM_006948.4	2	2,1909	2	0,41973
PH_hs_0000619	STAU1	staufen, RNA binding	6780	NM_001037328.1,NM	3	2,1934	2	0,18773
PH_hs_0019972	COX6B1	cytochrome c oxidase	1340	NM_001863.4	2	2,2018	2	0,52886
PH_hs_0004295	BRD2	bromodomain contain	6046	NM_001113182.1,NM	2	2,2174	2	0,31735
PH_hs_0009279	APEX2	APEX nuclease (apur	27301	NM_014481.2	3	2,2225	2	0,20853
PH_hs_0004585	EIF4E	eukaryotic translation	1977	NM_001130678.1,NM	2	2,2227	2	0,50923
PH_hs_0001829	CNN1	calponin 1, basic, sm	1264	NM_001299.4	2	2,2257	2	0,48451
PH_hs_0033202	ATP5O	ATP synthase, H+ tra	539	NM_001697.2	2	2,2279	2	0,54128
PH_hs_0013494	NUBP2	nucleotide binding pro	10101	NM_012225.2	2	2,2314	2	0,44653
PH_hs_0004730	TTLL12	tubulin tyrosine ligase	23170	NM_015140.3	2	2,2368	2	0,39283
PH_hs_0045613	CASP10	caspase 10, apoptosi	843	NM_032974.3	2	2,2453	2	0,4704
PH_hs_0046039	TMEM14C	transmembrane prote	51522	NM_001165258.1,NM	3	2,2491	2	0,27801
PH_hs_0046484	LOC100290317	similar to hCG202339	100290317	XM_002346903.1	3	2,2518	2	0,087802
PH_hs_0027111	SAG	S-antigen; retina and	6295	NM_000541.4	2	2,26	2	0,3642
PH_hs_0019280	PSAP	prosaposin	5660	NM_001042466.1,NM	2	2,2713	2	0,43424
PH_hs_0004521	SNAPC2	small nuclear RNA ac	6618	NM_003083.3,NR_03	3	2,2738	2	0,24798
PH_hs_0028961	GJA1	gap junction protein, a	2697	NM_000165.3	3	2,2765	2	0,29542
PH_hs_0047141	BNIP3	BCL2/adenovirus E1B	664	NM_004052.2	3	2,2801	2	0,071778
PH_hs_0047221	LPAR1	lysophosphatidic acid	1902	NM_057159.2,NM_0C	2	2,2808	2	0,36861
PH_hs_0048643	ODZ4	odz, odd Oz/ten-m ho	26011	NM_001098816.2	2	2,2889	2	0,44381
PH_hs_0035799	PSMA2	proteasome (prosome	5683	NM_002787.4	2	2,2946	2	0,36339
PH_hs_0030600	C5orf13	chromosome 5 open	9315	NM_001142483.1,NM	2	2,3167	2	0,50902
PH_hs_0025029	BAHCC1	BAH domain and coil	57597	NM_001080519.2	3	2,3234	2	0,25815
PH_hs_0024183	CARM1	coactivator-associate	10498	NM_199141.1	2	2,3499	2	0,4033
PH_hs_0017046	C21orf29	chromosome 21 open	54084	NM_144991.2	3	2,3547	2	0,22668
PH_hs_0012932	ATPIF1	ATPase inhibitory fac	93974	NM_178191.1,NM_17	3	2,3576	2	0,27825
PH_hs_0005777	RAGE	renal tumor antigen	5891	NM_014226.1	2	2,358	2	0,46952
PH_hs_0024800	MOBP	myelin-associated oli	4336	NR_003090.1	2	2,3607	2	0,42671
PH_hs_0004525	JUN	jun oncogene	3725	NM_002228.3	3	2,3715	2	0,24698
PH_hs_0003071	PLOD2	procollagen-lysine, 2-	5352	NM_182943.2,NM_0C	3	2,3812	2	0,2761
PH_hs_0030164	KRT16P3|KRT16	keratin 16 pseudogen	3868|644945	NR_029393.1|NM_005	2	2,3883	2	0,22727
PH_hs_0025361	PPIB	peptidylprolyl isomera	5479	NM_000942.4	2	2,4085	2	0,435
PH_hs_0015639	GLIPR2	GLI pathogenesis-rela	152007	NM_022343.2	3	2,4181	2	0,16937
PH_hs_0019840	ANAPC16	anaphase promoting c	119504	NM_173473.2	3	2,434	2	0,163
PH_hs_0032160	C17orf49	chromosome 17 open	124944	NM_174893.2,NM_0C	2	2,4534	2	0,34254
PH_hs_0000111	NF2	neurofibromin 2 (merli	4771	NM_181830.2,NM_01	2	2,4573	2	0,3812
PH_hs_0025750	DAZAP1	DAZ associated prote	26528	NM_018959.2,NM_17	2	2,462	2	0,38845
PH_hs_0024691	PLD4	phospholipase D fami	122618	NM_138790.2	3	2,4643	2	0,16504
PH_hs_0009944	C16orf7	chromosome 16 open	9605	NM_004913.2	3	2,4746	2	0,27471
PH_hs_0027174	NFE2L1	nuclear factor (erythro	4779	NM_003204.2	3	2,4964	2	0,28496
PH_hs_0035795	POLR3GL	polymerase (RNA) III	84265	NM_032305.1	2	2,4967	2	0,37741
PH_hs_0023612	MYO19	myosin XIX	80179	NM_001163735.1,NM	2	2,5016	2	0,47596
PH_hs_0003290	LEPREL2	leprecan-like 2	10536	NM_014262.3	2	2,5054	2	0,3706
PH_hs_0033554	HNRNPL|LOC644390	heterogeneous nuclea	3191|644390	NM_001005335.1,NM	3	2,5275	2	0,28319
PH_hs_0017280	RNF187	ring finger protein 187	149603	NM_001010858.2	2	2,537	2	0,31973
PH_hs_0000144	TBP	TATA box binding pro	6908	NM_001172085.1,NM	2	2,5534	2	0,4933
PH_hs_0027148	SSR2	signal sequence rece	6746	NM_003145.3	2	2,5537	2	0,41309
PH_hs_0011708	FOXP4	forkhead box P4	116113	NM_001012426.1,NM	2	2,5712	2	0,3317
PH_hs_0022388	ARPC5	actin related protein 2	10092	NM_005717.2	3	2,5835	2	0,084769
PH_hs_0004430	FBXL7	F-box and leucine-rich	23194	NM_012304.3	3	2,5854	2	0,19632
PH_hs_0005860	WNK4	WNK lysine deficient	65266	NM_032387.4	3	2,5932	2	0,12681
PH_hs_0014083	NRBP1	nuclear receptor bindi	29959	NM_013392.2	2	2,6075	2	0,33579
PH_hs_0027726	DYNC1I2	dynein, cytoplasmic 1	1781	NM_001378.1	2	2,6143	2	0,41407
PH_hs_0000242	PLP1	proteolipid protein 1	5354	NM_199478.1,NM_0C	3	2,6242	2	0,28135
PH_hs_0012265	GRK5	G protein-coupled rec	2869	NM_005308.2	2	2,6245	2	0,42189
PH_hs_0013484	NPAS4	neuronal PAS domain	266743	NM_178864.3	3	2,6308	2	0,21204
PH_hs_0009041	LAMP1	lysosomal-associated	3916	NM_005561.3	3	2,6449	2	0,17743
PH_hs_0002954	STRA13	stimulated by retinoic	201254	NM_144998.2	2	2,6694	2	0,34489
PH_hs_0049609	RCN1|LOC100287828	reticulocalbin 1, EF-h	5954|100287828	NM_002901.2|XR_07	2	2,6742	2	0,44869
PH_hs_0047260	COL1A2	collagen, type I, alpha	1278	NM_000089.3	3	2,7099	2	0,067371
PH_hs_0030270	TERT	telomerase reverse tra	7015	NM_198253.2,NM_19	2	2,7195	2	0,37662
PH_hs_0029073	ZBTB7A	zinc finger and BTB d	51341	NM_015898.2	2	2,7294	2	0,36772
PH_hs_0003436	DIO3	deiodinase, iodothyro	1735	NM_001362.3	2	2,7296	2	0,30022
PH_hs_0048010	PLEKHB2	pleckstrin homology c	55041	NM_001100623.1,NM	3	2,7474	2	0,24079
PH_hs_0002059	TFEB	transcription factor EI	7942	NM_001167827.1,NM	2	2,7602	2	0,49578
PH_hs_0023080	PDIA6	protein disulfide isom	10130	NM_005742.2	3	2,7717	2	0,23143
PH_hs_0005347	CCDC8	coiled-coil domain co	83987	NM_032040.3	3	2,808	2	0,20864
PH_hs_0049125	ALG9	asparagine-linked gly	79796	NM_001077692.1,NM	3	2,818	2	0,26678
PH_hs_0045348	LOC646127	similar to telomeric re	646127	XR_037301.2,XR_037	2	2,8305	2	0,34886

PH_hs_0031935	COPA	coatomer protein com	1314	NM_001098398.1,NM	2	2,8357	2	0,32912
PH_hs_0029963	PPA1	pyrophosphatase (ino	5464	NM_021129.3	3	2,8938	2	0,26825
PH_hs_0015334	AP2A1	adaptor-related protei	160	NM_130787.2,NM_01	2	2,9292	2	0,32067
PH_hs_0024614	TAF15	TAF15 RNA polymera	8148	NM_003487.2,NM_13	2	2,9471	2	0,38257
PH_hs_0040733	HSP90AA1	heat shock protein 90	3320	NM_005348.3	2	2,9526	2	0,36683
PH_hs_0018576	GABARAP	GABA(A) receptor-as	11337	NM_007278.1	3	2,9544	2	0,29383
PH_hs_0000700	GORASP2	golgi reassembly stac	26003	NM_015530.3	2	2,9816	2	0,41021
PH_hs_0001501	SPAG5	sperm associated ant	10615	NM_006461.3	2	2,986	2	0,37836
PH_hs_0043124	FKBP10	FK506 binding protein	60681	NM_021939.3	3	2,9982	2	0,27173
PH_hs_0029475	SSTR5	somatostatin receptor	6755	NM_001172560.1,NM	2	2,9997	2	0,33428
PH_hs_0013255	C19orf63	chromosome 19 open	284361	NM_175063.4,NM_20	3	3,0228	2	0,22922
PH_hs_0023910	DSC1	desmocollin 1	1823	NM_004948.3,NM_02	3	3,0431	2	0,085343
PH_hs_0027789	ACTN1	actinin, alpha 1	87	NM_001130004.1,NM	3	3,0585	2	0,13243
PH_hs_0011293	SEC61B|LOC100287	Sec61 beta subunit|si	10952|100287189	NM_006808.2|XM_00	2	3,1203	2	0,32075
PH_hs_0004492	SMPD1	sphingomyelin phospl	6609	NR_027400.1,NM_00	3	3,1229	2	0,368255
PH_hs_0001088	ERRFI1	ERBB receptor feedb	54206	NM_018948.3	3	3,1643	2	0,18728
PH_hs_0035456	IMPDH2	IMP (inosine 5'-monop	3615	NM_000884.2	3	3,2195	2	0,24141
PH_hs_0033736	TMEM119	transmembrane prote	338773	NM_181724.2	2	3,2398	2	0,35334
PH_hs_0024442	AHCY	adenosylhomocystein	191	NM_000687.2,NM_00	3	3,2501	2	0,26759
PH_hs_0002461	CRELD2	cysteine-rich with EG	79174	NM_001135101.1,NM	3	3,2727	2	0,29547
PH_hs_0009226	PLOD3	procollagen-lysine, 2-	8985	NM_001084.4	2	3,2934	2	0,35407
PH_hs_0025416	TH	tyrosine hydroxylase	7054	NM_199293.2,NM_19	3	3,3139	2	0,13591
PH_hs_0019152	TAS1R2	taste receptor, type 1	80834	NM_152232.2	3	3,3147	2	0,2815
PH_hs_0043131	RPP40	ribonuclease P/MRP	10799	NM_006638.2	3	3,3597	2	0,22692
PH_hs_0035939	COL6A2	collagen, type VI, alpl	1292	NM_058175.2,NM_05	3	3,365	2	0,29128
PH_hs_0032900	KAZ	kazrin	23254	NM_001017999.2,NM	3	3,388	2	0,25798
PH_hs_0005770	SLC5A5	solute carrier family 5	6528	NM_000453.2	3	3,4101	2	0,20619
PH_hs_0025581	COL4A1	collagen, type IV, alpl	1282	NM_001845.4	3	3,4532	2	0,23466
PH_hs_0004556	RABGGTB	Rab geranylgeranyltra	5876	NM_004582.2	2	3,5144	2	0,34968
PH_hs_0044737	FBLN2	fibulin 2	2199	NM_001165035.1,NM	3	3,5156	2	0,1724
PH_hs_0029086	CHSY1	chondroitin sulfate sy	22856	NM_014918.4	3	3,5296	2	0,17441
PH_hs_0000168	BMP1	bone morphogenetic p	649	NM_006129.4,NR_03	3	3,5755	2	0,17752
PH_hs_0004621	G6PD	glucose-6-phosphate	2539	NM_000402.3,NM_00	3	3,5993	2	0,28911
PH_hs_0025290	COL5A1	collagen, type V, alpl	1289	NM_000093.3	3	3,6518	2	0,18098
PH_hs_0020027	HSPA2	heat shock 70kDa pro	3306	NM_021979.3	3	3,6601	2	0,11584
PH_hs_0004001	CLIC3	chloride intracellular c	9022	NM_004669.2	3	3,6607	2	0,1424
PH_hs_0018698	RRM1	ribonucleotide reducta	6240	NM_001033.3	3	3,7652	2	0,23127
PH_hs_0043477	FHL1	four and a half LIM do	2273	NM_001159703.1,NR	3	3,822	2	0,045748
PH_hs_0002037	SYT5	synaptotagmin V	6861	NM_003180.2	3	3,8994	2	0,10394
PH_hs_0045424	LOC100130633	hypothetical LOC100	100130633	XM_001723998.2,XM_	3	3,9193	2	0,24393
PH_hs_0005671	LOX	lysyl oxidase	4015	NM_001178102.1,NM	3	3,9865	2	0,23761
PH_hs_0013028	TIMP3	TIMP metallopeptidas	7078	NM_000362.4	3	4,0595	2	0,19524
PH_hs_0001899	SERPINE2	serpin peptidase inhit	5270	NM_001136529.1,NM	3	4,0824	2	0,19071
PH_hs_0031282	PIGU	phosphatidylinositol g	128869	NM_080476.4	3	4,0958	2	0,25187
PH_hs_0012781	MYL12A	myosin, light chain 12	10627	NM_006471.2	3	4,1142	2	0,20638
PH_hs_0049537	TUBG1|LOC1001336	tubulin, gamma 1|sim	7283|100133673	NM_001070.4|XM_00	3	4,1579	2	0,21118
PH_hs_0045419	C3orf74	chromosome 3 open r	100128378	NR_027331.1,XR_078	3	4,2449	2	0,16246
PH_hs_0014165	NANS	N-acetylneuraminic a	54187	NM_018946.3	3	4,2877	2	0,2184
PH_hs_0004806	NT5DC2	5'-nucleotidase domai	64943	NM_022908.2,NM_00	3	4,3123	2	0,20284
PH_hs_0045643	RPS4Y2	ribosomal protein S4,	140032	NM_001039567.2	3	4,3183	2	0,19844
PH_hs_0001301	DPF2	D4, zinc and double P	5977	NM_006268.3	3	4,3335	2	0,11645
PH_hs_0047899	KDM5A	lysine (K)-specific de	5927	NM_001042603.1	3	4,3611	2	0,24067
PH_hs_0023770	CLPP	ClpP caseinolytic pep	8192	NM_006012.2	3	4,4058	2	0,20576
PH_hs_0014826	PRDM12	PR domain containing	59335	NM_021619.2	3	4,4447	2	0,20631
PH_hs_0018365	ZNF692	zinc finger protein 692	55657	NM_017865.2	3	4,5258	2	0,18185
PH_hs_0042616	OR4B1	olfactory receptor, fan	119765	NM_001005470.1	3	4,5503	2	0,20347
PH_hs_0025615	CCDC97	coiled-coil domain co	90324	NM_052848.1	3	4,6008	2	0,27416
PH_hs_0006930	TMEM52	transmembrane prote	339456	NM_178545.3	3	4,6161	2	0,24638
PH_hs_0047918	SPPL2B	signal peptide peptida	56928	NM_001077238.1,NM	3	4,6503	2	0,2061
PH_hs_0034387	METRNL	meteorin, glial cell dif	284207	NM_001004431.1	3	4,7026	2	0,22652
PH_hs_0047958	TNFRSF10D	tumor necrosis factor	8793	NM_003840.3	3	4,7605	2	0,18074
PH_hs_0043275	PABPN1	poly(A) binding protei	8106	NM_004643.2	3	4,7732	2	0,16459
PH_hs_0002110	CCNB1	cyclin B1	891	NM_031966.2	3	4,7941	2	0,1859
PH_hs_0023001	HNRNPH1	heterogeneous nuclea	3187	NM_005520.2	3	4,7978	2	0,18385
PH_hs_0045537	KIR3DP1	killer-cell Ig-like recep	768329	NM_001015070.1	3	4,9349	2	0,20443
PH_hs_0015557	PLXND1	plexin D1	23129	NM_015103.2	3	4,9561	2	0,18407
PH_hs_0010770	ABHD11	abhydrolase domain c	83451	NM_148912.2,NM_00	3	5,2801	3	0,18725
PH_hs_0000582	MGEA5	meningioma expresse	10724	NM_001142434.1,NM	3	5,3293	3	0,16621
PH_hs_0018644	TMEM145	transmembrane prote	284339	NM_173633.2	3	5,4296	3	0,19394
PH_hs_0032261	DCTPP1	dCTP pyrophosphatas	79077	NM_024096.1	3	5,6699	3	0,19485
PH_hs_0006027	SH3BGRL3	SH3 domain binding g	83442	NM_031286.3	3	5,7281	3	0,1155
PH_hs_0004359	MFSD2A	major facilitator super	84879	NM_001136493.1,NM	3	5,7729	3	0,15892
PH_hs_0030989	RNF181	ring finger protein 181	51255	NM_016494.3	3	5,9207	3	0,18271
PH_hs_0042159	CREB3L3	cAMP responsive ele	84699	NM_032607.1	3	6,0007	3	0,13685
PH_hs_0033361	ACOT7	acyl-CoA thioesterase	11332	NM_181866.2,NM_18	3	6,1786	3	0,17567
PH_hs_0049621	LOC100290309|LOC1	similar to Fc fragmen	8857|100290309|1001	XM_002347971.1|XM_	3	6,188	3	0,19184
PH_hs_0031045	RIC8A	resistance to inhibitor	60626	NM_021932.4	3	6,197	3	0,13738
PH_hs_0006045	NENF	neuron derived neurot	29937	NM_013349.4,NR_02	3	6,3014	3	0,18674
PH_hs_0035682	SF3B3	splicing factor 3b, sut	23450	NM_012426.4	3	6,5986	3	0,14607
PH_hs_0004994	PSMB4	proteasome (prosome	5692	NM_002796.2	3	6,7341	3	0,14176
PH_hs_0005109	H2AFY2	H2A histone family, m	55506	NM_018649.2	3	6,839	3	0,13921
PH_hs_0027429	PGD	phosphogluconate de	5226	NM_002631.2	3	6,9222	3	0,14198
PH_hs_0004346	TJP2	tight junction protein 2	9414	NM_001170416.1,NM	3	7,1313	3	0,15305
PH_hs_0043380	ZNF444	zinc finger protein 444	55311	NM_018337.2	3	7,1349	3	0,15784
PH_hs_0045590	EEF1B2	eukaryotic translation	1933	NM_001959.3	3	7,4046	3	0,16133
PH_hs_0000676	MPDU1	mannose-P-dolichol u	9526	NR_024603.1,NM_00	3	7,4194	3	0,13167
PH_hs_0025312	EMR4P	egf-like module conta	326342	NR_024075.1	3	7,458	3	0,089318
PH_hs_0024499	IFT140	intraflagellar transport	9742	NM_014714.3	3	8,2498	3	0,10531
PH_hs_0030167	ACYP2	acylphosphatase 2, m	98	NM_138448.3	3	9,7698	3	0,11632
PH_hs_0047963	SLC11A1	solute carrier family 1	6556	NM_000578.3	3	10,976	3	0,10995
PH_hs_0047838	IGFBP3	insulin-like growth fac	3486	NM_000598.4,NM_00	3	11,1906	3	0,068361
PH_hs_0002082	PRRT2	proline-rich transmem	112476	NM_145239.2	3	11,4025	3	0,092982
PH_hs_0047621	LOC100303728	hypothetical LOC100	100303728	NR_028443.1	3	12,7269	3	0,076896
PH_hs_0010621	SLC32A1	solute carrier family 3	140679	NM_080552.2	3	12,9034	3	0,063925
PH_hs_0029811	APOBEC3A|APOBEC	apolipoprotein B mRN	200315|9582	NM_145699.3|NM_00	3	13,5521	3	0,065379

10 Acknowledgements

I would like to express my sincere thanks to Prof. Dr. Thomas Scheper for giving me the opportunity to work on this interesting topic in the Institute of Technical Chemistry.

I express my thanks and appreciation to Prof. Dr. Cornelia Kasper for her support during my research. I wish good luck and many interesting discoveries to her new Tissue Engineering working group in Vienna.

I am grateful to Prof. Dr. Jürgen Alves for his willingness to be co-supervisor. I would also like to thank Prof. Dr. Ralf Hass for his collaboration and scientific support. I also thank Dr. Frank Stahl for valuable scientific discussions.

I would like to give big thanks to Iliyana Pepelanova for her friendship, warmth and constant moral and scientific support, for many funny evenings together and for so much help with Sebastian. Good luck with all your endeavors! I also thank Mike Büring, who keeps the spirit and traditions of TCI.

I thank my Life-Science-team Anne Schmidt and Yi Su for great years together and wish them big success with their careers.

Research is teamwork. Therefore I thank all people who were working with me during the last four years. Magda Thomala (I appreciate every day of our common work with all depths and heights - remember how we were trying to find the Petri-dish with our LIF-bacteria in the waste? ☺), Pierre Moretti (hope we will see each other at least once a year!), Tim Hatlapatka (how many billions of cells we raised together?), Daniel Landgrebe (thank you for being such a nice office mate and helping me with flow-cytometry and cell sorting), Alex Babitsky (thanks for the mitotracker!), Ingrida Majore for shearing her experience with stem cell cultivation and Johanna Walter for her help with the protein-microarray.

I hug and thank Sonja Kress (thanks for the great Feuerzangenbowle-evening!), Stefanie Wagner (I will always remember our flight from Vienna), Anne Neumann (we are the best neuron-makers!), Estabraq Abdulkerim (looking forward to hear you singing this summer again), Rebecca Bongartz (hope you don’t feel lonely now in the lab) and Christoph Wolff. Good luck with your theses!

Kai Mutz, my great office mate, I thank for his help with qRT-PCR, interesting scientific conversations, and for his help with my new computer. I wish you good luck with your thesis and hope you get a job you deserve!

I would also like to thank two fresh PhD students Alexandra Heilkenbrinker and Maren Lönne. It was really great to work with you both. I wish you much fun for the next three years in the science. Keep optimism and stay positive! “Success is going from failure to failure without loss of enthusiasm.” (W. Churchill)

My sincere appreciation to Martin Pähler for his help in DNA-microarray and to Martina Weiss for her help in HPLC and many other small everyday challenges (“By the way, Martina, do you have the brain?”☺). Thanks for helping me at any time and for helpful advices in experimental procedures.

I thank Friedbert Gellermann and Thorsten Strempel for their helpfulness when I had problems with my bioreactor (although sometimes I had a feeling that they hide when they see me coming with sad face and broken reactor☺). I also thank Michael Dors and Ivo Havlik for their constant help with collapsed software and broken USB-sticks.

I am grateful to the GMP-Musterlabor team: Dr. Ulrike Böer and Melanie Klingenberg for the help in everyday lab life and for establishing a good-functioning lab.

I thank Carmen Schirmaier, Ramona Winkler, Anne Stamm, André Jochum and Dominik Egger for common work. It was pleasure to accompany you on your scientific way.

Every single day I thank Joachim for his love, support and his presence in my life. Without you this work would not be possible. Thank you for your calming words, for your faith in me and for encouraging me to do what I believe in.

My dear son Sebastian I thank for his patience and love. You are the greatest discovery of my life.

Last but not least, I thank my family: Taisa, Valerii, Klara, Helmut, Maria, Sergey and Alexandra for unconditional support, love and everything what family can give. Thank you all…

11 List of Publications

Papers and manuscripts

1. **Lavrentieva A**, Hatlapatka T, Neumann A, Weyand B, Kasper C. Potential for osteogenic and chondrogenic differentiation of MSC. "Mesenchymal stem cells - basics and clinical application", Springer-Verlag Berlin Heidelberg 2012. *In press.*

2. **Lavrentieva A**, HatlapatkaT, Winkler R, Hass R, Kasper C. Strategies in umbilical cord-derived mesenchymal stem cells expansion: influence of oxygen, culture medium and cell separation. BMC Proceedings 2011 5(Suppl 8): P.88

3. Hass R, **Lavrentieva A**, Kasper C. Hypoxia – Implications of physiological normoxia for stem cell cultivation and tissue engineering. Rebirth News. 1.2011: P.3

4. **Lavrentieva A**, Majore I, Kasper C, Hass R. Effects of hypoxic culture conditions on umbilical cord-derived human mesenchymal stem cells. Cell Commun Signal. 2010 Jul 16; Volume 8: P.18.

5. **Lavrentieva A**, Hatlapatka T, Chen R, Scheper T, Kasper C. Investigations towards expansion efficiency of mesenchymal stromal cells under different cultivation conditions. *In preparation.*

6. Marten D, **Lavrentieva A**, Neumann A, Heilkenbrinker A, Röker S, Kasper C. Expansion and differentiation strategies of human umbilical cord derived cells in disposable rotating bed bioreactors. *In preparation.*

7. Hatlapatka T, Moretti P, **Lavrentieva A**, Hass R, Marquardt N, Jacobs R, Kasper C. Optimization of culture conditions for the expansion of umbilical cord-derived mesenchymal stem or stromal cell-like cells using xeno-free culture conditions. TISSUE ENGINEERING: Part C. 2011 Volume 17: P.465

8. Tomala M, **Lavrentieva A**, Moretti P, Rinas U, Kasper C, Stahl F, Schambach A, Warlich E, Martin U, Cantz T, Scheper T. Preparation of bioactive soluble human leukemia inhibitory factor from recombinant Escherichia coli using thioredoxin as fusion partner. Protein Expr Purif. 2010 Sep;73(1): P.51

9. Moretti P, Hatlapatka T, Marten D, **Lavrentieva A**, Majore I, Hass R, Kasper C. Mesenchymal stromal cells derived from human umbilical cord tissues: primitive cells with potential for clinical and tissue engineering applications. Adv Biochem Eng Biotechnol. 2010;123: P.29.

10. Tomala M, **Lavrentieva A**, Neubacher H, Zhao YX, Rinas U, Kasper C, Stahl F, Schambach A, Warlich E, Martin U, Cantz T, Scheper T. Production and purification of human Leukemia Inhibitory factor from recombinant E.coli. Protein Expr Purif. 2010 Sep;73(1): P.51

11. Hatlapatka T, Moretti P, Marten D, **Lavrentieva A**, Majore I, Hass R, Scheper T, Kasper C. Human umbilical cord-derived mesenchymal stem cell-like cells exhibit in vitro immunomodulatory properties. Human Gene Therapy. 2009. Volume 20: P.1488

12. Majore I, Moretti P, **Lavrentieva A**, Hass R, Kasper C. Characterization of mesenchymal stem cell-like cultures derived from human umbilical cord. Human Gene Therapy. 2009. Volume 20: P.1491

Poster presentations

1. World Conference on Regenerative Medicine, Leipzig , Germany 2011: **Lavrentieva A**, Kress S, Heilkenbrinker A, Lönne M, von Kaisenberg C, Hass R, Kasper C. GMP-conform Expansion of Umbilical Cord derived Mesenchymal Stem Cells

2. The 5th UK Mesenchymal Stem Cell (MSC) Meeting, Birmingham, UK, 2011: **Lavrentieva A**, Kress S, Heilkenbrinker A, Lönne M, von Kaisenberg C, Hass R, Kasper C. Expansion of Umbilical Cord-derived Mesenchymal Stem Cells with Regards to GMP-conform Production Process.

3. The 14th STS Meeting Signal Transduction - Receptors, Mediators and Genes. 2010, Weimar, Germany: Kasper C, Hatlapatka T, **Lavrentieva A**, Marquardt N, Jacobs R, Hass R. Shaping the Microenvironment of Umbilical Cord-derived Mesenchymal Stem Cell-like Cells for Bone Tissue Engineering

4. 27. Jahrestagung der Biotechnologen, 2009, Mannheim: Chen R, Tomala M, **Lavrentieva A**, Majore I, Kasper C, Stahl F. Expression and Purification of Recombinant human basic Fibroblast Growth Factor from Fed-Batch Cultivation of E. coli. Chemie Ingenieur Technik - CIT Volume 81 Issue 8: P.1290

5. 28. DECHEMA-Jahrestagung der Biotechnologen und ProcessNet-Jahrestagung 2010, Aachen, Germany. **Lavrentieva A**, Majore I, Kasper C, Scheper T. Wirkung der Hypoxie auf Zellkulturbedingungen von Nabelschnur-Abgeleiteten Stammzellen

6. 4th Annual Congress of the German Society for Stem Cell Research, 2009, Hannover, Germany: Hatlapatka T, Moretti P, Marten D, **Lavrentieva A**, Majore I, Hass R, Scheper T, Kasper C. Human Umbilical Cord-derived Mesenchymal Stem Cell-like cells exhibit in vitro immunoprivileged and immunomodulatory properties

7. World Conference of Regenerative Medicine, 2009, Leipzig, Germany: Hatlapatka, T., Moretti, P., **Lavrentieva, A**., Majore, I., Hass, R., Scheper, T., Kasper, C. Immunologic Properties of Human Umbilical Cord-derived Mesenchymal Stem Cell-like cells.

8. 2th Annual Stem Cell and Regenerative Medicine Europe Conference, 2009, Edinburgh: Hatlapatka, T., Moretti, P., **Lavrentieva, A**., Majore, I., Hass, R., Scheper, T., Kasper, C. Human Umbilical Cord-derived Mesenchymal Stem Cell-like cells exhibit similar in vitro immunologic properties as described for Bone-Marrow-MSCs

9. 4th congress of Regenerative Biology and Medicine (BioStar), 2010, Stuttgart, Germany: Hatlapatka, T., **Lavrentieva, A**., Hass, R., Marquardt, N., Jacobs, R., Kasper, C. Shaping the Microenvironment of Umbilical Cord-derived Mesenchymal Stem Cell-like Cells

10. 22nd ESACT Meeting, 2011, Vienna, Austria: **Lavrentieva, A**., Hatlapatka, T., Winkler, R., Hass, R., Kasper, C. Strategies in Umbilical Cord-derived mesenchymal stem cells expansion: influence of oxygen, culture medium and cell separation

11. 1st European Congress of Applied Biotechnology, 2011, Berlin, Germany**: A. Lavrentieva**, T. Hatlapatka, R. Hass, C. Kasper. In vitro expansion of the umbilical cord-derived mesenchymal stem cells for tissue engineering: influence of hypoxia, glucose concentration and number of passages

Curriculum Vitae

Persönliche Daten

Name	Antonina Lavrentieva
Geburtsdatum	21.05.1976
Geburtsort	Dmitrow, Russland
Staatsangehörigkeit	Russisch

Schulbildung

1983-1993	Mittlere allgemeinbildende Schule (Hochschulqualifikation) Dmitrow, Russland

Studium

1993-1998	Studium der Biologie Fakultät für Biologie, Schwerpunkt Embryologie, Staatliche Lomonosov Universität, Moskau, Russland. Diplom Physiologie
1998-2004	Promotion am Institut für Physiologie, Russische Akademie der Medizinischen Wissenschaft, Moskau, Russland (Ph.D. für Physiologie)
2005-2007	Master Studiengang „Life Science“, Gottfried Wilhelm Leibniz Universität Hanover, Deutschland
2008-2012	Promotion am Institut für Technische Chemie, Gottfried Wilhelm Leibniz Universität Hanover, Deutschland

Förderungen

2007	Förderpreis der Christian-Kuhlemann-Stiftung für herausragende Leistungen und Hochschulengagement internationaler Studierender
2011	Reisestipendium der *European Society of Animal Cell Technology* (ESACT)